

CAPITAL UNIVERSITY OF SCIENCE AND
TECHNOLOGY, ISLAMABAD



In- Silico Analysis of Human
Head Lice (*Pediculus humanus
capitis*) Genome for Insecticide
Resistance

by

Muneeba Ishtiaq

A thesis submitted in partial fulfillment for the
degree of Master of Science

in the

Faculty of Health and Life Sciences

Department of Bioinformatics and Biosciences

2022

Copyright © 2022 by Muneeba Ishtiaq

All rights reserved. No part of this thesis may be reproduced, distributed, or transmitted in any form or by any means, including photocopying, recording, or other electronic or mechanical methods, by any information storage and retrieval system without the prior written permission of the author.

All praise is due to Allah, the One and Only, by Whose the blessing and favour, perfected deeds of virtues are accomplished. This thesis was dedicated to Allah Almighty, Hazrat Muhammad (S.A.W.W) and my parents. My mother prayers have always enlightened my way throughout my life. It's also dedicated to all my respected teachers, my brother, sister and all other family members who taught me that the best kind of knowledge to have is that which is learnt for its own sake. They taught me that even the largest task can be accomplished if it is done one step at a time with dedication.



CERTIFICATE OF APPROVAL

In- Silico Analysis of Human Head Lice (*Pediculus humanus capitis*) Genome for Insecticide Resistance

by

Muneeba Ishtiaq

(MBS203028)

THESIS EXAMINING COMMITTEE

S. No.	Examiner	Name	Organization
(a)	External Examiner	Dr. Uzma Azeem Awan	NUMS, Rawalpindi
(b)	Internal Examiner	Dr. Arshia Amin Butt	CUST, Islamabad
(c)	Supervisor	Dr. Sahar Fazal	CUST, Islamabad

Dr. Sahar Fazal
Thesis Supervisor
October, 2022

Dr. Syeda Marriam Bakhtiar
Head
Dept. of Bioinformatics & Biosciences
October, 2022

Dr. Sahar Fazal
Dean
Faculty of Health & Life Sciences
October, 2022

Author's Declaration

I, **Muneeba Ishtiaq** hereby state that my MS thesis titled “***In- Silico Analysis of Human Head Lice (*Pediculus humanus capitis*) Genome for Insecticide Resistance*** ” is my own work and has not been submitted previously by me for taking any degree from Capital University of Science and Technology, Islamabad or anywhere else in the country/abroad.

At any time if my statement is found to be incorrect even after my graduation, the University has the right to withdraw my MS Degree.

(Muneeba Ishtiaq)

Registration No: MBS203028

Plagiarism Undertaking

I solemnly declare that research work presented in this thesis titled “***In- Silico Analysis of Human Head Lice (*Pediculus humanus capitis*) Genome for Insecticide Resistance*** ” is solely my research work with no significant contribution from any other person. Small contribution/help wherever taken has been dully acknowledged and that complete thesis has been written by me.

I understand the zero tolerance policy of the HEC and Capital University of Science and Technology towards plagiarism. Therefore, I as an author of the above titled thesis declare that no portion of my thesis has been plagiarized and any material used as reference is properly referred/cited.

I undertake that if I am found guilty of any formal plagiarism in the above titled thesis even after award of MS Degree, the University reserves the right to withdraw/revoke my MS degree and that HEC and the University have the right to publish my name on the HEC/University website on which names of students are placed who submitted plagiarized work.

(Muneeba Ishtiaq)

Registration No: MBS203028

Acknowledgement

My first word of thanks to the one who taught words to Adam, Who blessed man with knowledge, who is the sublime without Whose “Kun” nothing is possible. Secondly my humblest thanks from the core of my heart, to our beloved **Prophet Hazrat Mohammad (S.A.W.W)** who is the eternal fountain of knowledge and guidance for the whole mankind. Then I would like to pay my deepest gratitude to my admirable teacher and supervisor Prof. Dr. Sahar Fazal, Dean Faculty of Health & Life Sciences, Capital University of Science and Technology Islamabad. I am grateful to her for approving research topic, her disciplinarian attitude, and strictness in punctuality and working in organized manner makes possible to complete this work. Not to be forgotten, my best friend Narjis Khatoon who helped me morally for accomplishment of this goal.

I now turn to those who were and are first in my mind but are mentioned last, my parents, my brother, my sister, friends and all teachers of my career. I believe their most sincere and innocent prayers which were a constant source of strength and inspiration to me that resulted in the completion of this work. I pray to Allah Almighty to give me the strength and resources to serve them to the best of my efforts and wisdom not to neglect them in future; Ameen.

(Muneeba Ishtiaq)

Abstract

Head louse is an obligate ecto-parasite of the humans which lives on the scalp of human's head. Head louse infestation is a main public health issue and a big threat for the children's personal hygiene which is very common in the children of age five to thirteen years. Head louse are the vectors of many pathogenic microorganisms and they are transmitting the diseases among the people suffering from head louse infestation. Head louse infestations are treated with different insecticides like Lindane, Permethrin, Pyrethroids and Malathion but they are developing resistance against these chemicals and their treatment has become very difficult. Genome sequencing and genome annotation is a new approach in the field of Biological Sciences, by the help of which one can understand the genomes of different organisms. In the current study, the whole genome of the human head louse was sequenced and annotated using different computational tools. The objectives of this study were to sequence the whole genome of the head louse and to understand the role of the resistance genes in the genome of human head lice. The DNA of the head lice was extracted by using Phenol-chloroform method of DNA extraction, after that the whole DNA was sequenced using Next Generation Sequencing (Illumina 1.9). The raw data was then assembled and a de novo assembly was obtained. The data of the sequencing was then analyzed and mapped using different computational tools like Genious Prime and Velvet assembler. The results of this study revealed the outcome of whole genome of the head louse was sequenced and the resistance genes were identified. The total genes in the head louse genome were 9942, total proteins were 9907 and the total open reading frames were 988226. There were total nine novel resistance causing genes i.e. the knockdown resistance genes and the voltage sensitive sodium channels were identified in the head louse's genome. The mutations in the resistance causing genes were identified and the mutations were successfully predicted using different computational tools. There were different mutations such as at 34th position the methionine is replaced with Isoleucine and the other mutation was that at the 34th position, the Isoleucine was replaced with the Phenylalanine. Then the mutations were verified through the PROVEAN tool and among those mutations, the mutation M34I was deleterious

and the other mutation i.e. I34F was neutral and the third one was the mutation M34I was deleterious. And the prediction of 2D and 3D structures of the mutated genes for the analysis such as for the docking was done. The mutations were functionally annotated and their impacts on the genes in causing the resistance was studied. They have different functions which includes the cell communication, neurological system process, intrinsic component of membrane and transmembrane transporter activity. The novel mutations were submitted in the National Centre for Biotechnology Information (NCBI) and the accession ID is **OP136150**. The study of the resistance genes, mutations and their structures helped to understand the role of these genes and these mutations in causing the resistance among human head louse which have shown resistance against the insecticide (*pediculide*) such as Lindane and have not shown resistance against the Malathion, Pyrethroids and Carbaryl. The impacts of these mutations on causing the resistance in the head louse was studied and this study is helpful for researchers in designing the control and treatment for the head louse infestation or *pediculosis*.

Contents

Author’s Declaration	iv
Plagiarism Undertaking	v
Acknowledgement	vi
Abstract	vii
List of Figures	xiii
List of Tables	xvi
Abbreviations	xvii
1 Introduction	1
1.1 Problem Statement	4
1.2 Objectives	5
2 Review of Literature	6
2.1 Background	6
2.2 Pathogens Associated with Head Lice	6
2.3 Evolutionary History of Human Lice	10
2.4 Lice are the Markers of Evolution of Humans	12
2.5 Life Cycle	13
2.5.0.1 Egg	13
2.5.0.2 Nymph	13
2.5.0.3 Adult	14
2.6 Louse Nit Sheath Proteins	14
2.7 Treatment of Human Head Louse	15
2.8 Resistance in the Lice Against Insecticides	16
2.8.1 Pyrethroids as the <i>Pediculides</i>	17
2.8.2 Malathion as the <i>Pediculides</i>	18
2.8.3 Lindane as the <i>Pediculides</i>	19
2.8.4 Carbaryl as the <i>Pediculides</i>	20
2.9 Gap Analysis	20

2.10	Research Questions	21
3	Research Methodology	22
3.1	Methodology Flowchart	22
3.2	Materials and Chemicals	23
3.3	Preparation of Solutions	23
3.3.1	70% Ethanol	23
3.3.2	TET Buffer	23
3.3.3	TE Buffer	24
3.3.4	TAE Buffer	24
3.4	Ethical Approval	24
3.5	Sample Collection	24
3.6	Preservation of Head Lice	25
3.7	Extraction of DNA from <i>Pediculus humanus capiti</i>	25
3.8	Agarose Gel Electrophoresis	26
3.9	Quantification of DNA	26
3.10	Lyophilization of DNA	27
3.11	Whole Genome(WG) Sequencing Data Assembly	27
3.12	Genome Annotation	28
3.13	Sequence Analysis	29
3.13.1	Mapping of the Contigs with the Reference Sequence	29
3.13.2	Translation of the Mapped Contigs	29
3.14	Mutational Analysis	30
3.14.1	Prediction of Mutations	30
3.14.2	Verification of Mutations	30
3.15	Prediction of the Structures of Mutated Proteins	31
3.15.1	Prediction of the 2D Structure of Mutated Proteins	31
3.15.2	Prediction of the 3D Structure of Mutated Proteins	32
3.16	Validation of the Mutations through Molecular Docking	32
3.17	Retrieval and Preparation of Ligands (<i>Pediculides</i>) Structure	33
3.18	Steps Involved in the Mutational Analysis	33
3.19	Functional Annotation of the Mutated Proteins	34
4	Results and Discussions	35
4.1	Results of DNA Extraction	35
4.2	Whole Genome Sequencing(WGS)	37
4.3	Raw Reads/ Contigs of the Whole Genome Sequencing	37
4.4	Assembly of the Raw Reads/Contigs	38
4.5	Genome Annotation	39
4.5.1	De Novo Assembly	39
4.5.2	Genes and Open Reading Frames (ORFs)	40
4.6	Mapping Of The Contigs With The Reference Sequence	41

4.6.1	Resemblance Shown by Sequence 1, 2 and 3 with MW057882	41
4.6.2	Resemblance Shown by Sequence 4, 5 and 6 with KX301993	42
4.6.3	Resemblance Shown by Sequence 7, 8 and 9 with KX302005	43
4.7	Translation of the Mapped Sequences	44
4.8	Mutational Analysis	44
4.8.1	Prediction of Mutations in the Mapped Sequences by Blast X	45
4.8.1.1	Prediction of Mutation in the Sequence 1, 2 and 3	45
4.8.1.2	Prediction of Mutation in the Sequence 4, 5 and 6 .	45
4.8.1.3	Prediction of Mutation in the Sequence 7, 8 And 9	46
4.9	Verification of Mutations	47
4.9.1	Verification of Mutation in the Sequence 1, 2 and 3	47
4.9.2	Verification of Mutation in the Sequence 4, 5 and 6	47
4.9.3	Verification of Mutation in the Sequence 7, 8 And 9	48
4.10	2D Structure Prediction	49
4.10.1	2D Structure of Sequence 1	49
4.10.2	2D Structure of Sequence 2	50
4.10.3	2D Structure of Sequence 3	52
4.10.4	2D Structure of Sequence 4	53
4.10.5	2D Structure of Sequence 5	55
4.10.6	2D Structure of Sequence 6	56
4.10.7	2D Structure of Sequence 7	58
4.10.8	2D Structure of Sequence 8	59
4.10.9	2D Structure of Sequence 9	61
4.11	3D Structure Prediction	63
4.11.1	Sequence 1 3D Structure	63
4.11.2	3D Structure of Sequence 2	64
4.11.3	3D Structure of Sequence 3	66
4.11.4	3D Structure of Sequence 4	67
4.11.5	3D Structure of Sequence 5	69
4.11.6	3D Structure of Sequence 6	70
4.11.7	3D Structure of Sequence 7	72
4.11.8	3D Structure of Sequence 8	73
4.11.9	3D Structure of Sequence 9	75
4.12	Molecular Docking of <i>Pediculides</i> (Insecticides) with KRD Sequences of Head Louse	77
4.12.1	Molecular Docking of <i>Pediculides</i> with the Reference Se- quences	77
4.13	Reasons of Binding of <i>Pediculides</i> with the Reference Sequences . .	79
4.14	Functional Annotation and Interactions of the Reference Sequences	83
4.15	Submission of Mutations in NCBI	88
5	Conclusions and Recommendations	89
	Bibliography	91

An Appendix

List of Figures

2.1	Life Cycle of the Head Lice.	14
3.1	Flowchart	22
3.2	Steps involved in Mutational Analysis in Knockdown Resistance Genes (KDR) of Human Head Lice.	33
4.1	Agarose Gel Electrophoresis of the DNA recovered. Lane 1 represents the 2kb ladder, lane 2 represents the negative control sample, lane 3, 4, 5, 6, 7 and 8 represents the human head lice samples.	36
4.2	Results of Whole Genome Sequencing in the form of Raw Reads/-Contigs.	37
4.3	Assembly of the Raw Reads of the Whole Genome Sequencing by Velvet Assembler Software.	38
4.4	De Novo Assembly of the 7,933 contigs.	40
4.5	The Open Reading Frame of a contig of the genome of head lice.	40
4.6	Resemblance shown by sequence 1, 2 and 3 with MW057882.	42
4.7	Resemblance shown by sequence 4, 5 and 6 with KX301993.	43
4.8	Resemblance shown by sequence 4, 5 and 6 with KX301993.	43
4.9	Translation of the mapped sequences.	44
4.10	Predicted Mutation in the Sequence 1, Sequence 2 and Sequence 3.	45
4.11	Predicted Mutation in the Sequence 4, Sequence 5 and Sequence 6.	46
4.12	Predicted Mutation in the Sequence 7, Sequence 8 and Sequence 9.	46
4.13	Verification of the Mutation in the Sequence 1, Sequence 2 and Sequence 3.	47
4.14	Verification of the Mutation in the Sequence 4, Sequence 5 and Sequence 6.	48
4.15	Verification of the Mutation in the Sequence 7, Sequence 8 and Sequence 9.	48
4.16	2D Structure Prediction of the Sequence 1.	49
4.17	Components and graphical representation of the 2D Structure of the Sequence 1.	50
4.18	2D Structure Prediction of the Sequence 2	51
4.19	Components and graphical representation of the 2D Structure of the Sequence 2.	51
4.20	2D Structure Prediction of the Sequence 3.	52
4.21	Components and graphical representation of the 2D Structure of the Sequence 3.	53

4.22	2D Structure Prediction of the Sequence 4.	54
4.23	Components and graphical representation of the 2D Structure of the Sequence 4.	54
4.24	2D Structure Prediction of the Sequence 5.	55
4.25	Components and graphical representation of the 2D Structure of the Sequence 5.	56
4.26	2D Structure Prediction of the Sequence 6.	57
4.27	Components and graphical representation of the 2D Structure of the Sequence 6.	57
4.28	2D Structure Prediction of the Sequence 7.	58
4.29	Components and graphical representation of the 2D Structure of the Sequence 7.	59
4.30	2D Structure Prediction of the Sequence 8.	60
4.31	2 Components and graphical representation of the 2D Structure of the Sequence 8.	60
4.32	2D Structure Prediction of the Sequence 9.	61
4.33	Components and graphical representation of the 2D Structure of the Sequence 9.	62
4.34	3D Structure of the Sequence 1.	63
4.35	Ramachandran Plot of the Sequence 1.	64
4.36	3D Structure of the Sequence 2.	65
4.37	Ramachandran Plot of the Sequence 2.	65
4.38	3D Structure of the Sequence 3.	66
4.39	Ramachandran Plot of the Sequence 3.	67
4.40	3D Structure of the Sequence 4.	68
4.41	Ramachandran Plot of the Sequence 4.	68
4.42	3D Structure of the Sequence 5.	69
4.43	Ramachandran Plot of the Sequence 5.	70
4.44	3D Structure of the Sequence 6.	71
4.45	Ramachandran Plot of the Sequence 6.	71
4.46	3D Structure of the Sequence 7.	72
4.47	Ramachandran Plot of the Sequence 7.	73
4.48	3D Structure of the Sequence 8.	74
4.49	Ramachandran Plot of the Sequence 8.	74
4.50	3D Structure of the Sequence 9.	75
4.51	Ramachandran Plot of the Sequence 9.	76
4.52	Molecular Docking of Sequence 1, sequence 2 and sequence 3 with the <i>Pediculides</i> (Malathion, pyrethroids and carbaryl).	78
4.53	Molecular Docking of Sequence 4, sequence 5 and sequence 6 with the <i>Pediculides</i> (Malathion, pyrethroids and carbaryl).	78
4.54	Molecular Docking of Sequence 7, sequence 8 and sequence 9 with the <i>Pediculides</i> (Malathion, pyrethroids and carbaryl).	79
4.55	Binding due to Aromatic Compounds in Sequence 1, 2, 3.	79
4.56	Binding due to Hydrophobicity in Sequence 1, 2, 3.	80

4.57	Binding due to Aromatic Compounds in Sequence 4, 5, 6.	80
4.58	Binding due to Hydrophobicity in Sequence 4, 5, 6.	81
4.59	Binding due to Hydrogen Bonding in Sequence 4, 5, 6.	81
4.60	Binding due to Hydrogen Bonding in Sequence 7,8,9.	82
4.61	Graphical Representation of the Binding Affinities of the Ligands.	83
4.62	The Interactions of the Reference (query) Protein of head louse with Proteins of human body lice.	84
4.63	Submission of KDR gene in NCBI.	88
5.1	A1 (Basic Statistics of the Sequence)	110
5.2	A2 (Per Base Quality of the Sequence).	110
5.3	A3 (Quality of the Sequence per Tile)	111
5.4	A4 (Per Sequence Quality Scores.).	111
5.5	A5 (Per Base Sequence Content)	112
5.6	A6 (Per Base GC Content)	112
5.7	A7 (Per Base N Content.)	113
5.8	A8 (Sequence Length Distribution.)	113
5.9	A9 (Sequence Duplication Levels)	114
5.10	A10 (Adapter Content.)	114
5.11	A11 (The Assembly Report provided by the Genious Prime tool.)	115

List of Tables

2.1	Insecticide used for the treatment of head louse.	18
4.1	Components of 2D Structure of the Sequence 1.	50
4.2	Components of 2D Structure of the Sequence 2.	52
4.3	Components of 2D Structure of the Sequence 3.	53
4.4	Components of 2D Structure of the Sequence 4.	55
4.5	Components of 2D Structure of the Sequence 5.	56
4.6	Components of 2D Structure of the Sequence 6.	58
4.7	Components of 2D Structure of the Sequence 7.	59
4.8	Components of 2D Structure of the Sequence 8.	61
4.9	Components of 2D Structure of the Sequence 9.	62
4.10	Binding Affinities of the <i>Pediculides</i> (Ligands) with the Reference Sequences.	82
4.11	Functional Annotation of the Mapped Knockdown Resistance Genes.	85

Abbreviations

BLAST: Basic Local Alignment Search

DNA: Deoxyribonucleic Acid

dsRNA: Double Stranded RNA

dNTP: Deoxynucleotide

ddNTPs: Dideoxynucleotide

EDTA: Ethylene Diamine Tetra Acetic Acid

FTIS: Fourier Transform Infrared Spectroscopy

NaCl: Sodium Chloride

NCBI: National Center for Biotechnology Information

NGS:Next Generation Sequencing

PCR: Polymerase Chain Reaction

PROVEAN: Protein Variation Effect Analyzer

RNA: Ribonucleic Acid

RNAi: RNA Interference

siRNA: Small Interfering RNA

WG: Whole Genome

WGS: Whole Genome Sequencing

Chapter 1

Introduction

Head lice infestation occurs throughout the world which is caused by *Pediculus humanus capitis* [1]. Head lice are obligatory human hematophagous ecto-parasites belonging to the *Pediculidae* family [2]. Its transmission occurs by means of clothing, such as, hats, jackets, and scarves, as well as the shared use of hairbrushes and combs [3]. Close body contact is strongly associated with louse transmission, and infestation occurs more frequently in crowded environments, such as homeless shelters, refugee camps, and jails, especially when hygienic standards are lacking [4]. *Pediculosis* is a term used to defined infestation caused due to eggs, larvae and adult head louse also termed as a source of the parasitism [4]. The louse injects the biologically active proteins in skin that include an anticoagulant and an anesthetic [5]. These antigens provoke an allergic reaction within 3–4 weeks after the bite.

Pediculosis is a major public health concern because it can transmit intracellular pathogenic bacteria: *Rickettsia prowazekii* and *Bartonella Quintana*, which belong to a subgroup of *Proteobacteria*, and the spirochete *Borrelia recurrentis* [6]. Head lice are responsible for the Trench fever that was first described during World War I, so named because the disease affected Allied and German troops crowded into trenches during World War I [7]. The disease is caused by *Bartonella. Quintana*, a Gram-negative bacterium. The incidence of *Bartonella Quintana* dramatically fell after World War II [8], [9]. In the early 1990s, trench fever was recognized

as a major reemerging disease in the poor living conditions of urban homeless populations in developed countries [10], [11]. It was recovered in soldiers from Napoleon's army [12], [13] and in the dental pulp of a person who died 4000 years ago [14]. Epidemic relapsing fever is caused by the spirochete *Borrelia Recurrentis*, and *Pediculus humanus capitis* are the sole reservoir [15]. Although the disease has disappeared in extensive regions of the world, it remains an important endemic disease in northeastern Africa [16]. It was initially described in Ireland and was one of the first infectious lice disease identified by microscopy [17]. Relapsing fever spreads in humans through feces [18], [19], [20] and, as with epidemic typhus, primarily affects military and civilian populations disrupted by war and other disasters [21]. After becoming infected by the ingestion of an infected blood meal, a louse remains infected throughout its lifetime [22]. As the disease frequently causes jaundice, it has been reported as the yellow plague, which ravaged Europe in 550. AD. During World War I, a half million people contracted relapsing fever in Serbia. During civil war in Russia and Eastern Europe between 1919 and 1923, 13 million cases were reported, leading to 5 million deaths [23].

The major phenotypic differences between the head and body louse relate to the ecology and color [24]. No similarity among those characteristics could be assessed, and phenotypic studies were subsequently challenged by genetic studies [25]. Three clades (A, B and C) of head lice were described by analyzing the mitochondrial DNA (cytochrome b and cytochrome oxidase subunit 1), and of them, only one (clade A) was present in body lice [26]. Clade A can be subdivided in two subclades: the Eurasian subclade A1 and the Sub-Saharan subclade A2 [27]. A third clade, named A3, was recently characterized using high polymorphic intergenic spacers in the American lice and represents a specific Amazonian genotype that is putatively pre-Columbian [28]. This multi spacer typing technique was previously used to show a correlation between genotypes and ecotypes [29].

Clade B head lice are found in North and Central America (USA and Honduras, respectively), in Europe, and in Australia. The third type (clade C) is only found in head lice from Nepal, Ethiopia and Senegal [30] and the clade C head lice always have a dark color. Further complicating the study of the different groups

of lice, a recent study showed possible interbreeding events between lice of different clades, and identical genotypes of highly variable spacers were found between lice on different continents. Another study based on multi-spacer typing of doubly infested homeless individuals showed that, at least among Clade A lice, head and body lice are ecotypes of the identical species. Recently, genetic structure of the human louse was assessed through an analysis of variation at 15 new microsatellite loci in 93 human lice from four regions of the world and confirmed a high level of inbreeding in human lice [28].

Resistance is an established trait that pests acquire over time through selective pressure from continued or inappropriate pesticide use. Resistance is an inherited genetic trait caused by recessive allelic mutations that occur in various insects that have been exposed to DDT or pyrethroids or both at some point in their evolutionary history. Kdr-causing point mutations (e. g., M815I, T917I, and L920F) in the VSSC alpha subunit gene have been identified in resistant lice and used as markers of pyrethroid resistance. Although the detection of kdr gene mutations alone may not directly predict clinical failure, their increased frequency in head lice populations is consistent with reports of product failure in controlled trials. Unfortunately, due to the widespread use of conventional pediculicides in many parts of the world, resistant louse populations have emerged and are spreading rapidly.

Moreover, although ivermectin is the only drug currently used for oral therapy and its high potency has been clinically approved for the treatment of both louse ecotypes, empirically identified ivermectin resistance has increased in Senegal. It is beginning to be reported in the field [29]. There is also an increasing use of natural products such as *pediculicides* based on plant essential oils such as eucalyptus and tea tree oils and *pediculicides* with purely physical mechanisms of action such as dimethicone and benzyl alcohol. Insecticide resistance, which leads to treatment failure, is thought to be a major cause in the rising prevalence of head louse infections [151], [152]. The freshly sequenced louse genome provides a once-in-a-lifetime chance to answer fundamental issues about the molecular pathways that govern pesticide resistance. This is critical to extending the active life of

current pesticides and accelerating the development of new, more effective, and sustainable pesticide tactics [153].

There are many treatment options for head louse, along with chemical pesticides, topical remedies, natural preparations, and mechanical techniques (combs and heaters). However, the use of chemical pesticides with insect neurotoxic effects is the most widely used and preferred method. These include organic chlorides (lindane), organic phosphates (malathion), carbamates (carbaryl), pyrethrins (chrysanthemum extract), pyrethroids (synthetic derivatives of pyrethrins). Among them, malathion and permethrin remain the most commonly used *pediculicides*, given that they were launched in 1971 and 1992 respectively. A proteomic comparison of laboratory-susceptible (wild-type) and ivermectin-selection-resistant lice also found that complexins were considerably decreased in resistant lice. Taken together, their findings show that complexins play an important role in controlling ivermectin resistance in lice, and they are the first to relate complexins to pesticide resistance [30].

In general, pesticide resistance has resulted in the failure or partial treatment of *pediculosis*, which has increased its varying incidence and intensity globally during the previous three decades. As a result, different pesticides or other treatment methods are required. It is critical to have a preliminary understanding of the incidence of hereditary resistance among human head lice with local pesticides in order to apply effective treatment methods. In current study, insecticide resistance genes of the human head lice of Pakistan were identified, their protein structures were predicted and their networks were determined using different computational tools [31].

1.1 Problem Statement

In the different parts of the world, the spread as well as appearance of resistance among the head louse is due to indiscriminate use of insecticide that has raised the questions of addressing the factors and mechanisms responsible for resistance.

1.2 Objectives

The objectives of this research were:-

1. Identification of the resistance causing by mutations from whole genome of head louse.
2. Mutational Analysis including the identification and verification of the mutation in the resistance genes.
3. Prediction of the protein structures of mutated genes.
4. Functional annotation of the mutated genes that cause the resistance in human head louse.

Chapter 2

Review of Literature

2.1 Background

The head louse is suggested to be originated with the origin of humans. Because in the process of evolution, the humans have also evolved from other placental mammals so same is the case with human head lice that they are also originated from the other lice which are parasitizing the other placental mammals like monkeys, gorilla and chimpanzees [44], [45].

2.2 Pathogens Associated with Head Lice

In the current decades, it has been identified that the head louse is also a carrier of the multiple pathogenic microorganisms which has transformed the traditional thinking that only the body louse is the vector of different diseases. The body louse has been reported to be the carrier of the different diseases but the capability of the head louse as the vector of the diseases has not been fully understood. At the onset of the challenges to the immune system, a lot of research has been conducted on comparing the immune responses of the head louse and the body louse and it is noticed that body louse has relatively a weak immune response as compared to the head louse, these studies have been done by using in-vitro rearing system [45].

A comparative study of head and body louse revealed that the head louse can survive the infections of the *B. quintana* for many days and can transfer it in its feces [46]. In the gut of the body louse the rate of the multiplication of the *B. quintana* was 2.0 to 12.1 times more than in the head lice up to twelve days. In the feces of the body louse, the rate of the survival of the *B. quintana* was 6.4 to 10.6 times higher as compared to the head louse. The decrease in the immune response of the body louse as compared to the head louse can be the outcome of the enhanced competence as a vector. While the head louse has a very effective immune system to support the replication of the bacteria [47]. The transcriptional analysis of the immune response of the alimentary canal revealed the reduced immune response in the body louse due to the decreased expression of some genes such as defensin, peptidoglycan recognition protein and defensin 1. It is suggested that these regulations could be due to the alterations in the post transcription miRNA-mediated factors and in the epigenetic pathways [48]. In the guts of insects the level of the reactive oxygen species is thought to be the crucial mediator of the antimicrobial innate immunity defense, it has been noticed that in the body lice this important mediator was in a very lower level as compared to the head louse [49]. In many insects, the effects of the endosymbionts on the antibacterial immunity has been described already [50].

Moreover, there is a fact that the head louse and the body louse have different ecological niches and have distinct feeding methods are the additional features which may have impacts on the transferring of the pathogens. Body louse is very exposed to harsh conditions because it lives on the clothes of the humans and it has more movements on body to suck the blood as compared to head louse [51]. The stress has severe impacts on immunity of insect vectors that can cause changes in their immune responses of body louse against the infectious bacteria. Moreover, the head louse ingests less blood as compared to body louse [52].

The absorption of the more blood meals in the midgut causes increase in the infections in the lice as compared to small meals. The human head lice can transmit the *R. prowazekii* under the laboratory conditions. The first prove of it was reported by the *Anderson* and *Goldberger*, who have successfully recovered the

head louse from the epidemic *Typhus* fever and they have transferred the typhus to the *R. macaques* by using the hypodermic inoculation of the crushed infected head louse [53]. Another study disclosed that the head louse feeding on the rabbits infested with the *R. prowazekii* were responsible for spreading and infecting the virulent organisms through the feces and the head louse has the capability of transferring the infectious bacteria under suitable conditions [54].

Recently, the DNA of multiple infectious bacteria have been reported from head louse of many parts of the world. The head lice which belong to the clade D, C, E and A, contains the *B. quintana* in their bodies. A lot of studies have revealed that the incidence of the *B. quintana* in the different countries of the world contained by head louse, it has noticed that this bacteria is present in the rural populations in the Senegal and most other counties of the world [55]. In the Marseille, the DNA of the *B. quintana* was received from the individuals who were homeless. In the Ethiopian populations, it was noticed that the infections of the *B. quintana* in the head louse was associated with the high altitudes. Based on the head louse collection from the higher altitudes were infected with the bacteria and the body louse were not infected by the bacteria [56]. The capability of the head louse to act as vector may depend on the factors of the environment which are forcing the head louse to transfer the pathogenic bacteria in some geographical areas. In the Ethiopia and in the Republic of Congo, from the head louse of the poor people, the *B. recurrentis* was identified in the clade C. These patients were suffering from the disease which is caused by lice and is called relapsing fever [57].

In the eastern Congo, the DNA of the *Y. pestis* was found in the head louse of the clade A which infested the people in an endemic area of the plague. There are some bacterial species which were not considered previously to be transferred by the lice but recently have been also found to be associated with the head louse such as *R. aeschlimannii*, *C. burnetii*, *Ehrlichia* and *Anaplasma* [58]. The researchers have concluded that the head louse is continuously feeding on the blood of humans, so it can acquire all the infections from the blood of the infected people with the bacteria or other pathogens. The head lice infestations and head lice infections with all the infectious bacteria or pathogens are mostly occurring in the people

of the poor and vulnerable populations who lived in poor hygiene and poverty, so the ecotypes of the head lice proliferate there. This finding is supported with the facts that school going children and the people living in the good hygienic conditions are suffering from the head lice infestations but they are not having any type of the infections caused due to head lice. *Acinetobacter* is an exception which is thought to not cause any type of the disease in the humans, because it has been detected in the head lice with great prevalence and it was also identified in the body lice [59].

It is unclear that these species of the *Acinetobacter* are the same as they cause infections in the humans. Currently, the vulnerability of the *Acinetobacter* species to antibiotics is unknown. A study conducted to check the multidrug resistance and phenotypic and genotypic features in the *Acinetobacter baumannii* species of the humans and also of those isolated from the body lice indicated that these are totally different bacteria genotypically and phenotypically [30]. On the basis of the combined proves from the laboratory and epidemiological studies, it is believed that under suitable conditions human lice are capable to transfer the diseases to their hosts which are humans but its capacity of being a vector is lower than the body lice.

There are a lot of the pathogens associated with the human head lice, which are causing different types of infectious diseases in the people of different regions of the world. The head louse infestation is caused and widely spread due to the hygiene problems, sharing of beds, hair brushes or combs and head to head contact of the children. Head lice infestation cause irritation and itching in the head of the affected person [31]. The lice infestation also depends upon the number of family members in a family because if family members are less in number then a proper attention can be paid on this issue but if the family members are in large number then attention cannot be paid to this issue. The risk factors of causing the head lice infestation include the unwashed hairs, unwashed body weekly, combine family system because the mother cannot pay attention towards the cleanliness of the children. It has been found that the head louse infestation is the most harmful thing for the human health because the person gets into depression because of the

itching. Hence, counseling of the people is needed for the head louse infestation so that they can take care of their life style conditions [32].

2.3 Evolutionary History of Human Lice

The body louse and head louse have almost similar biological features and morphology but their nutritional modes are different and their ecology is different [11]. For more than a century, the taxonomy of the head lice and body lice is under discussion, also they belong to the ecotypes of the same species [29], [11], [30]. The evolutionary relationships and the genetic basis of the head louse and body louse are unclear spite of the lots of studies. Till now, it is considered that the body lice and head lice have been descended from each other in the nature [11].

The body lice lay eggs and live on the clothes of the host so it was thought that when the humans started wearing clothes after that the body lice have been seemed to emerge [22], [31]. Although, the current data is not showing the same information. But lately, a new theory for the emergence of the body louse has been reported. According to this theory, it is said that because of the poor hygien conditions the head louse infestation is turning to the different multiple types of infestations of the phenotypic and genotypic variants of the head lice like pubic louse infestation or body louse infestation. And when it turns to body louse infestation, it then colonizes the clothes of the hosts and ingests a great quantity of the blood [32], [33].

The assumption is made on the basis of the phylogenetic and genotypic analysis by using the intergenic spacers of the nuclear genome which has showed that body and head louse are not indistinguishable [34]. Moreover, there are some scientists who have also said that if the head louse is raised under certain suitable conditions then head louse can emerge as the ecotypes of the body lice [35], [36]. Hence, it is clear that the divergence of the body louse and head louse is not the outcome of the single occasion, but this has happened continuously between the two lice clades i.e. clade A and clade D and this transformation can be supported by

the large amount of infestations [11]. When the transcriptomes of the body lice and head lice were compared with differential expression of the 14 genes, it was noticed that there is a gene missed in the head lice, which is present in the body lice which is responsible for coding a protein with the unknown function called the hypothetical protein containing 69 amino acids [37].

The gene was also present in head lice, according to the study, but the sequence of this gene was altered. Real-time PCR was used to confirm sequence variations. This was the first tool to show that body lice and head lice are separate ecotypes [38]. According to these studies, white lice and head lice clearly share the same genomic content, but differ in gene expression and have different phenotypes [37].

Studies have shown that variations in the transcript pools of head lice and white lice and their alternative splicing phenomena are observed from transcription data. These mutations have been identified in transcription studies of genes involved in ovarian follicle cell development, nutrition, and the nervous system of the body and head lice [30]. These findings indicate, for example, that genes involved in the development of eating habits play an important role in the development of an open tracheal system and the formation of salivary glands, making body lice less likely to spread around clothing. Which accommodates irregular eating habits to a more regular diet of head lice [40].

The variation in the Proteome of the body louse is due to the alternative splicing in their genomes [39]. There are some studies which have considered the relation of the alternative splicing with the variations in the phenotypes of the insects which live in groups or families and are social. Head lice were comparison with the body lice, it was revealed that there were some variations in the body louse observed in the phenotypes due to which they were thought to be separate community [37], [38].

The differences in the phenotypes has also been seen in some other insects for example, termites, honey bees and migratory locusts [41], [42], [43]. These all questions could be answered after the whole genome sequencing of the head louse and then thorough study of the epigenomics, proteomics and transcriptomics [44].

2.4 Lice are the Markers of Evolution of Humans

For thousands of years, lice have been evolved from their primate hosts and the lice of humans are very much hosts specific. As they have been found on the fossils of the humans, this is the evidence that they are considered to be the markers of the evolution of the humans and they have certain unique properties which shows the evolutionary history of the humans and also their migration from Africa [44], [45], [46].

Some happenings of the evolution of the humans have been confirmed from the analysis of the phylogeny of the *Pediculus*. For example, about six million years ago, the lice of the chimpanzees and the lice of the humans shared a common ancestor which showed that they have diverged from their respective hosts [47], [44]. About 100,000 years ago, when the humans migrated out of Africa, the human lice also migrated with them and they represent a vast population of the lice which have genetic variations in them. It is the source of studying and understanding the migration of the humans like their time of travel and their time of populating the new world [48].

According to the research, it is suggested that before the modern *Homo sapiens*, the ancient clades of the head lice are clade B and clade C originated [48]. Also it was found that when the Neanderthals used to populate the continent of Eurasia, the head lice of clade B diverged from the clade A about 0.7 to 1.2 million years ago, while the clade C of the head lice is very primitive and it is thought to have evolved from the *Homo erectus*. The ancient humans have direct contact with the modern humans, so the head louse is transmitted through head to head contact which is a physical contact of the hosts, in this way modern humans have attained diverse lineages of the head louse [49]. Lice have also helped us to understand the important events occurred in the evolution of the humans that were unclear in the DNA of the host's fossils. Some events include

- The estimation of the time from when the humans started wearing the clothes because the lice were living in the clothes of the humans [50], [51].

By calculating the molecular dating of the body lice, the use of the clothes by the humans has been estimated as 170,000 and 83,000 years ago in Africa [52], [53].

2.5 Life Cycle

Head lice completely depend upon the scalp of human's head for their survival and reproduction, and they remain attached to the human head and suck the blood as their meal for about 6-7 times a day. As a result, they inject a little amount of the saliva into the scalp of the human's head after that human becomes sensitive to the waste material of the lice and this leads to an allergic reaction and irritation in the head [52]. Their life cycle has three stages.

2.5.0.1 Egg

The adult fertile female used to lay eggs on the scalp of the head of humans and secretes special type of the proteins from its reproductive system through which the eggs remain attached to the human head and this protein acts like a glue. The eggs at this stage are called nits which are not visible to human eyes properly. At this stage, the size of the egg is about 0.8 mm and the color is whitish yellow which sometimes look like dandruff in hair. The nit sheath is hardened by the glue, this glue covers whole nit but not the cap like structure called operculum by which the embryo respire [52].

2.5.0.2 Nymph

A single nymph is hatched by a single egg. Pale yellow color of the nits become more visible at this stage. The size of the nymph is like the size of the pinhead and the nymph becomes mature after 3 instars and in 7-10 days it becomes adult lice. In the stage of 1st and 2nd instars the nymph is not able to move and the lice spread occurs in the 3rd instar because the lice can move from one place to the other in the 3rd instar [52]. This was the initial stage of life cycle of head lice.

2.5.0.3 Adult

The adult louse has 6 legs with claws and its color turns to grayish white but in the people having dark black hair the color of the head lice will be darker because of the characteristic of insects. Females are larger in size than males because it has to lay eggs, the size of male is smaller as compared to the female and male dies after the copulation. Head lice can move with the speed of 23cm/mm. Their reproductive mode is sexual reproduction [53].

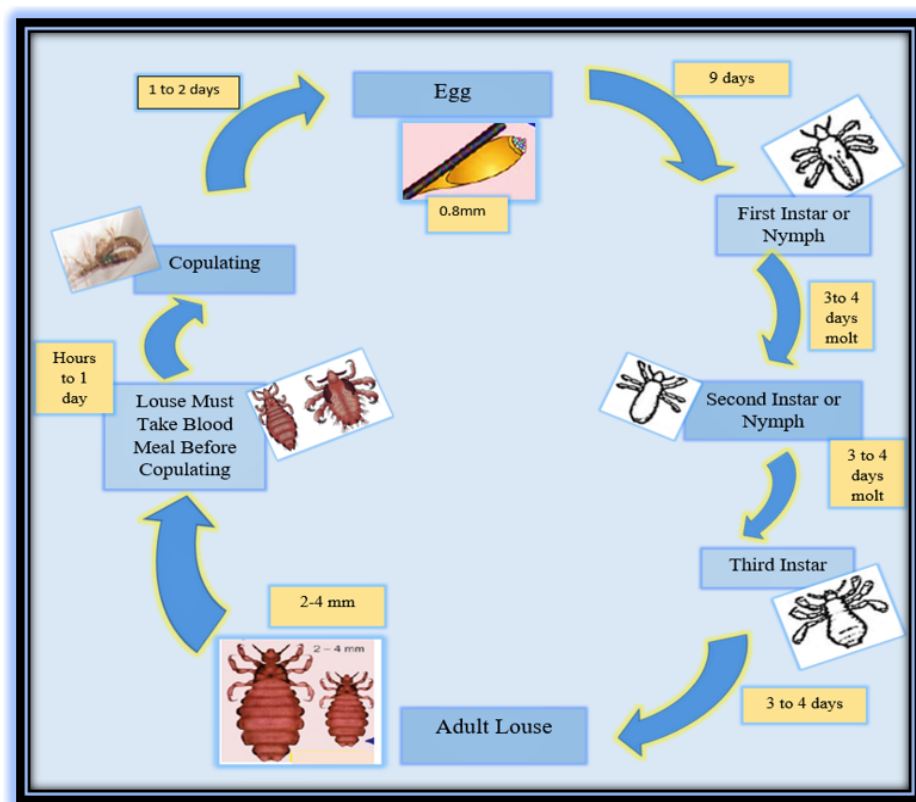


FIGURE 2.1: Life Cycle of the Head Lice [53].

2.6 Louse Nit Sheath Proteins

The female head lice secrete certain type of glue that is protein in nature that helps them to attach to the scalp of the human head [53], [54]. These proteins are secreted on the scalp of human and they form a nit sheath protein [55], [56]. These are the proteins which are helping the head lice eggs on the scalp of the

human head and protect eggs from environmental hazards. The composition of the nit sheath protein is chitin based. The sheath is composed of the four bands of the proteins and the beta sheets in their tertiary structures [57], [58], [59].

2.7 Treatment of Human Head Louse

There are many treatment options of the *Pediculosis* which includes mechanical methods like heating devices and combs, herbal formulations, chemical insecticides and the physically applied agents [60], [61]. Among these methods, the mostly used method for the treatment of the *pediculosis* is the chemical method in which different insecticides are used for the removal of the head lice [62]. These chemicals include the organophosphates (malathion as insecticide), organochloride (lindane as insecticide), extracts of the carbamates (carbaryl as insecticide) and the pyrethroids which are the synthetic derivatives of the pyrethrins (phenothrin, permethrin and the deltamethrin).

In 1971, the Malathion was introduced in the market and in the 1992, the permethrin was introduced in the market and they were mostly used to treat the *pediculosis*. Intensive use of these insecticides to remove the lice throughout the world has lead to an increase in the resistance of the head lice against these all chemicals [62].

While looking at the resistance of the head lice, the researchers were forced to develop some other strategies for their treatment which have different mode of action like they developed the spinosad and ivermectin and they were having high hopes for the treatment of the pediculosis. They have produced new neurotoxic modes of action which have low resistance for commonly used pediculicides and they were having low toxicity for mammals [63], [64]. The people are interested in using the natural products the *pediculicides* which are based on the essential oils derived from plants like tea tree oil and eucalyptus oil or some *pediculicides* which are based on the chemical agents like the benzyl alcohol and dimeticone but clinically a very less importance is given to chemical agents such as DDT [65].

2.8 Resistance in the Lice Against Insecticides

Resistance in insects (lice) is a time-honored attribute of the organisms which is tailored with the passage of the time with the selective stress of the normal use of the unsuitable pesticides [66]. The entire genome of the human's physique louse was once sequenced and has opened the new opportunity to obtain the new targeted, new, sustainable and tremendous remedy for the manipulate of the *pediculosis* [67]. Permethrin resistance was discovered to be the result of a polymorphism with in voltage-gated sodium channel -subunit gene. A better reproduction of the enzyme's carboxylesterase was further discovered to be mostly liable for Malathion resistance [68]. The ivermectin is the drug which is taken orally for the therapy of the *pediculosis* and it is very high-quality for each ecotypes of the lice however in the Senegal the resistance in opposition to the ivermectin has additionally been suggested [69]. It is regarded for the insecticide resistance web site in the nematodes and arthropods. From the different article it was observed that the three associated non-synonymous mutations had been discovered [70]. The foremost regulator of the launch of neurotransmitter is the neuronal protein referred to as the complexin. It was once determined that the complexin was once inhibited in the lice which have developed resistance. A untimely give up codon is taken by using the transcripts of the complexin of the lice which have developed the resistance and it used to be published from the evaluation of the DNA mutations. The relation of the ivermectin resistance and the complexin has been similarly demonstrated from the RNA interfering, which used to be seen by way of blocking off the expression of the complexin which leads to the resistance in the prone lice in opposition to the ivermectin. From all these studies, it has been concluded that the complexin is the protein in which mutation is accountable for the resistance in opposition to ivermectin in the physique lice [71].

Traditional *pediculicide* stress induced by enormous pesticide disintegration has resulted in the establishment and spreading of resistance in various regions of the world. Pesticide resistance can also result in healing failures, which can lead to persistent infestations requiring multiple treatments against head lice [72].

2.8.1 Pyrethroids as the *Pediculides*

Natural pyrethrum was given around 1945 (Table 2.1), it was eventually replaced with the aid of synthetic derivatives known as pyrethroids. Pyrethroids make up the majority of commercial pesticides used to control head lice. Pyrethroids are neurotoxins that cause spastic paralysis and louse death by keeping voltage-gated sodium channels open for excessively extended periods of time. Pyrethroids have a quick knockout effect that immobilises insects and typically precedes their fatal impact. The precise influence of resistance rates on quality checks is unknown at this time. Pyrethroid resistance appears to be widespread in various countries, but it fluctuates in depth and is now barely homogenous. A Panamanian investigation from 1983 discovered that this medicinal effectiveness was formerly good [73], [74].

Based on a randomised controlled research, medical and parasitological resistance to pyrethroids first was described in France (1994) [75]. By the seventh day of this trial, the medicinal effectiveness of d-phenothrin was really only 39 percent. This is most likely due to the area's head lice's are well resistance to pyrethroids. The clinical effectiveness of drugs tested on day 7 following software application such as docking varied from 10 percent [76] to 79.5 percent [76] in Europe, on the other side (Czech Republic [77], UK [78], Denmark [79]), Israel [80], the U.S [81], Argentina [82], Tokyo [83], and Australians [84] have show the less effectiveness. The cellular activity that affects pyrethroid resistance has been partially explained. Permethrin resistance of head lice were previously thought to be predominantly given by a recessive *kdr* [85].

Three-factor mutations in the α -subunit VGSC gene (M815I, T917I, and L920F) linked with the pyrethroid phenotype have been proposed to be essential for knock-down resistance [86]. Sequence analysis of replicated cDNA and genomic DNA from human samples indicated that all mutations were present as resistant haplotypes. Further tests involved the application of site-directed mutation at the relevant amino acid sequence. Using a *kdr*-type neural unresponsiveness mechanism, *Xenopus laevis* oocytes demonstrated that the T917I mutation was earlier the primary motif for pesticide resistance in head lice [87].

TABLE 2.1: Insecticide used for the treatment of head louse.

Insecticides Names	Name of Classes	Introducing Year	Reference
Pyrethrum in Natural	Pyrethrin	1945 year	[73]
Permethrin	Synthetic-Pyrethroid	1992 year	[74]
Phenothrin	Synthetic-Pyrethroid	1992 year	[75]
Malathion	Organo-phosphorus	1971 year	[76]
Carbaryl	Carbamate	1977 year	[77]
Lindane	Organo-chlorine	1940 year	[78]

2.8.2 Malathion as the *Pediculides*

Malathion is a neurotoxic organophosphate pesticide, when converted to its oxone form, binds to and inhibits the action of acetylcholinesterase, producing spastic paralysis and louse death [87].

Malathion is used in a 0.5% formulation that kills lice fast (within 20 minutes), but has been validated in partnership with the FDA and French fitness authorities to have an 8-hour duration of action. Malathion was taken off of the US market in 1990 (Prioderm; Purdue Frederick Company, Norwalk, Connecticut, USA) and 1994 (Ovide; Medicis Pharmaceutical Corporation, Lakewood, NJ, USA), owing to high costs and low sales. Due to reports of decreasing efficacy of other insecticides such as organochlorins and pyrethroids, Ovide was returned to the US market in 1999 [88].

During the same time period, malathion was progressively entering the European market. Malathion is only accessible through prescription in the U.S. Malathion appears to be substantially less toxic to head lice than pyrethroids. In the early 1990s, a randomised controlled experiment in France demonstrated that a 0.5 percent malathion lotions was much more ovicidal or pediculicidal than just a 0.3 percent d-phenothrin lotions [89]. In both gels and obiid lotions, a recent

big randomised, blinded research found that his 0.5 percent malathion was highly efficacious as 1% permethrin (Nix, Creme Rinse) [90].

Ovide shampoo contains 0.005g of malathion per millilitre of isopropyl alcohol (78%), terpineol, dipentene, and pines oil. Interestingly, using 0.5% miticide solution for 30min, 60min, or 90 minutes yielded effects comparable to ovide shampoo. Using pesticides in a shorter system instance can also help to reduce pesticide solubility and residual concentrations. This may eventually result in the appearance and rise of resistance. Malathion resistance was initially proven in France [91], subsequently in the U.K. [92], Australia [93], and Denmark [94]. Malathion previously had a poor effectiveness in a single-blind randomised study in the U.K., with treatment costs of just 17% (n=30) [95].

2.8.3 Lindane as the *Pediculides*

Lindane, also known as *c-hexachlorocyclohexane*, is an *organochlorine* insecticide that is not aromatic [96]. When the white louse developed a high resistance to DDT through kdr in the 1950s, the it was exposed to lindane, a pesticide that works on c-aminobutyric acid-gated ion channel rather than VGSC, and quickly lost his appetite. The head of an immunosuppressive medication evolved. Lindane was the most frequently prescribed *pediculicide* in the U. S. prior to the advent of pyrethroids [97] [98]. Lindane, which is only available by prescription as a 1 percent shampoo, is a neurotoxic chemical that stimulates the CNS and kills insects [99] [100]. It is, however, only somewhat ovicidal (today, 30-50% of eggs are not harmed) [101] [102]. For many years, global resistance has been proposed. In the 1980s, spa rates increased between 43% and 91% 14 days after his administration of 0.5% antilice lotion or 1% shampoos [103]. In Florida and Panama, lindane, malathion, pyrethrins, and permethrin are effective against treatment-resistant and treatment-sensitive lice, respectively. Only 61 percent were beneficial [104]. Linden, on the other hand, is still stunning in her 1999 Korea, and he has a 93% success rate in all other in vitro tests [105]. The undesirable effects of lindane cause reuse and overuse, increasing the likelihood of damaging events,

some of which are significant, such as severe seizures in children. Lindane is no longer suggested by Americans when applied to the entire body floor area [106] and because to its low effectiveness during activity [107]. Lindane usage is forbidden in California. Finally, its prescriptions range from usage with exaggerated cautions to total market withdrawal [108]. In 2007, the European Union banned the use of lindane as an insecticide.

2.8.4 Carbaryl as the *Pediculides*

Carbaryl is a carbamate pesticide that operates by reversibly blocking acetylcholinesterase, causing stiffness and death. It is utilised at a concentration of 0.5-1% in lotions or shampoos. In 1981 [109], its scientific validity was characterised as flawless, and in 1991 [110], it varied from 78% to 92%. *Lebwohl et al.* identified two of his medication risks (n = 18) in 1998 in Leeds, England, when using single carbaryl lotion [111].

Head lice were exposed to carbaryl doses ranging from 0.8 to 3.2 g/100 mL, and enzymatic studies verified alterations in the acetylcholinesterase reactivity in head lice to carbaryl in this range [112]. Carcinogenic concerns have required a prescription since 1995 [113].

Nonetheless, in 2008, a suggestion based completely on an update to Stafford's research recommended using the 1% cararil in waterbodies, which is no longer produced in the U.K. [114] to [118]. As carbaryl, lindane and pyrethroids was extensively used insecticide in the world.

2.9 Gap Analysis

The mutations are responsible for the insecticide resistance in head louse of Pakistan and their functional impact has not been studied. There is a need to study and identify the mutations responsible for insecticidal resistance in the head lice of Pakistani population.

2.10 Research Questions

1. What type of mutations are present in the insecticide resistance genes of human head lice of Pakistani Population?
2. What is the functional impact of these mutations and play major role in causing the resistance against the insecticides?

Chapter 3

Research Methodology

3.1 Methodology Flowchart

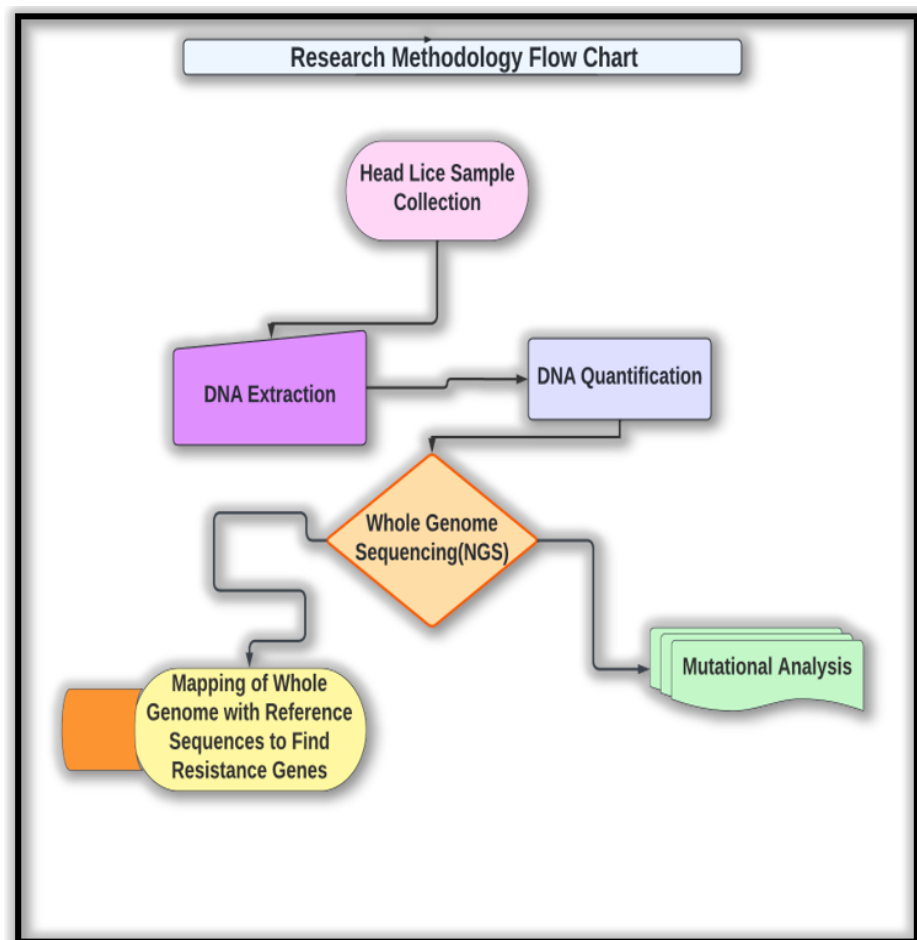


FIGURE 3.1: Methodology of the Research.

3.2 Materials and Chemicals

The materials and chemicals needed for the extraction of the DNA and quantification of the DNA were Gloves (Latex), Auto-clave (TOMY), Labelling tape (Biologs), 1.5 ml Micro-centrifuge tubes (Biologs), Micro-pipettes (Thermo Scientific), Micro-pipette tips tips (Biologs), Vertex Machine (China Mx-S), Thermal Block (Thermo Scientific), Mortar and Pestle (Biologs), Centrifuge Machine (Heraeus Sepatech), 500 ml Reagent Bottles (Biologs), 50 ml Folcan Tubes (Biologs), 0.2 ml PCR Tubes (Biologs), Weighing Balance (Sartorex), 500ml Beakers (Amber Glass), Gel Dock (Protein Simple), Gel Loading Tank (SCIE-PLAS), Gel Cassette (SCIE-PLAS), Combs (SCIE-PLAS), Ethidium Bromide (Thermo Scientific), Loading Dye (Blue Dye) (Thermo Scientific), Microwave Oven (Dawlance), Drying Oven (Touch Science), Freezer (Dawlance), Power Pack (ENDUROTM), Thermo Cycler (BIOER XP cycler), 70% Ethanol, Tris-HCl, Acetic Acid, NaCl, Triton-X, Ethylene Diamine Tetra Acetic Acid (EDTA), Phenol, Chloroform, Isoamyl Alcohol, Isopropanol, $MgCl_2$, Taq polymerase (Mol Bio), PCR Buffer (KCl or NH_4Cl) (Mol Bio), dNTPs (Mol Bio), Distilled Water, Agarose, Electric Comb (LICETEC), Nano drop plate (Thermo Scientific), MultiSkan Go Nanodrop Spectrophotometer, Lint free papers (Safetiss) and Lyophilizer (Labconko).

3.3 Preparation of Solutions

3.3.1 70% Ethanol

30 ml of the distilled water was mixed in the 70 ml of the absolute ethanol to prepare 100 ml of 70% ethanol.

3.3.2 TET Buffer

For the preparation of the 10 ml TET buffer solution, 1 ml of the 25 mM EDTA, 0.33 ml of the 50 mM Tris-HCL with pH 7.5, 0.4 ml of the 100 mM NaCl and 0.08

ml of the 0.4% Triton X-100 were mixed in the 8.19 ml of the distilled water.

3.3.3 TE Buffer

The 100 ml of TE buffer solution was prepared by mixing the 1.67 ml of the 50 mM Tris-HCL and 5 ml of the 25 mM EDTA were mixed in the 93.33 ml of the distilled water.

3.3.4 TAE Buffer

The 100 ml of TAE buffer was prepared by mixing the 11.4 ml of Acetic Acid, 3.7 ml of 25 mM EDTA and 48.4 ml of 50 mM Tris-HCL were mixed in the 63.5 ml of the distilled water.

3.4 Ethical Approval

The Ethical Committee of the Capital University of Science and Technology Islamabad Pakistan authorized the study overview. The participants from whom the head lice were collected were informed about this research work and the informed consents were signed by the guardians or parents of the children.

3.5 Sample Collection

Approximately 300 *Pediculus humanus capitis* (head lice) samples were collected from the people suffering from head lice *pediculosis* were also known as infestation from the diverse regions of Pakistan such as Azad Jammu and Kashmir (AJK), Punjab, Parachinar (KPK), Karachi, Gilgit Baltistan, Thar and Cholistan Desert by using physical method and mechanical method as electric combs which are used for the removal of head lice from the head and this electric comb also removes the eggs of the head lice from the head [119].

3.6 Preservation of Head Lice

After collecting *Pediculus humanus capiti* samples, they were kept in 70% ethanol and stored in a freezer at -20 °C [119].

3.7 Extraction of DNA from *Pediculus humanus capiti*

The phenol-chloroform technique of DNA extraction was used to extract DNA from the archival samples [120] [121]. A pestle and mortar was used to grind the head lice. Then re-suspended the powder in 400 μ L of Tris-EDTA-Triton-x (TET) buffer in a 1.5 mL micro-centrifuge tube. The pH of the TET buffer was kept constant at 50 mM Tris-HCl. After 20 minutes, 30 μ L (20 mg/ml) proteinase-K and 50 μ L (20 mg/ml) sodium dodecyl sulphate (SDS) were added to the tubes on a heat block at 65 °C. Transfer to a centrifuge tubes and incubated at 65°C overnight. The next day, 600 μ L of phenol, chloroform, isoamyl alcohol (25:24:1) solution was transferred to the tube and centrifuged for 10 minutes at 14000 rpm [122], [123].

The supernatant was transferred to a newly labelled microcentrifuge tube, 500 μ L of chloroform, isoamyl alcohol (24:1) was added to the supernatant, and the supernatant was recentrifuged at 14,000 rpm for 10 minutes. The supernatant was collected once again, transferred to a newly labelled microcentrifuge tube, 300 μ L of cold isopropanol was added, and the tube was kept in a -20°C freezer for 4 hours. The refrigerated tubes were then centrifuged for 10 minutes at 14,000 rpm. The supernatant was collected, and the pellet was rinsed with 70% ethanol before being centrifuged at 7500 rpm for 5 minutes.

The supernatant was collected once again, and the particle was washed for 5 minutes in 300 μ L of 70% ethanol at 7500 rpm. The particle was air dried after the supernatant was carefully removed [124]. The DNA pellet was kept in 150 μ L of TE buffer (10 mM Tris pH 8.0 and 1 mM EDTA).

3.8 Agarose Gel Electrophoresis

After the extraction of DNA, for the confirmation of the DNA 1% Agarose Gel was prepared by dissolving 1g of the agarose in 100ml of Tris Acetic Acid EDTA (1X TAE) buffer and was boiled in the microwave oven to melt the agarose and after melting 8 micro-liter (μ l) of the Ethidium Bromide was mixed with the gel and then the gel was put in the cassette for cooling down.

After that the DNA was loaded in the vials of the gel by mixing 7 micro-liter (μ l) of DNA with 3 micro liter (μ l) of loading dye. Then the DNA was allowed to run in the gel tank which contained the 1X TAE buffer at 70 volts and 1 hour. The gel picture was visualized on the Gel Dock Machine [125].

3.9 Quantification of DNA

The quantity of the DNA was checked by using the Multiskan GO Nanodrop plate spectrophotometer. The purpose of the quantification of DNA was to check that whether the quantity of the DNA was sufficient for the Next Generation Sequencing or not. The spectrophotometer works on the principle of the measurement of the UV light absorbance by the DNA sample present in a particular liquid media. The DNA samples absorbs the maximum UV light at 260 nm, the proteins absorb maximum UV light at 280 nm and other salts and organic molecules absorb the maximum UV light at 230 nm.

The ratio of the 260/280 is taken for finding the quantity of the DNA. The samples which have the value of ratio of 260/280 equals to 1.8 are said to be the best quantity of the DNA for the Next Generation Sequencing. The samples were loaded on the Nanodrop plate and the plate was inserted in the Multiskan GO Nanodrop plate spectrophotometer (Thermo Scientific) and the samples were quantified by using the Skaned software on the PC. The sample having the 260/280 ratio equals to 1.8 was noted and was further processed for the Next Generation Sequencing [126]. The NGS (Illumina) made it easy for the scientist in analysis.

3.10 Lyophilization of DNA

The lyophilization of the DNA was done by the Lyophilizer machine (China Biobase). The purpose of the lyophilizing the DNA was to protect the DNA from any harm during the shipment time because the lyophilizer converts the DNA sample into powder form. After that the DNA samples were properly labelled and were shipped for the Next Generation Sequencing (Whole Genome Sequencing). The samples were sent to Genewiz Sequencing Company China from the Alpha Genomics Lab. Genewiz Sequencing Company uses the Illumina platform of NGS [127].

3.11 Whole Genome(WG) Sequencing Data Assembly

The FASTQC report of the whole genome of the head lice was generated and was sent us by the Genewiz through email in as mentioned in Appendix (5.1,5.2, 5.3, 5.4,5.5, 5.6, 5.7, 5.8, 5.9, 5.10). After that the results were received as a huge raw data through email, that data was assembled in the proper form by using different Bioinformatics tools like Velvet Assembler and Genius Prime (version 2022.0.2) [128]. These tools trimmed the extra contigs from the raw data and provided the De Novo assembly in a proper trimmed form of our whole genome sequencing of the head lice. There were a large number of contigs because the data was in the raw form and after that with the help of using the Bioinformatics tools i.e. Velvet Assembler and Genius Prime (version 2022.0.2), the raw data was converted into a usable form. The number of contigs used for the annotation were reduced to almost 7933 and the genome was then annotated [129].

Velvet assembler software is a very useful tool which is used for assembling the data of the Next Generation Sequencing and for getting the De novo assembly. In 2008, the Velvet software was developed by Ewan Birney and Daniel Zerbino in the European Institute of Bioinformatics. It is the package of algorithms which was

designed for dealing with the alignment of the short reads and the de novo assembly of the genomes sequenced by the Next Generation Sequencing. This software uses the de Bruijn graphs for the assembly of the sequences of the genomes through the simplification of the regions which are repeated and by removing the errors in the sequences. This software is very frequently used by the researchers to get the de novo assemblies of the data of Next Generation Sequencing. Velvet software can be downloaded by using the link (<https://velvet-for-windows.soft112.com>).

Genious Prime (version 2022.0.2) is a platform which contains all the necessary tools for the researchers for the analysis of the molecular biology data of the Next Generation Sequencing. It helps in the transformation of the raw data into the visualizations which help the researchers to analyze the sequencing data very easily and it is user friendly as well. Genious Prime increases the insights and visibility of the sequence, decreases the risks and errors and increases the productivity of the sequencing [130].

3.12 Genome Annotation

The structural and functional annotation of the human head lice was done by using different computational tools like Genious Prime (version 2020.0.2) and BLAST. BLAST stands for Basic Local Alignment Search Tool, which is used by researchers for different purposes like annotation of the genomes, mapping of the DNA, finding of new species and finding the phylogenetic relationships among the different organisms.

It is actively used by the researchers in the initial step of their research because when the data is obtained from research, the researchers use the BLAST for alignment and searching their data that in which direction their research is going on. It takes the sequence data in the FASTA format, then the sequence is processed by identifying the homologous sequences by finding the matches in the short fragments of the sequences after that the local alignment is done and the homologous sequences are displayed on the screen [131]. The functional annotation of the genes

was done by using the UniProt Consortium. UniProt, short for Universal Protein Resource, is a strong, comprehensive, and publicly available protein sequence repository that also provides data on protein function. The key actions done by UniProt include sequence archiving, collecting of information relating to a protein supplied by other websites, and manual correction of protein sequences backed by bioinformatics research [132]. After every three weeks the UniProt is updated and it is freely useable and downloadable by the researchers at (www.uniprot.org). The functional annotation of the genome made us able to find out the functions of the genes. By the help of functional annotation, the genes which are responsible for developing resistance in the head lice against insecticides were found. These genes were also confirmed from the literature because they are causing resistance in the body lice [132].

3.13 Sequence Analysis

The sequence analysis was performed to identify the resistance genes in the WG (whole genome) sequence of *Pediculus humanus capitis*. For this purpose, the contigs of the genome were mapped with the reference sequences and translated.

3.13.1 Mapping of the Contigs with the Reference Sequence

The contigs of the whole genome of head louse were mapped with the reference sequences available on the NCBI. This step was performed to find out the reference sequences for the resistance genes in the head lice genome. The mapping of the contigs was done with the help of Genious Prime tool [134].

3.13.2 Translation of the Mapped Contigs

When the reference sequences were found for the head lice's genome contigs and it was noticed that they were the contigs of the resistance genes in the head lice

genome, then those contigs were translated into amino acid sequences to predict the structures of proteins. The mapped contigs were translated into amino acids with the help of Genious Prime tool [135].

3.14 Mutational Analysis

3.14.1 Prediction of Mutations

The mutations in the resistance genes were firstly found from the literature. Keeping in view those mutations, novel mutations were predicted in the contigs of resistance genes of the human head louse genome. The mutations were found by the help of BLAST-X (NCBI) in the form of the FASTA format. BLASTX operates at a slower rate because it must match all six reading frames to protein databases. The end result is a match between the open reading frame and its homolog sequence [136].

BLASTX is a strong tool for gene discovery and prediction. Protein-coding genes in cdna should be identified using this method. It also has the potential to determine proteins encoded by transcriptome or transcript variations and to assess whether a novel genetic material is a protein-coding gene. Identify the open reading frame and gene name based on the codon (CDS) [136].

(www.blastx.ncbi.nlm.nih.gov/Blast.cgi)

3.14.2 Verification of Mutations

The mutations predicted in the resistance genes of the head louse genome were then verified by using the Provean and SIFT tools. The PROVEAN (Protein Variation Effect Analyzer) (www.jcvi.org/seq_submit.php) programme predicts if amino acid changes or indels alter protein biological activity. PROVEAN aids in the filtering of sequence variations in order to discover non-synonymous or indel polymorphisms that are likely to be functionally significant [136]. PROVEAN's efficiency

is equivalent to those of well-known tools like SIFT (sift.bii.a-star.edu.sg/www/SIFT_seq_submit2.html) and PolyPhen-2 (www.genetics.bwh.harvard.edu/pph2/). A quick computational strategy to obtaining sequence similarity homology total score resulted in the production of pre-computed PROVEAN estimates of 20 single amino acid changes and single amino acid removals at every amino acid location of all both mouse and human protein sequences. It is now feasible. SIFT predicts if amino acid changes impact protein function based on amino acid sequence homology and physical characteristics. SIFT may be used to detect natural compounds non-synonymous polymorphisms as well as laboratory-induced missense mutations [137].

3.15 Prediction of the Structures of Mutated Proteins

The 2D and 3D structures of the mutated proteins were predicted.

3.15.1 Prediction of the 2D Structure of Mutated Proteins

The 2D structures of the mutated proteins of the resistance genes were predicted with the help of the NPS @ SOPMA (npsa-prabi.ibcp.fr/cgi-bin/npsa_automat.pl?page=/NPSA/npsa_sopma.html) and PSI-PRED (bioinformatics.ucl.ac.uk/psipred/).

Users can submit protein sequences to the PSIPRED secondary structure prediction server, execute predictions in FASTA format, and get prediction results in text through email and dynamically on the web. To attach to the array, the user can select one of her 3 prediction techniques. PSIPRED is regarded as the most accurate tool for structure prediction. MEMSAT 2 (<http://www.sacs.ucsf.edu/cgi-bin/memsat.py>) is an updated version of a popular approach for predicting membranes topology. Or GenTHREADER (<https://swmath.org/software/35746>), a sequence profile-based fold identification approach [138].

3.15.2 Prediction of the 3D Structure of Mutated Proteins

The SWISS model (www.swissmodel.expasy.org/), trRosetta (ww.yanglab.nankai.edu.cn/trRosetta/), and I-Tasser (zhanggroup.org/I-TASSER/tools) were used to determine the 3D structure of the resistance gene's mutant protein.

SWISS-MODEL is a service for completely automated protein molecular structure determination that may be accessed via the Expasy web server or the DeepView software (Swiss Pdb viewer). The goal of this site is to make protein modelling available across life science researchers all over the globe. The resource models all 13 nucleotide sequences on a weekly basis using the most recent UniProtKB proteome [139].

3.16 Validation of the Mutations through Molecular Docking

The molecular docking of the mutated protein structures with the ligands of Pyrethroids, Malathion and carbaryl was performed to validate the mutations in the resistance genes. This was done to check the binding of the insecticides like pyrethroids and Malathion with the mutated genes of the head louse [140], [141]. It was done by the help of Bio Discovery Studio and PyRx is considered the computational drug discovery programme that may be used to test libraries of chemicals against putative therapeutic targets [142].

PyRx (<https://pyrx.io/>) allows medicinal chemists to conduct virtual screens from any platform and guides users through every stage of the procedure, from data preparation to order submission to results analysis [143]. While there are no magic buttons in the drug discovery process, PyRx features a docking wizard with an intuitive interface, making it a useful tool for computational drug design.

PyRx also has chemical spreadsheet capabilities and a sophisticated visualisation engine, both of which are required for rational drug design [144].

3.17 Retrieval and Preparation of Ligands (*Pediculides*) Structure

The 3D structures of the pediculides such as Malathion, pyrethroids, lindane and carbaryl were download from PDB (www.rcsb.org/) in the PDB format. The structures of these molecules were stabilized in the Bio-Discovery studio tool and using this tool the hydrogen atoms, water molecules and HETAM molecules were removed. The HETAM molecules are the previously docked ligands. After removing above mentioned atoms the missing hydrogen were added and energy of minimalization was performed [145], [146].

3.18 Steps Involved in the Mutational Analysis

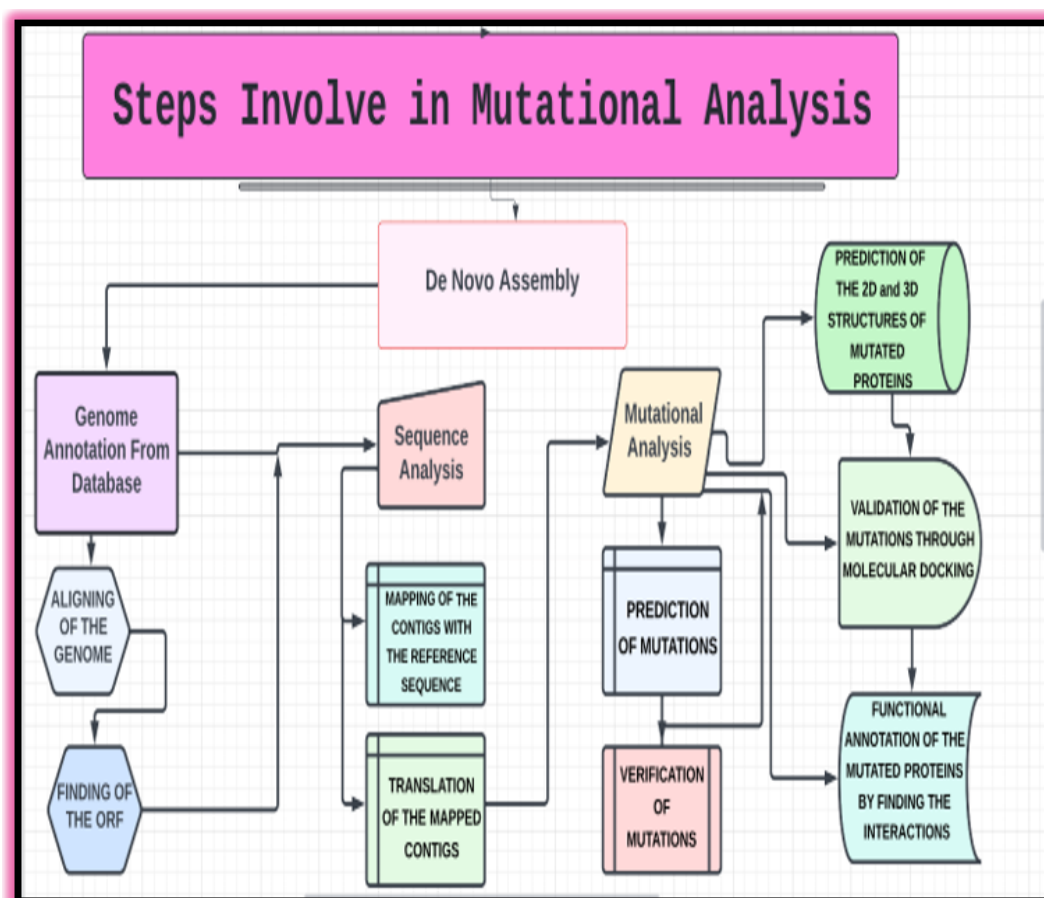


FIGURE 3.2: Steps involved in Mutational Analysis in Knockdown Resistance Genes (KDR) of Human Head Lice.

3.19 Functional Annotation of the Mutated Proteins

The functional annotation of the mutated proteins was done to find out the functions of the mutated proteins. Their interactions were found by using the STRING and Cytoscape tools. By the help of functional annotation, the role of these mutations were predicted in causing the resistance in the head lice against the insecticides [147].

Chapter 4

Results and Discussions

4.1 Results of DNA Extraction

The phenol-chloroform extraction technique was used to obtain DNA. The extraction of DNA was validated by agarose gel electrophoresis. This procedure was conducted after the DNA extraction to ensure the purity of the DNA and the success of the retrieved DNA from the head lice samples (Figure 4.1). The working principle of agarose gel electrophoresis is that an electric field is applied for the movement of the charged molecules in the matrix of the agarose and on the basis of the size, the biomolecules are separated.

The use of the agarose gel electrophoresis for the separation of the DNA has brought a revolution in the extraction of the DNA because firstly the DNA was confirmed by using the high density centrifugation and other physical or chemical methods in which there were chances of degradation of the DNA [146], [147]. The bands of the DNA can be seen in the (Figure 4.1).

Through the agarose gel electrophoresis, the DNA of the size from 100bp to 25kb can be separated. It can be seen that there are eight different vials on the gel labelled as ladder, negative control. The bands produced were interpreted according to their size, intensity and presence.

The following band in the (Figure 4.1) explained as:-

- In the vial labelled as ladder, the ladder of the molecular weight of 2 kb is present which is used as the standard for the rest of the DNA samples.
- The vial labelled as negative control contained the negative control sample which means that it is not passed through any type of the treatment.
- The vial labelled as 1, 2, 3, 4, 5 and 6 contained the DNA samples of the head lice of the Parachinar, Rawalpindi, Kashmir, Cholistan, Gilgit Baltistan and Thar regions of the Pakistan, respectively.
- The bands of DNA samples of the human head lice observed on the gel were between 600 base pairs and 800 base pairs. The molecular weight of the DNA of head lice observed was almost 700 base pairs.



FIGURE 4.1: Agarose Gel Electrophoresis of the DNA recovered. Lane 1 represents the 2kb ladder, lane 2 represents the negative control sample, lane 3, 4, 5, 6, 7 and 8 represents the human head lice samples.

4.2 Whole Genome Sequencing(WGS)

The Whole Genome Sequencing of the human head lice was performed using the Sequencing by Synthesis approach (Illumina) of the Next Generation Sequencing, firstly the FastQC report was generated by the Genewiz Company which indicated the accuracy of the sample. The FastQC report provided the important information about the sequence which includes the basic statistics of sequences, depended on GC, levels of duplication of sequence, distribution of the length of sequence and the sequences which are overrepresented.

4.3 Raw Reads/ Contigs of the Whole Genome Sequencing

The results of the sequence of the whole genome were received in the form of raw reads/contigs (Figure 4.2) and they are available in the link given below. <https://drive.google.com/drive/folders/165qrZuByCod0PV1pmH7rbQ-JN5eU4R3h>.

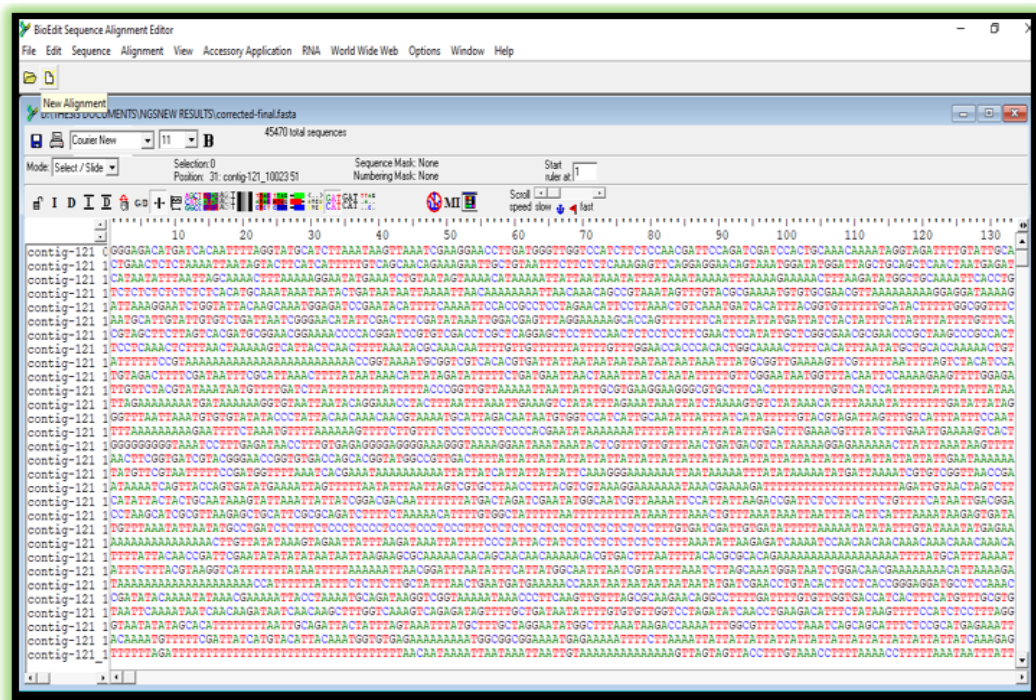


FIGURE 4.2: Results of Whole Genome Sequencing in the form of Raw Reads/Contigs.

Raw reads were basically the results of the Next Generation Sequencing which were significant for the analysis of the sequence data. The raw reads are called so because they contain the contaminations and the sequence of the primer as well. There were 45470 total sequences and 1002351 contigs in the raw form. These raw reads cannot be analyzed until they were converted to a proper format. By using different Bioinformatics tools like Velvet assembler and Genious Prime, the data was converted to a standard format.

4.4 Assembly of the Raw Reads/Contigs

The genome of the human head lice was sequenced with the average coverage of 1014.028. The scaffolds and contigs were assembled and their average size was 124 Mb and 118 Mb respectively. This showed that the size of the genome of the human head louse was very small as compared to the other insects whose genomes have been sequenced till now. The raw reads/contigs were assembled by using the Velvet assembler tool (Figure 4.3). This tool is a package of algorithms which is designed for the de novo assemblies of the genomes and for the alignments of the short read sequencing <https://www.ebi.ac.uk/~zerbino/velvet/>.

```

contigs - Notepad
File Edit Format View Help
>NODE_1_length_141_cov_17.219858
CTTTCTGTCGTATTCTCTCCTTCATAAGAGCCCTTTTACTACCAATAATTTTCATAGCTA
GCTTATTATCCGTGGGTTGGAAGAGTGCCTGTAGCTGGTTTTTGAGGAAGCTTTGTTTAC
CGGAATCCACGGCACCGATAGGTGTCGGACCCGGTTCCTCTTTAGGCGTACCATATAAAC
TAACATCGTCACCTCCGAAATGCACCTTTCC
>NODE_2_length_286_cov_4.548951
CTGAAAGCCCTTTGATTTCTTTTTTTTCCCGGGGGGGAGGGGAGGGAAGGGGAAGGAGTGG
AAGGAGGAGGGAAAAGGGGGAGGAAATATCTAGGTGACCAACAACAGGATATTTATTCA
TTGATTCAAAAAATTTTAAATAAAATCTTGCCATTTTTTTTAAAAATCGAATCGATTAAC
ACATATTTTCGCGGAAACGCCATTTTTTTTTTTTTTTGTTTTTTTTTGGTGAACAATACA
TTCCGGCTTTATACGGATAAGATAATAATAATAATAATAATGATGATAATAAATGATAC
ATTTGCCACCATGTAAAAAGTAAAAAATAGAAAAAGGAAAAAACCTCAAGTAGTCA
>NODE_20_length_271_cov_9.269373
TATTTTTTTTAAATACATATCAATGAATGATGTTTTGTAATGCTTTTTTATTATACAAAA
ATTAATATTTGTAATATAAATGACTATTTAAGAAAAATGAAATTATACTTGATAATTATT
TATTTAATAATCCTTTGATATTATATACATAAAATAATTAATTTATTTTAAAGCCTTAAAT
GTAATATGCTAAATATTTATATAAACATAAAATCAATAATGAAAAAATGAATAAAAAT
ATATTGCTTTTACAAAAATTTACAAAAAGTAAAAAATATTCTAAAAAATAAATCGGCAAAA
TATTATACTGTGTAACATTTCTTTAAATTTTATACAAAAA
>NODE_21_length_457_cov_6.962801
CTTTTTTATTATAATTTACTCCTTTTTTCAAAACGAAATTTTGTTTAACAACAATTTCA
ATTTTTTTTTGTTTAAACATAAAAAACGAGGAGGAAAAAAAAAAAAAATTAAGTTGCGCACTT
TAAAAATTTTTTTCTTTAATTTAAAAAATAAATTTATTTCTTATTACGGTACTGAAATCT
ACTTACGATCGTTTAAATGGATGGTTTTCCCTTTTAAATAAATCAACGGGGGGAATGGGAAG
AGGGGAGGGTGGGAGGAAGAGTAGGAGGAGAGAATACGAGAAAAACCGTTAATTTATCATCG
TATTGTTATTTATCATTTCATCGTTTCGAATTTAAAAATCGATTTTTCTTTTTTAAAAAATAAAA
CCTTATTAATTAATTTATTTAAACAATTTTCATTTGTTTAAACAATAAAAAAACGTTTCGA
ATTTACTCGATTTAATAATAATAATAAATTTAAAAAGCGATCGATAGAATTCAAACGAACGC
AATTCATCGTCTCTTATAAATTTATTCGTCAAATTTATTTTCAACCC
>NODE_27_length_154_cov_16.162338
AAAAAATAATCGTATTTAATATTAGGATTGAATTAATAAACATTTCAATAGGGTGACCCA
CATCGTTTAAATTTATTATTATTCATTATTATTAATAAAATGTATTATGCGTGCCTGTG
CGTGTGCGTGCCTGCTTTTCATTTTAAATAAATTTAATAAATCGGTTGGTAATACTGCGTT
ATATAAAAAAGCAAAAAATGGTTCTGACTGTTTAAACACGCCCTTTA
>NODE_28_length_72_cov_3.736111
TAATAATCGGTTGGTAATACTGCGTTATATAAAAAAGCAAAAAATGGTTCTGACTGTTAAC

```

FIGURE 4.3: Assembly of the Raw Reads of the Whole Genome Sequencing by Velvet Assembler Software.

This tool removed all the errors and the repeated sequences from the genome and provided the purified genome assembly. By using this tool, total 45,470 reads were obtained.

4.5 Genome Annotation

The genome of the human head lice was annotated once its contigs were assembled. Genome annotation consisted of the two major steps. First was the structural annotation and second was the functional annotation. For this purpose, the following steps were performed.

4.5.1 De Novo Assembly

The Genious Prime (version 2022.0.2) tool was used for the De 'Novo assembly. The purpose of using this tool was to clean the data of the sequencing because by the help of the Velvet assembler tool, there were total 45,470 reads obtained. But for the annotation of the genome these reads needed to be more purified. So, by using the Genious Prime tool, these reads were purified and a total of 18,607 out of the 45,470 reads were analyzed to generate 7,933 contigs. The de 'novo assembly was obtained because there was no reference sequence for the whole genome of the head lice. The significance of De 'Novo assembly was that this assembly was used for the annotation of the genome which contained the purified sequences and from this assembly complete information regarding the genome were obtained. The contigs were stored on the notepad (Figure 4.4). The assembly report given by the Genious Prime tool is mentioned in the (Figure in Appendix (Figure 5.11)). The assembly report provided with all the information about the sequence of the genome which was cleaned i.e. the number of unused reads were 26,863, minimum length of the base pairs was 2,228 bp, maximum length of the base pairs was 111,223 bp, N50 length was 7,416, total sum of the length of base pairs was 54,222,862 and the number of contigs greater than or equal to N50 were 2460. This information was very important when the submission have done in NCBI.

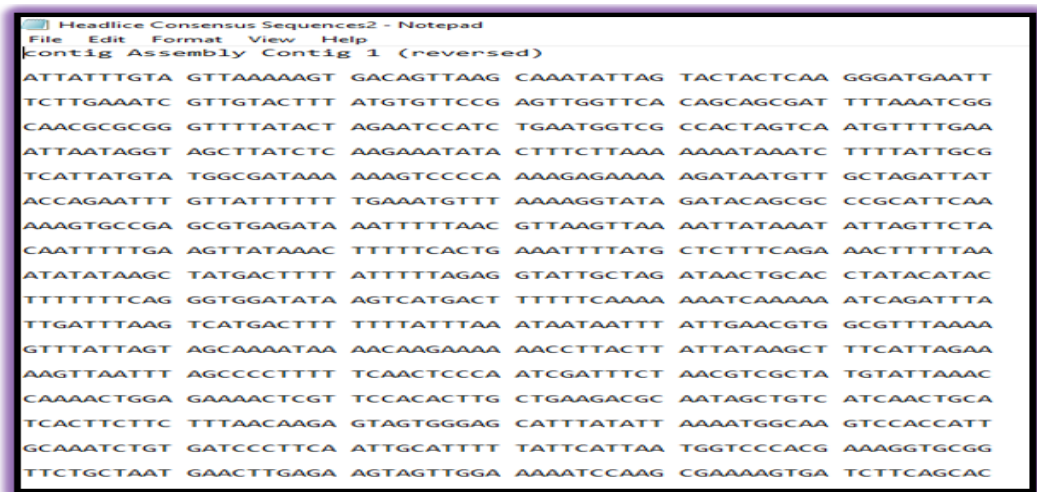


FIGURE 4.4: De Novo Assembly of the 7,933 contigs.

4.5.2 Genes and Open Reading Frames (ORFs)

In the genome of the head lice there are total 988,226 open reading frames (Figure 4.5). The length of one of the ORF as shown in figure is 138, its name is ORF 248 frame 1 with intervals of 7862 to 7725, its sequence is also given, its genetic code is standard and all the information regarding this ORF are shown in the (Figure 4.5). And the total no. of genes found in whole genome(WG) of human head louse(*Pediculus humanus capitis*) were 9942.



FIGURE 4.5: The Open Reading Frame of a contig of the genome of head lice.

All of the ORFs of the human head louse genome are given in the table available drive.google.com/drive/folders/165qrZuByCod0PV1pmH7rbQ-JN5eU4R3h.

Open reading frames are the regions or sequences of the DNA between the start codon and the stop codon. The gene which encodes for the proteins consists of the open reading frames. For the gene prediction, it is the major step to find the open reading frames in the genome because the ORFs are used to identify regions in the DNA which are responsible for the coding of the functional RNA and also the regions responsible for encoding the proteins in the genome.

4.6 Mapping Of The Contigs With The Reference Sequence

The de novo assembly was mapped with the reference sequences which were available on the NCBI, i.e., MW057882, KX301993 and KX302005. There were nine sequences of the de novo assembly of human head louse which showed resemblance with these three reference sequences and these sequences have been reported in the NCBI as Knockdown Resistance Genes (KDR). The sequences of the de novo assembly which showed the resemblance with the KDR were renamed as sequence 1, 2, 3, 4, 5, 6, 7, 8 and 9 [134].

4.6.1 Resemblance Shown by Sequence 1, 2 and 3 with MW057882

The sequence of nucleotides having Accession ID MW057882 reported in NCBI have shown resemblance with the sequence 1, 2 and 3 of human head louse. In the (Figure 4.6).

The green bar showed the *kdr* gene, yellow bar showed the CDS which is coding region, blue bar showed source of mapped *kdr* genes which was *Pediculus humanus humanus* and the red bar showed the mRNA. The figure (4.6) showed the voltage

sensitive sodium channels which are important factors of the resistance in the head louse. The interval of the sequence was from 24000 to 38000.

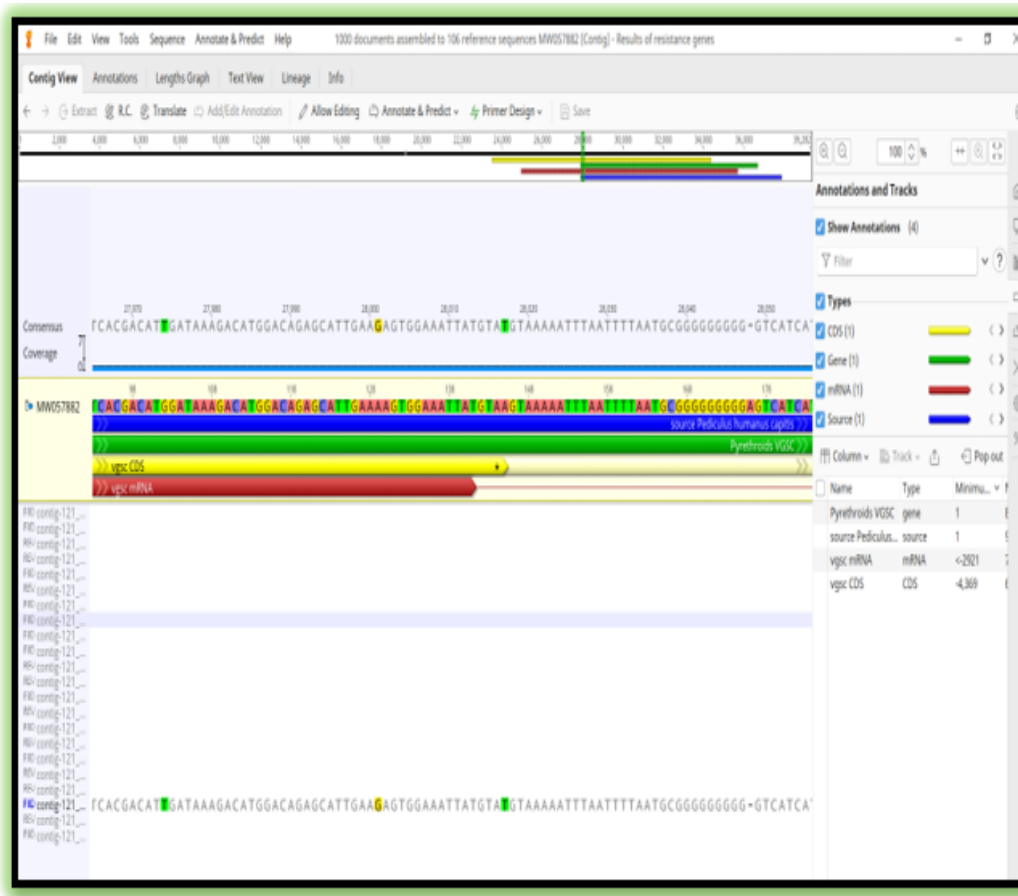


FIGURE 4.6: Resemblance shown by sequence 1, 2 and 3 with MW057882.

4.6.2 Resemblance Shown by Sequence 4, 5 and 6 with KX301993

The sequence of nucleotides having Accession ID KX301993 reported in NCBI have shown resemblance with the sequence 4, sequence 5 and sequence 6 of human head louse. In the figure (4.7). The green bar showed the *kdr* gene, yellow bar showed the CDS which is coding region, orange bar showed ORF, blue bar showed source of mapped *kdr* genes which was *Pediculus humanus humanus* and the red bar showed the mRNA. The interval of the sequence was from 13000 to 26000. The figure (4.7) showed the voltage sensitive sodium channels which are important factors of the resistance in the head louse.

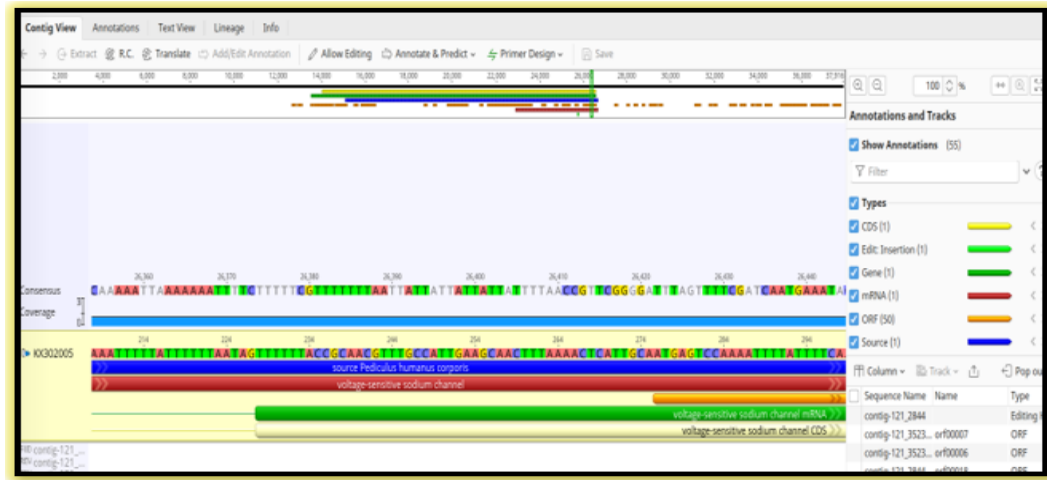


FIGURE 4.7: Resemblance shown by sequence 4, 5 and 6 with KX301993.

4.6.3 Resemblance Shown by Sequence 7, 8 and 9 with KX302005

The sequence of nucleotides having Accession ID KX302005 reported in NCBI have shown resemblance with the sequence 7, 8 and 9 of human head louse. In the figure (4.8). The green bar showed the *kdr* gene, yellow bar showed the CDS which is coding region, orange bar showed ORF, blue bar showed source of mapped *kdr* gene which was *Pediculus humanus humanus*, the peach color showed the miscellaneous features such as poly-beta-1,6-N-acetyl-D-glutamine and multidrug effect, and the pink bar showed the tRNA. The interval of the sequence was from 1 to 50071.



FIGURE 4.8: Resemblance shown by sequence 4, 5 and 6 with KX301993.

4.7 Translation of the Mapped Sequences

The sequences which showed the resemblance with the *kdr* genes were translated into the amino acid sequences to predict their protein structures. The purpose of translating the sequences into amino acid sequences was to find the novel mutations in the sequences due to which the resistance was occurring in the head louse against insecticides. In the figure (4.9) the blue bar showed the source of the mapped genes which *Pediculus humanus humanus*, yellow bar showed the CDS which is coding regions and the red bar showed the mRNA [135].



FIGURE 4.9: Translation of the mapped sequences.

4.8 Mutational Analysis

Mutational analysis was done for the prediction of the mutations other than reported in the DNA sequences. The mutational analysis was done to find out the novel mutations for resistance in the knockdown resistance gene (*kdr*) sequences that were obtained by mapping the head louse's de novo assembly with the reference sequence on NCBI.

4.8.1 Prediction of Mutations in the Mapped Sequences by Blast X

4.8.1.1 Prediction of Mutation in the Sequence 1, 2 and 3

The novel mutation was predicted in the sequence 1, 2 and 3 by using the BLAST X tool. The mutation occurred at the 34 sites where the M was replaced by I at the 34th position. M stands for methionine and I stands for Isoleucine shown in the figure (4.10). The reported mutations in the head louse of Thailand were T917I and L920F which were point mutations [133].

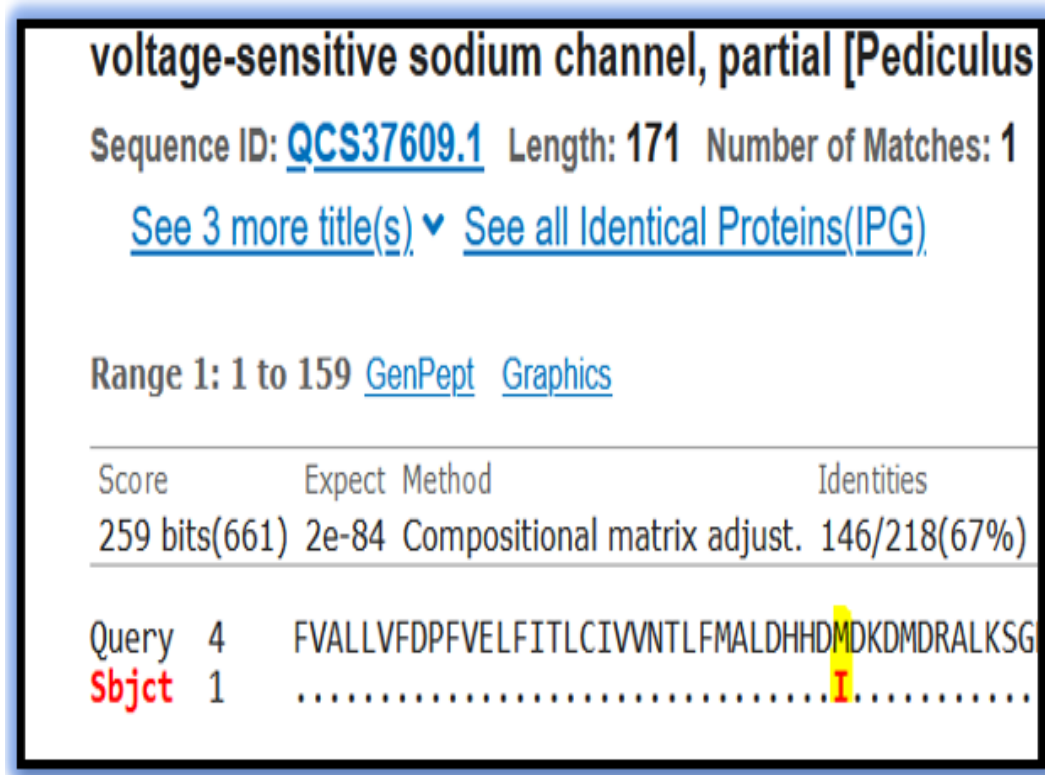


FIGURE 4.10: Predicted Mutation in the Sequence 1, Sequence 2 and Sequence 3.

4.8.1.2 Prediction of Mutation in the Sequence 4, 5 and 6

The novel mutation was predicted in the sequence 4, 5 and 6 by using the BLAST X tool. The mutation occurred at the 34 site where the 'I' was replaced by 'F' at the 34th position. I stands for Isoleucine and F stands for Phenylalanine shown

in the figure (4.11). The reported mutations in the head louse of Thailand were T917I and L920F which were point mutation [133], [136].

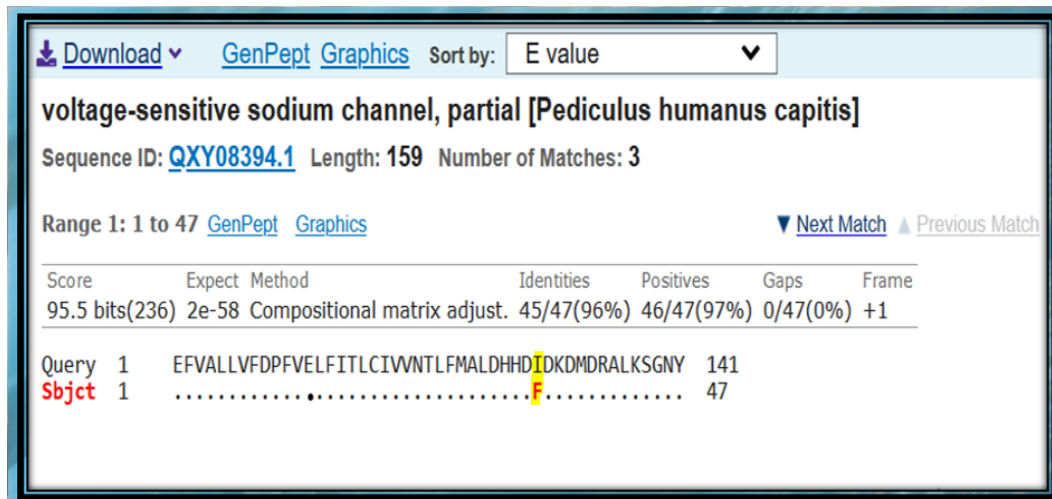


FIGURE 4.11: Predicted Mutation in the Sequence 4, Sequence 5 and Sequence 6.

4.8.1.3 Prediction of Mutation in the Sequence 7, 8 And 9

The novel mutation was predicted in the sequence 7, 8 and 9 by using the BLAST X tool. The mutation occurred at the 34 site where the M was replaced by I at the 34th position. M stands for methionine and I stands for Isoleucine shown in the figure (4.12). The reported mutations in the head louse of Thailand were T917I and L920F which were point mutations [133], [136].

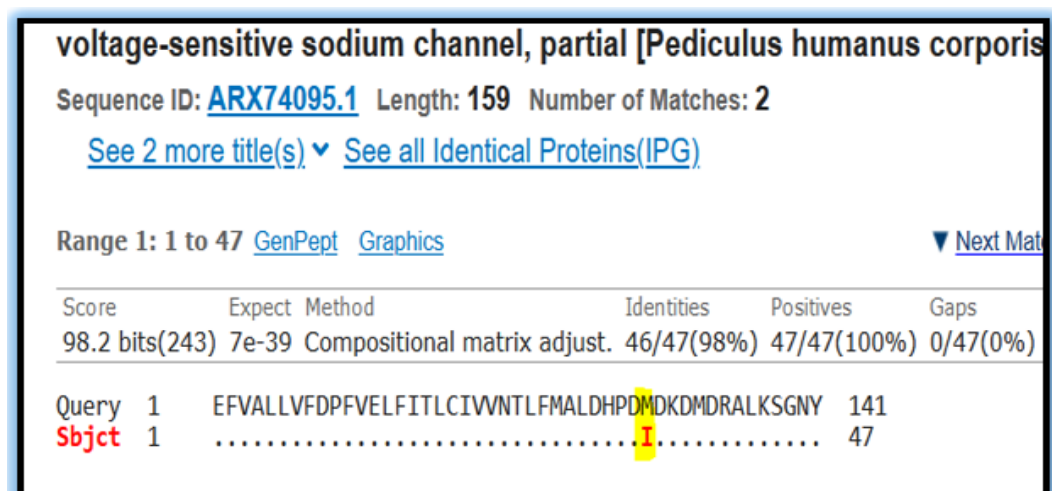


FIGURE 4.12: Predicted Mutation in the Sequence 7, Sequence 8 and Sequence 9.

4.9 Verification of Mutations

4.9.1 Verification of Mutation in the Sequence 1, 2 and 3

The novel mutations which were predicted by using the BLAST X tool were verified by using the PROVEAN tool [137]. The figure (4.13) showed the verification of the mutation in the sequence 1, sequence 2 and sequence 3. The mutation has occurred at 34th position where Methionine was replaced by Isoleucine and the PROVEAN score of the mutation was -6.0 and this score indicate that the mutation was deleterious which means that the resistance was existing in the head louse [133].

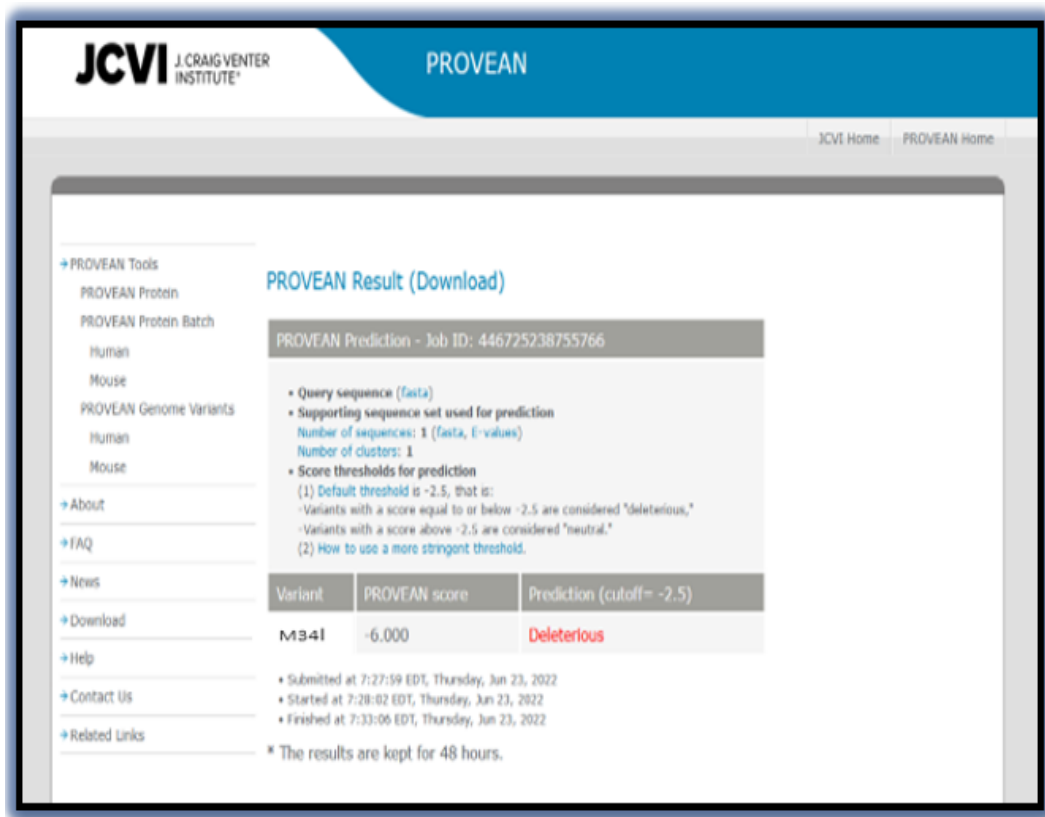


FIGURE 4.13: Verification of the Mutation in the Sequence 1, Sequence 2 and Sequence 3.

4.9.2 Verification of Mutation in the Sequence 4, 5 and 6

The novel mutations which were predicted by using the BLAST X tool were verified by using the PROVEAN tool [137]. The figure (4.14) showed the verification of

the mutation in the sequence 4, sequence 5 and sequence 6. The mutation has occurred at 34th position where Isoleucine was replaced by Phenylalanine and the PROVEAN score of the mutation was -0.981 and this score indicate that the mutation was neutral which means that the resistance was existing in the head louse.

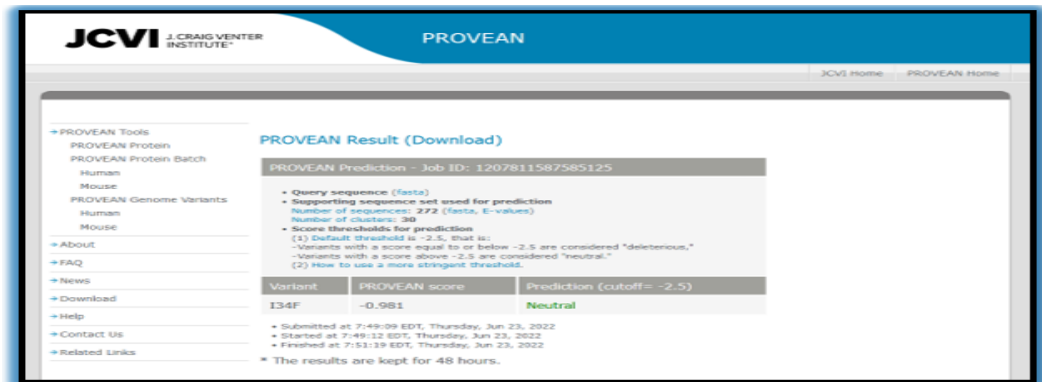


FIGURE 4.14: Verification of the Mutation in the Sequence 4, Sequence 5 and Sequence 6.

4.9.3 Verification of Mutation in the Sequence 7, 8 And 9

The novel mutations which were predicted by using the BLAST X tool were verified by using the PROVEAN tool [137]. The figure (4.15) showed the verification of the mutation in the sequence 7, sequence 8 and sequence 9. The mutation has occurred at 34th position where Methionine was replaced by Isoleucine and the PROVEAN score of the mutation was -6.0 and this score indicate that the mutation was deleterious which means that the resistance was existing in the head louse.

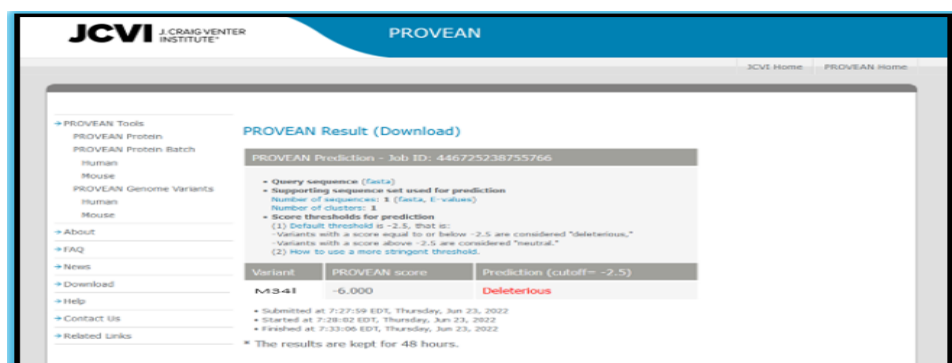


FIGURE 4.15: Verification of the Mutation in the Sequence 7, Sequence 8 and Sequence 9.

4.10 2D Structure Prediction

4.10.1 2D Structure of Sequence 1

The figure (4.16) showed the 2D structure of the sequence 1. The alpha helices were represented in the pink color, beta strands were represented in the yellow color and the coils were represented with the grey lines [138].

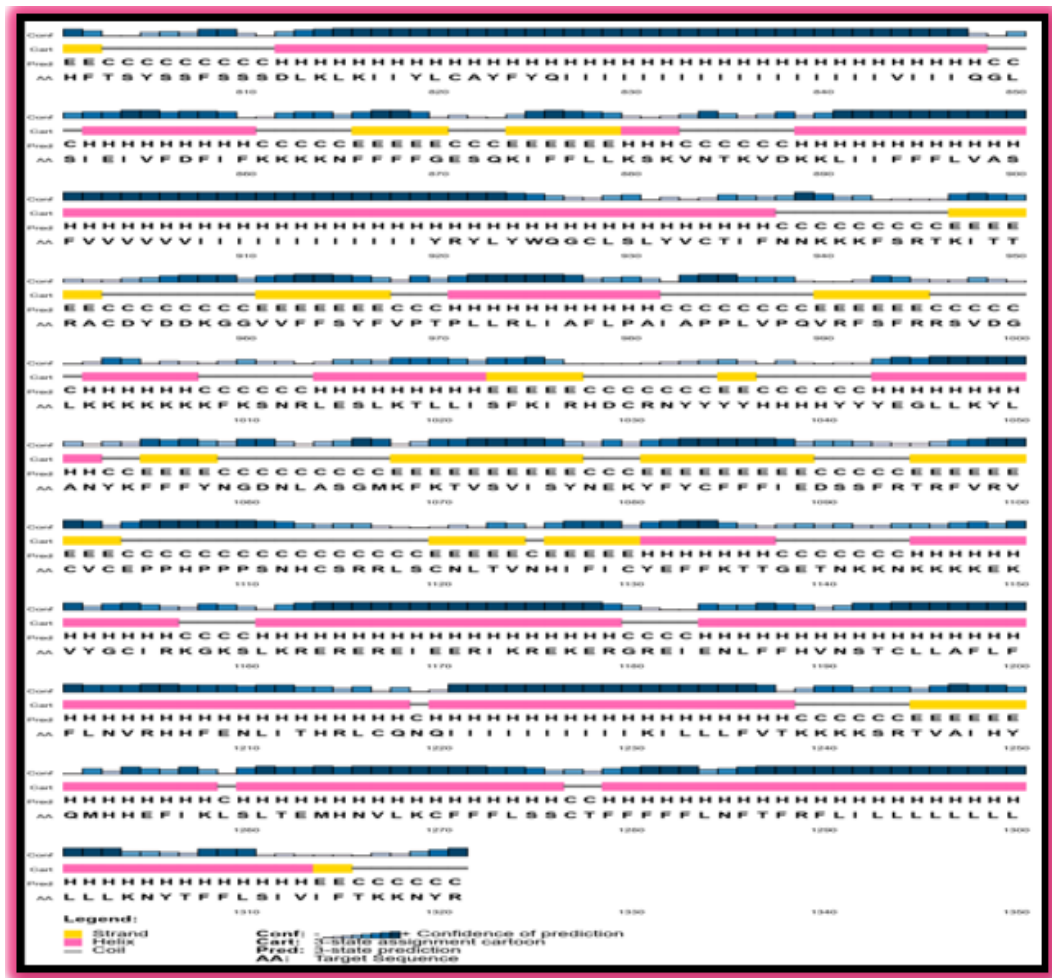


FIGURE 4.16: 2D Structure Prediction of the Sequence 1.

The Figure (4.17) showed the graphical display of 2D structure of sequence 1. The blue color in the (figure 4.17) represented the helices and the total number of the helices were 1107, the beta bridges were represented in the red color and the total number of beta bridges were 0, the green color represented the beta turns and the total number of beta turns were 351 and the coils were represented in the yellow

color and total number of coils in sequence 1 were 1001 shown in the table 4.1. These component like Helix, Beta turns, Beta sheets & bridges and coil made the protein structure different from one another.

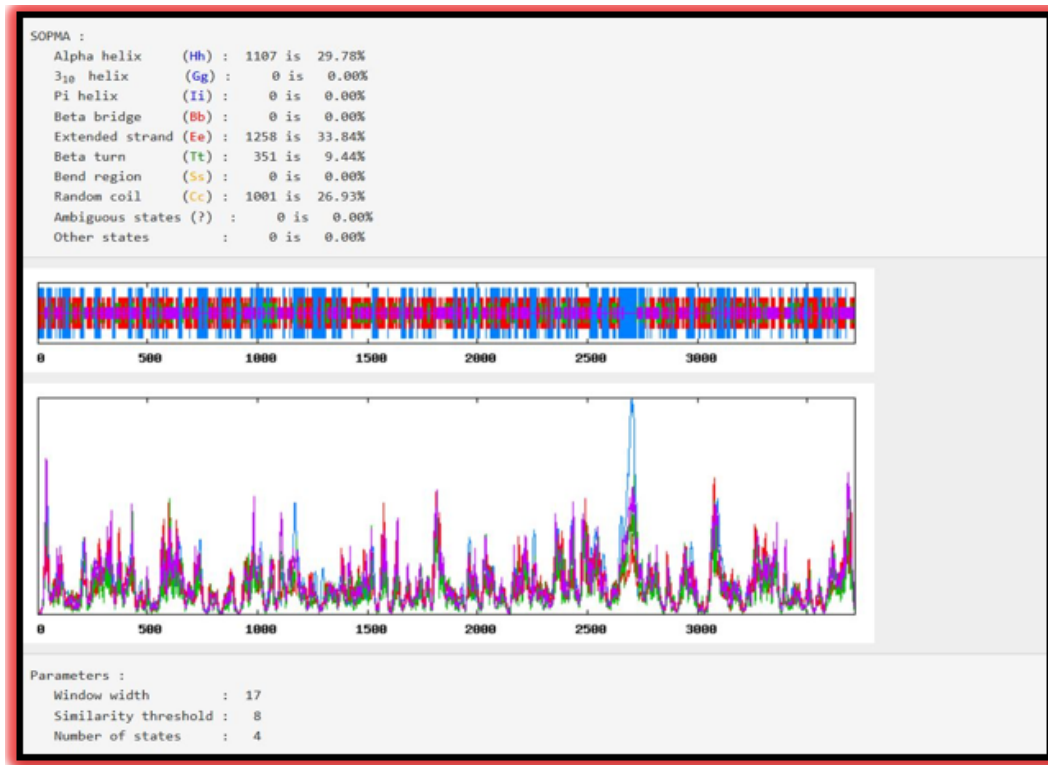


FIGURE 4.17: Components and graphical representation of the 2D Structure of the Sequence 1.

TABLE 4.1: Components of 2D Structure of the Sequence 1.

Serial. No	2D Structure Components	Color	Total Number
1.	Helix	Blue	1107
2.	Beta bridges	Red	0
3.	Beta turns	Green	351
4.	Coil	Yellow	1001

4.10.2 2D Structure of Sequence 2

The figure (4.18) showed the 2D structure of the sequence 2. The alpha helices were represented in the pink color, beta strands were represented in the yellow

color and the coils were represented with the grey lines [138].

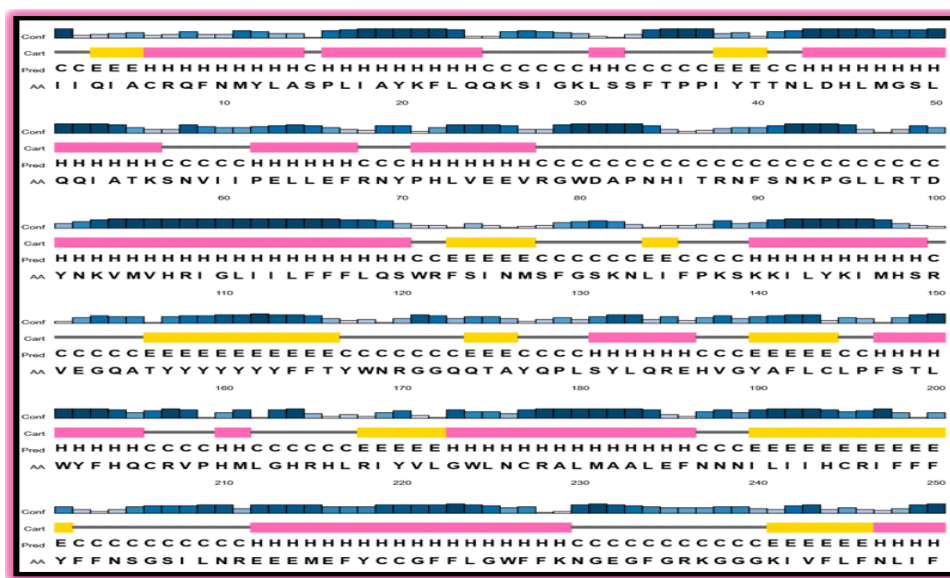


FIGURE 4.18: 2D Structure Prediction of the Sequence 2

The Figure (4.19) showed the graphical display of 2D structure of sequence 2. Blue color in (figure 4.19) represented the helices and the total number of the helices were 185, the beta bridges were represented in the red color and the total number of beta bridges were 0, the green color represented the beta turns and the total number of beta turns were 48 and the coils were represented in the yellow color and total number of coils in sequence 2 were 112 shown in the table 4.2.

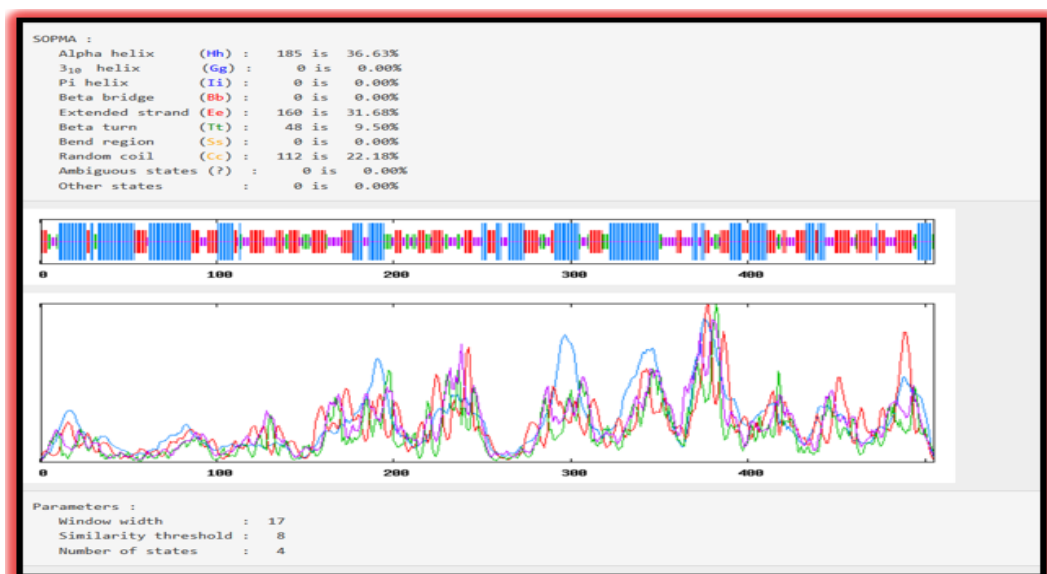


FIGURE 4.19: Components and graphical representation of the 2D Structure of the Sequence 2.

TABLE 4.2: Components of 2D Structure of the Sequence 2.

Serial. No	2D Structure Components	Color	Total Number
1.	Helix	Blue	185
2.	Beta bridges	Red	0
3.	Beta turns	Green	48
4.	Coil	Yellow	112

4.10.3 2D Structure of Sequence 3

The figure (4.20) showed the 2D structure of the sequence 3. The alpha helices were represented in the pink color, beta strands were represented in the yellow color and the coils were represented with the grey lines.

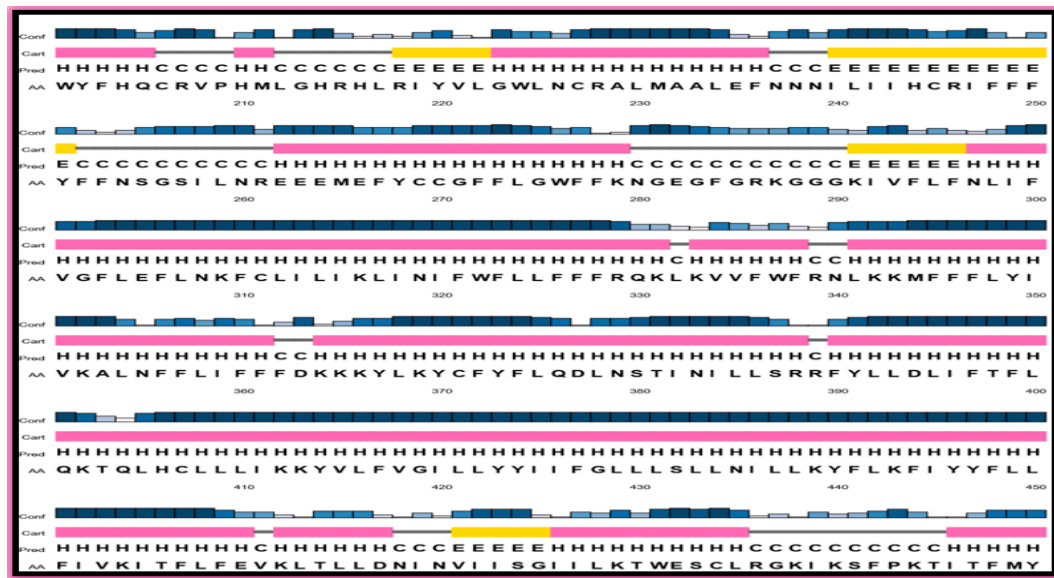


FIGURE 4.20: 2D Structure Prediction of the Sequence 3.

The Figure (4.21) showed the graphical display of 2D structure of sequence 3. The blue color in the figure (4.21) represented the helices and the total number of the helices were 335, the beta bridges were represented in the red color and the total number of beta bridges were 0, the green color represented the beta turns and the total number of beta turns were 59 and the coils were represented in the yellow color and total number of coils in sequence 3 were 171 shown in the table 4.3.

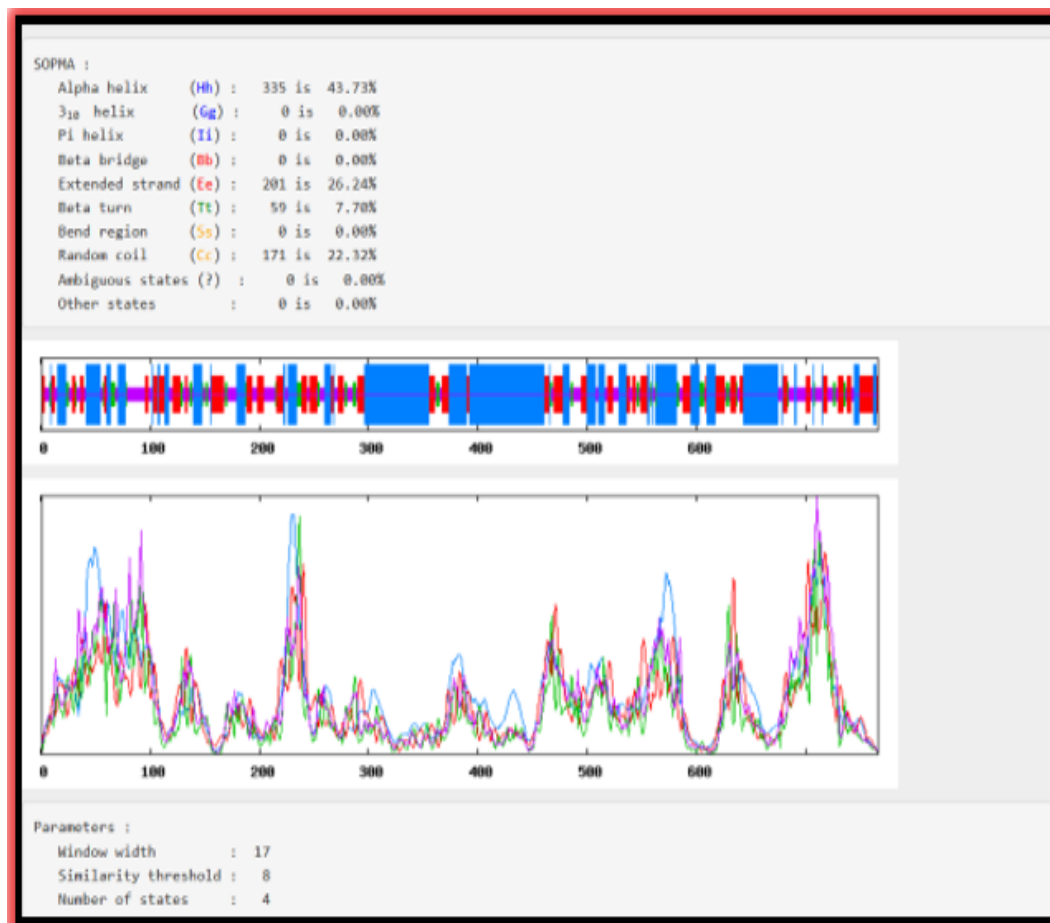


FIGURE 4.21: Components and graphical representation of the 2D Structure of the Sequence 3.

TABLE 4.3: Components of 2D Structure of the Sequence 3.

Serial. No	2D Structure Component	Color	Total Number
1.	Helix	Blue	335
2.	Beta bridges	Red	0
3.	Beta turns	Green	59
4.	Coil	Yellow	171

4.10.4 2D Structure of Sequence 4

The figure (4.22) showed the 2D structure of the sequence 4. The alpha helices were represented in the pink color, beta strands were represented in the yellow color and the coils were represented with the grey lines.

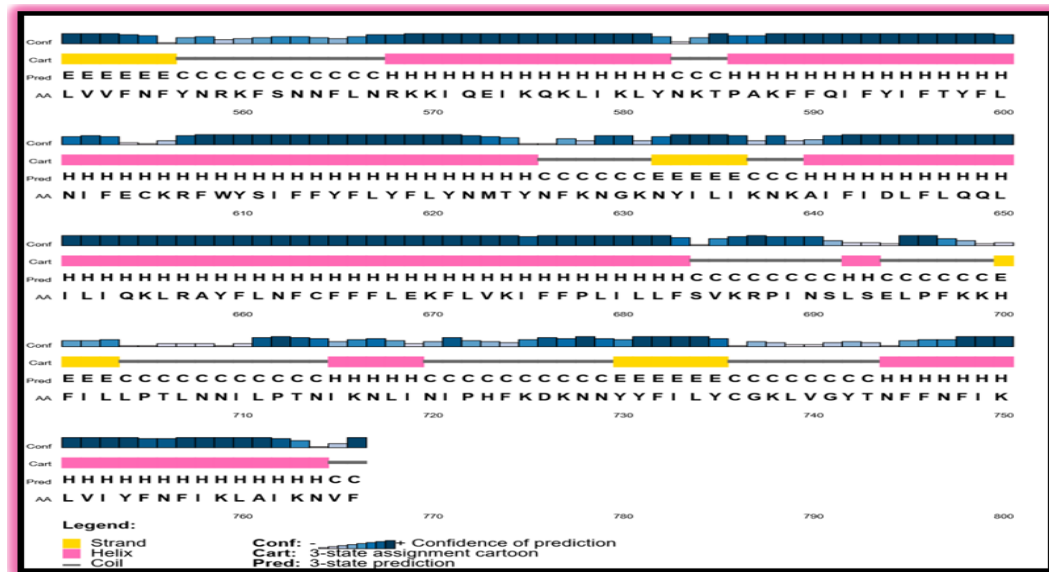


FIGURE 4.22: 2D Structure Prediction of the Sequence 4.

The Figure (4.23) showed the graphical display of 2D structure of sequence 4. Blue color in the (figure 4.23) represented the helices and the total number of the helices were 409, the beta bridges were represented in the red color and the total number of beta bridges were 0, the green color represented the beta turns and the total number of beta turns were 122 and the coils were represented in the yellow color and total number of coils in sequence 4 were 343 shown in the table 4.4.

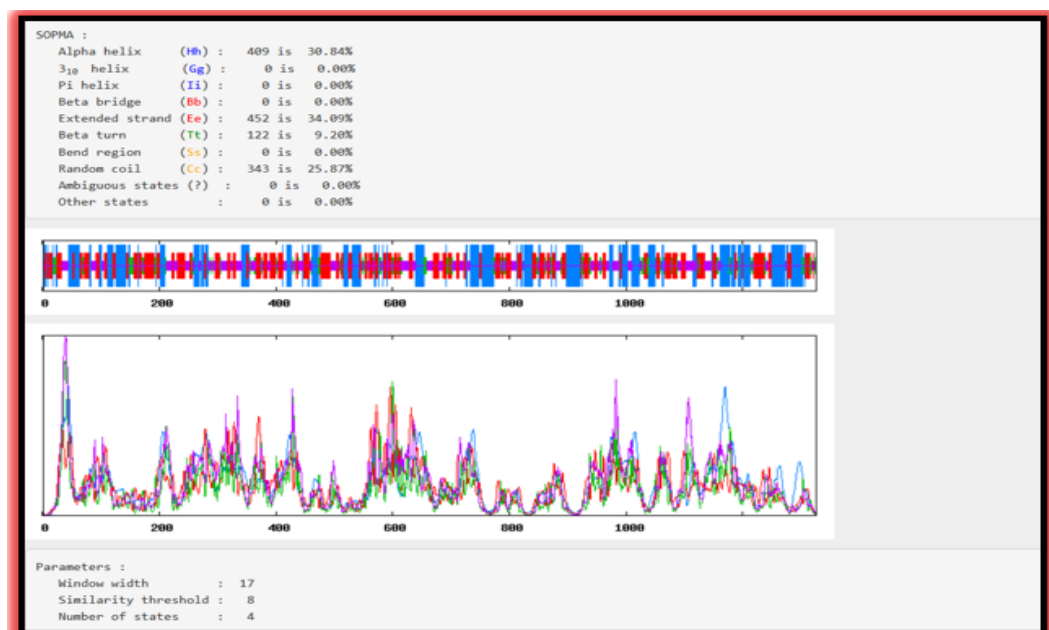


FIGURE 4.23: Components and graphical representation of the 2D Structure of the Sequence 4.

TABLE 4.4: Components of 2D Structure of the Sequence 4.

Serial. No	2D Structure Components	Color	Total Number
1.	Helix	Blue	409
2.	Beta bridges	Red	0
3.	Beta turns	Green	122
4.	Coil	Yellow	343

4.10.5 2D Structure of Sequence 5

The figure (4.24) showed the 2D structure of the sequence 5. The alpha helices were represented in the pink color, beta strands were represented in the yellow color and the coils were represented with the grey lines.



FIGURE 4.24: 2D Structure Prediction of the Sequence 5.

The Figure(4.25) showed the graphical display of 2D structure of sequence 5. Blue color in the figure (4.25) represented the helices and the total number of the helices were 185, the beta bridges were represented in the red color and the total number of beta bridges were 0, the green color represented the beta turns and the total

number of beta turns were 48 and the coils were represented in the yellow color and total number of coils in sequence 5 were 112 shown in the table 4.5.

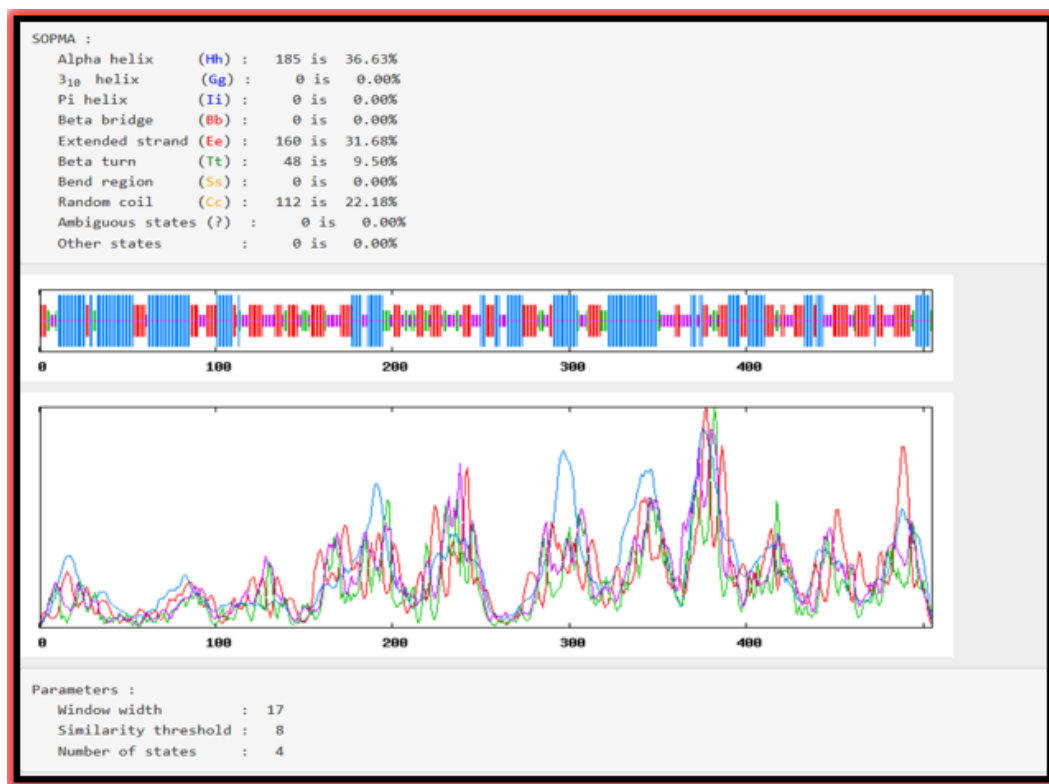


FIGURE 4.25: Components and graphical representation of the 2D Structure of the Sequence 5.

TABLE 4.5: Components of 2D Structure of the Sequence 5.

Serial. No	2D Structure Components	Color	Total Number
1.	Helix	Blue	185
2.	Beta bridges	Red	0
3.	Beta turns	Green	48
4.	Coil	Yellow	112

4.10.6 2D Structure of Sequence 6

The figure (4.26) showed the 2D structure of the sequence 6. The alpha helices were represented in the pink color, beta strands were represented in the yellow color and the coils were represented with the grey lines.

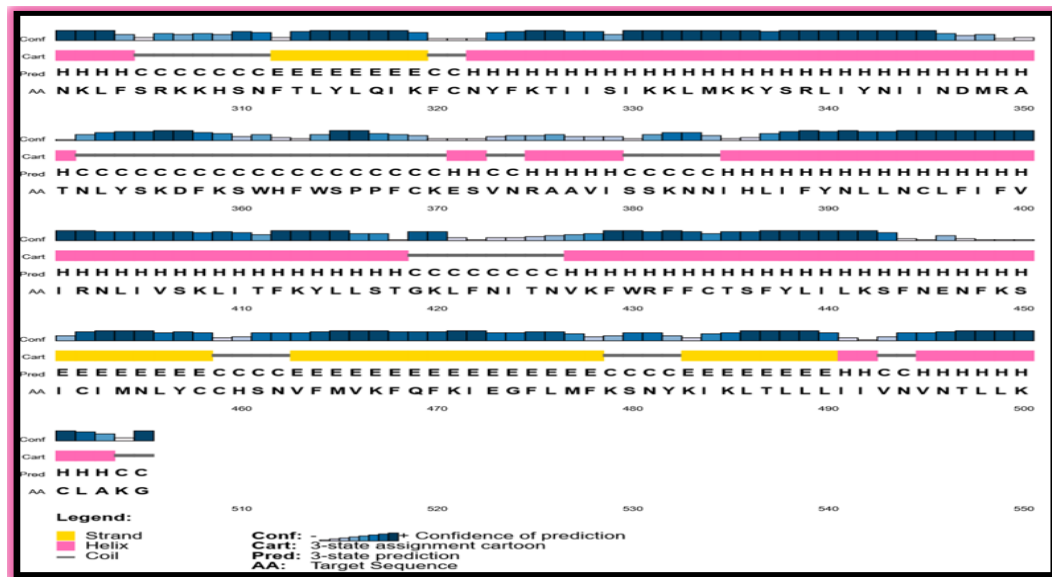


FIGURE 4.26: 2D Structure Prediction of the Sequence 6.

The Figure (4.27) showed the graphical display of 2D structure of sequence 6. Blue color in the (figure 4.27) represented the helices and the total number of the helices were 335, the beta bridges were represented in the red color and the total number of beta bridges were 0, the green color represented the beta turns and the total number of beta turns were 59 and the coils were represented in the yellow color and total number of coils in sequence 6 were 171 shown in the table 4.6.

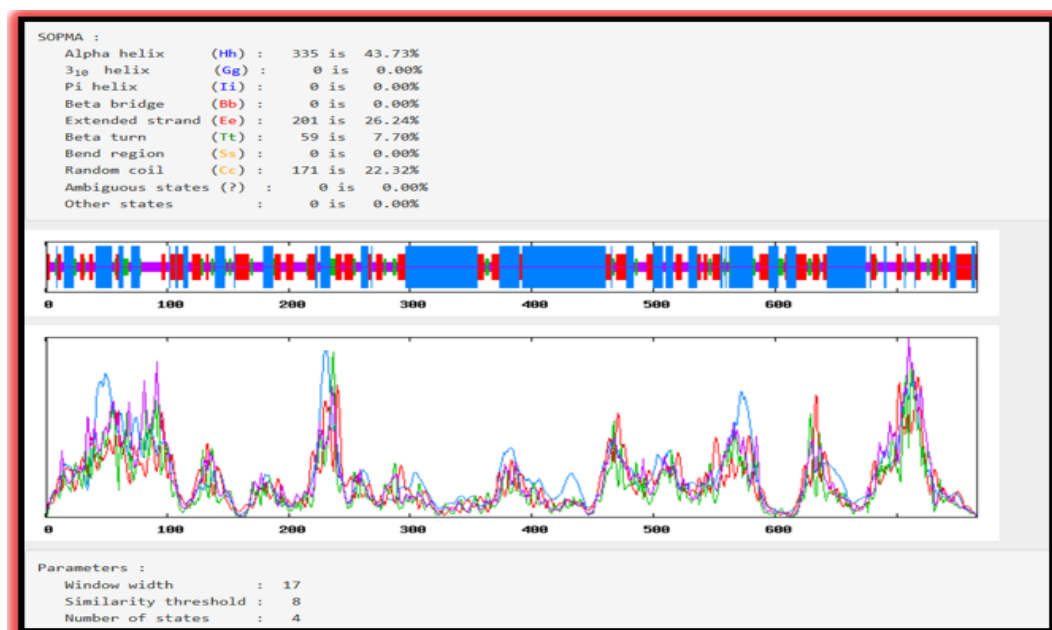


FIGURE 4.27: Components and graphical representation of the 2D Structure of the Sequence 6.

TABLE 4.6: Components of 2D Structure of the Sequence 6.

Serial. No	2D Structure Components	Color	Total Number
1.	Helix	Blue	335
2.	Beta bridges	Red	0
3.	Beta turns	Green	59
4.	Coil	Yellow	171

4.10.7 2D Structure of Sequence 7

The figure (4.28) showed the 2D structure of the sequence 7. The alpha helices were represented in the pink color, beta strands were represented in the yellow color and the coils were represented with the grey lines.



FIGURE 4.28: 2D Structure Prediction of the Sequence 7.

The Figure (4.29) showed the graphical display of 2D structure of sequence 7. Blue color in the figure (4.29) represented the helices and the total number of the helices were 309, the beta bridges were represented in the red color and the total number of beta bridges were 0, the green color represented the beta turns and the

total number of beta turns were 85 and the coils were represented in the yellow color and total number of coils in sequence 7 were 266 shown in the table 4.7

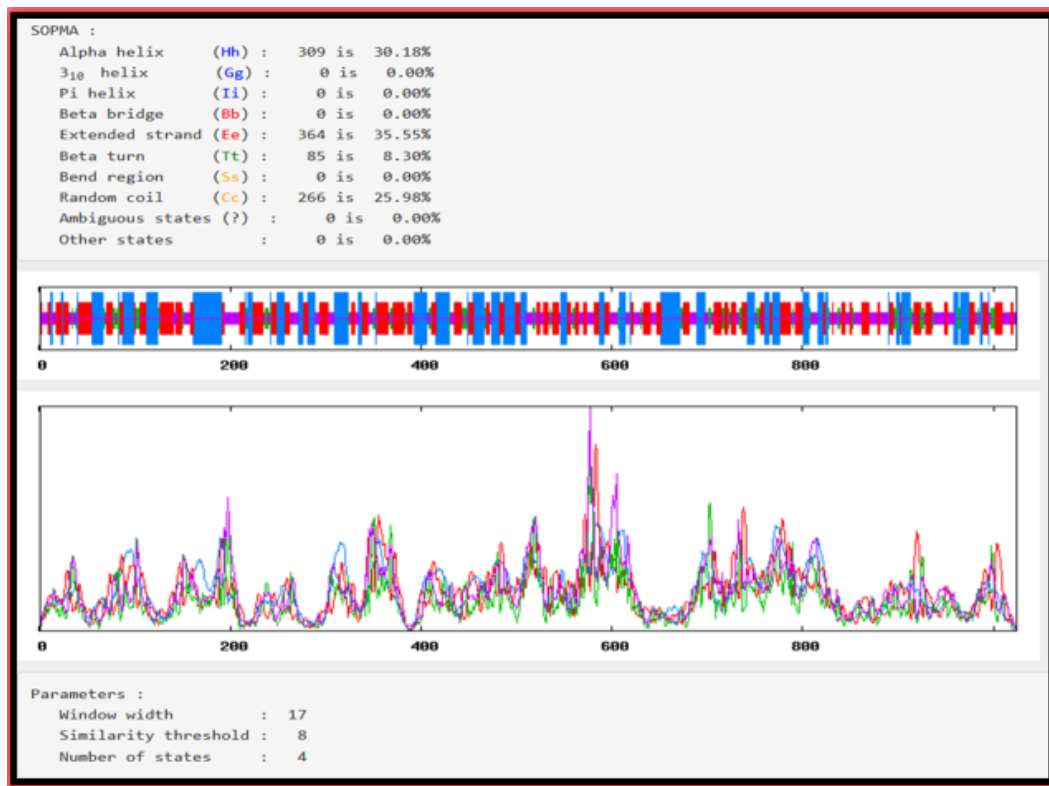


FIGURE 4.29: Components and graphical representation of the 2D Structure of the Sequence 7.

TABLE 4.7: Components of 2D Structure of the Sequence 7.

Serial. No	2D Structure Components	Color	Total Number
1.	Helix	Blue	309
2.	Beta bridges	Red	0
3.	Beta turns	Green	85
4.	Coil	Yellow	266

4.10.8 2D Structure of Sequence 8

The figure (4.30) showed the 2D structure of the sequence 8. The alpha helices were represented in the pink color, beta strands were represented in the yellow color and the coils were represented with the grey lines.

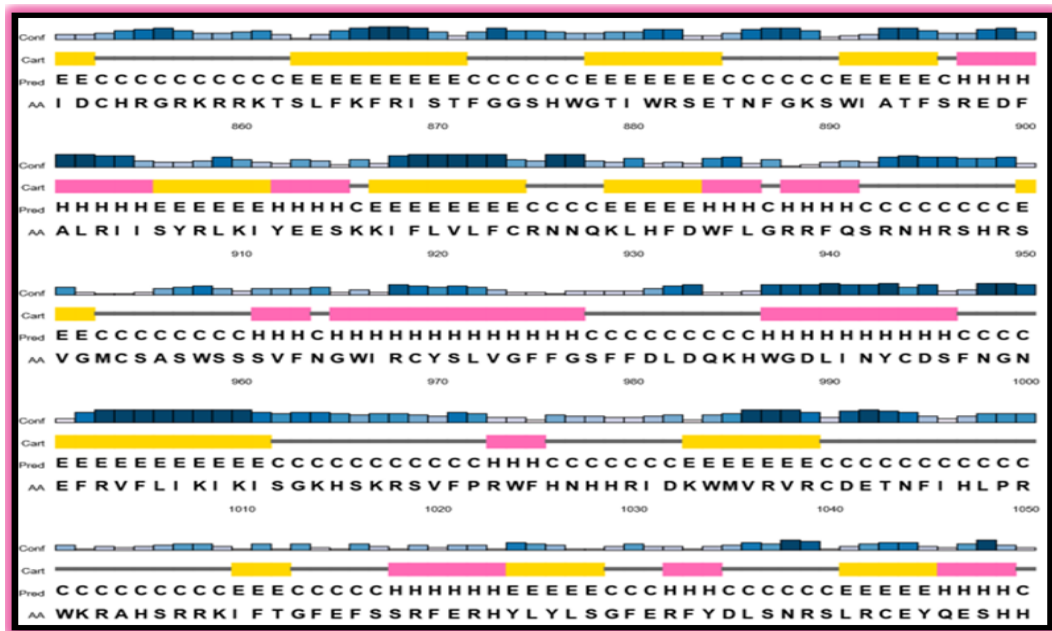


FIGURE 4.30: 2D Structure Prediction of the Sequence 8.

The Figure (4.31) showed the graphical display of 2D structure of sequence 8. Blue color in the figure (4.31) represented the helices and the total number of the helices were 370, the beta bridges were represented in the red color and the total number of beta bridges were 0, the green color represented the beta turns and the total number of beta turns were 114 and the coils were represented in the yellow color and total number of coils in sequence 8 were 338 shown in the table 4.8.

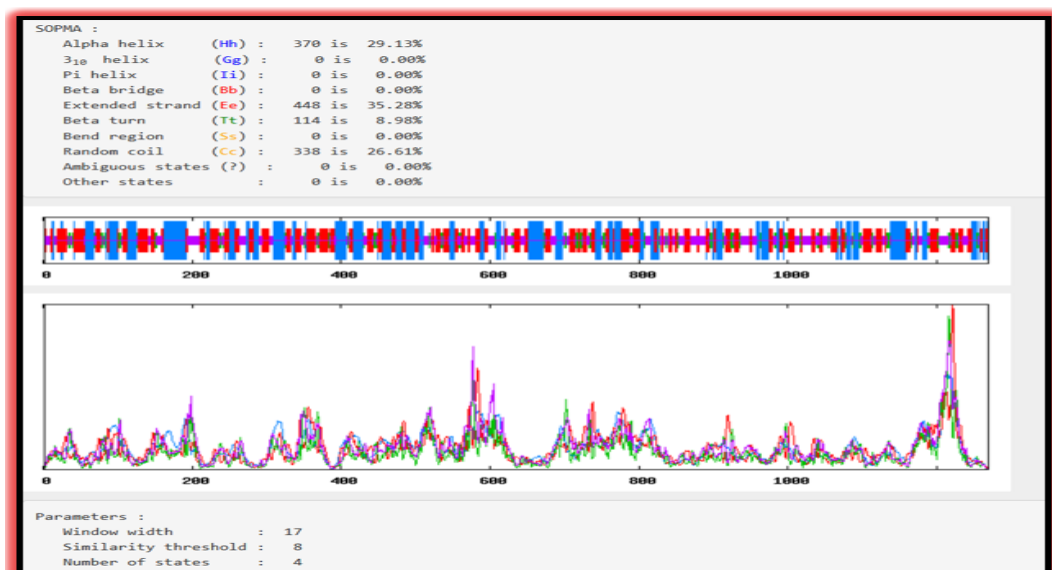


FIGURE 4.31: Components and graphical representation of the 2D Structure of the Sequence 8.

TABLE 4.8: Components of 2D Structure of the Sequence 8.

Serial. No	2D Structure Components	Color	Total Number
1.	Helix	Blue	370
2.	Beta bridges	Red	0
3.	Beta turns	Green	114
4.	Coil	Yellow	338

4.10.9 2D Structure of Sequence 9

The figure (4.32) showed the 2D structure of the sequence 9. The alpha helices were represented in the pink color, beta strands were represented in the yellow color and the coils were represented with the grey lines.



FIGURE 4.32: 2D Structure Prediction of the Sequence 9.

The Figure (4.33) showed the graphical display of 2D structure of sequence 9. The blue color in the figure (4.33) represented the helices and the total number

of the helices were 625, the beta bridges were represented in the red color and the total number of beta bridges were 0, the green color represented the beta turns and the total number of beta turns were 120 and the coils were represented in the yellow color and total number of coils in sequence 9 were 371 shown in the table 4.9.

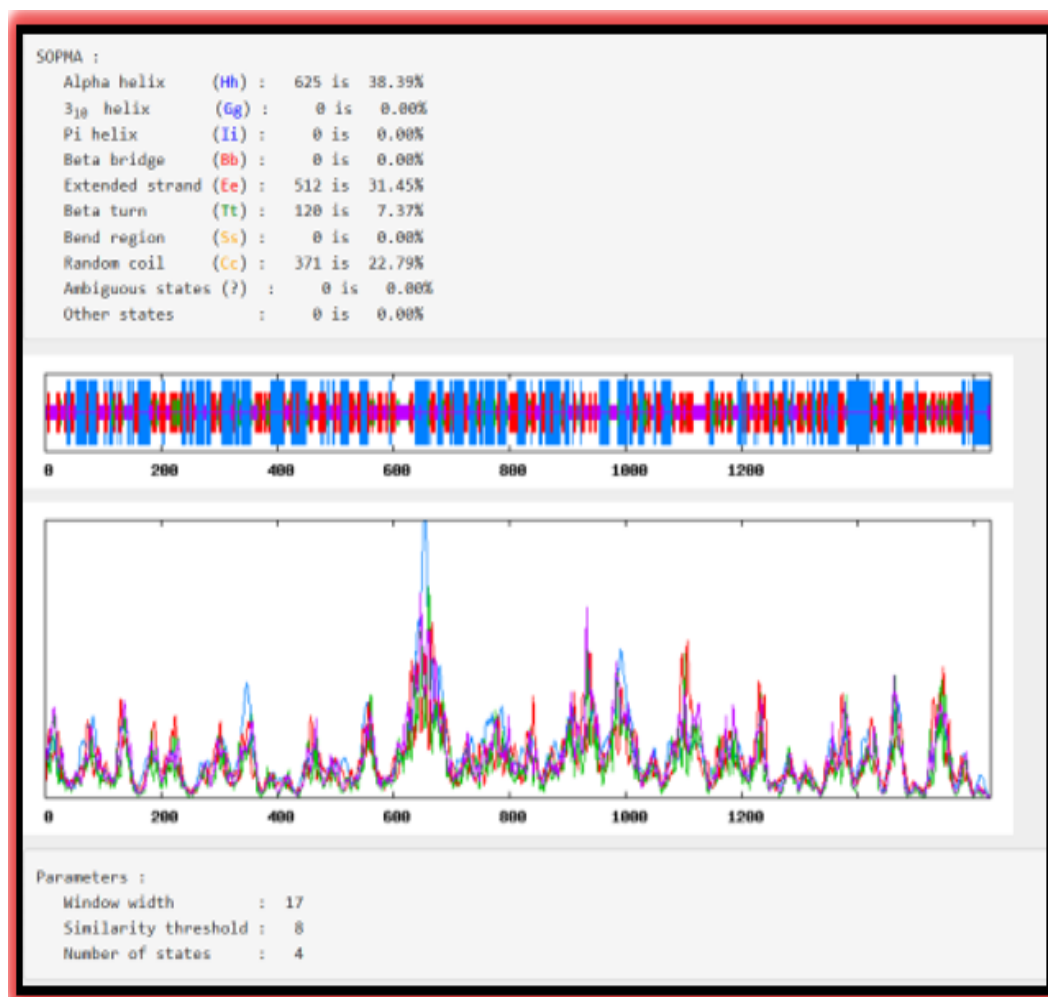


FIGURE 4.33: Components and graphical representation of the 2D Structure of the Sequence 9.

TABLE 4.9: Components of 2D Structure of the Sequence 9.

Serial. No	2D Structure Components	Color	Total Number
1.	Helix	Blue	625
2.	Beta bridges	Red	0
3.	Beta turns	Green	120
4.	Coil	Yellow	371

4.11 3D Structure Prediction

4.11.1 Sequence 1 3D Structure

The figure (4.34) showed the 3D structure. The 3D structure was predicted by using the Swiss Modeler tool and the alpha helices, beta sheets and coils were shown in the 3D structure of the sequence 1 [139].

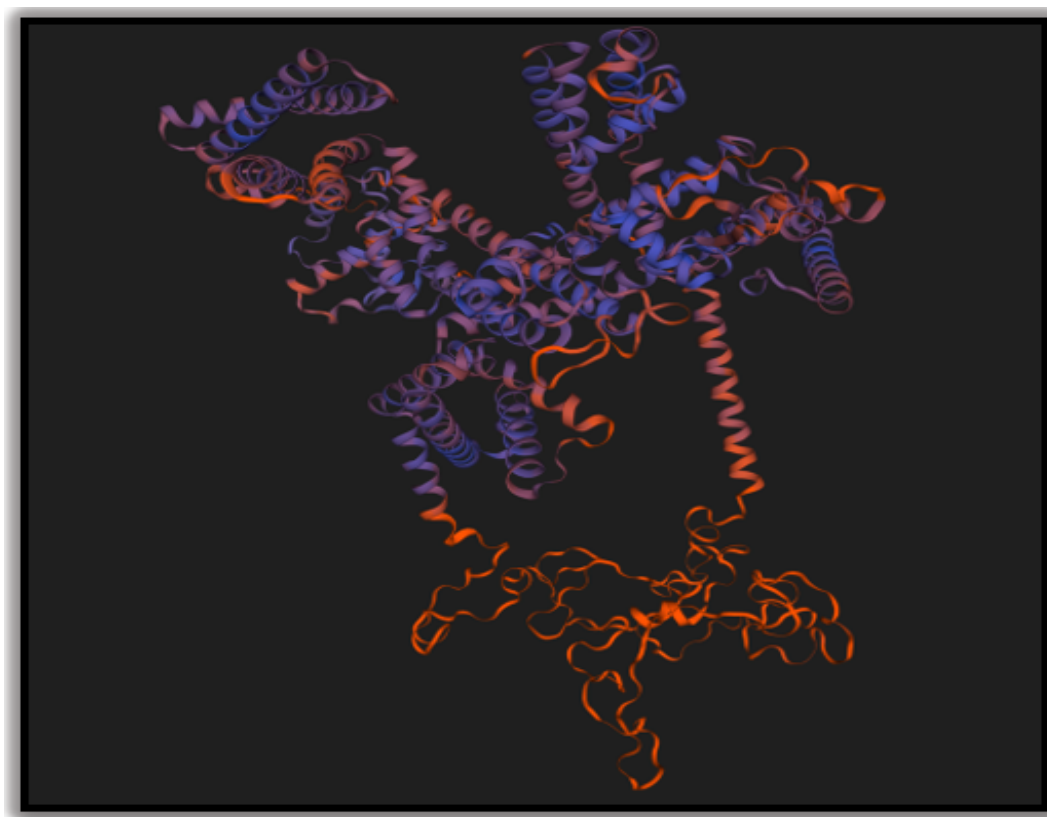


FIGURE 4.34: 3D Structure of the Sequence 1.

The Ramachandran plot was generated by the help of the Swiss Modeler tool. The (x-axis) of ramachandran diagram shows phi angle and (y-axis) of ramachandran diagram shows psi angle. From 0-180 degree the beta sheets were shown on the left hand. On the right hand from 0-180 degree, the left handed alpha helices were shown and on the left hand from 0 to -180 degree, the right handed alpha helices were represented. The area of the plot was divided into four regions, dark green was the mostly favored region, tea green region was the generously allowed region, the light green region was the additional allowed region and the white region was

the disallowed region in the Ramachandran plot of the sequence 1 as shown in the figure (4.35).

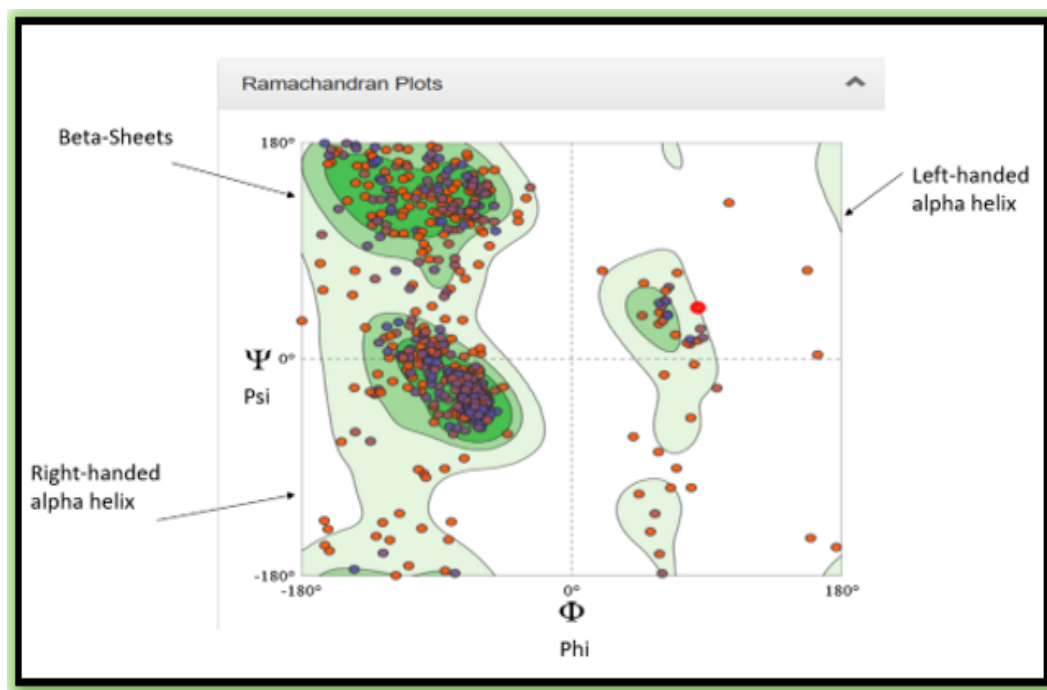


FIGURE 4.35: Ramachandran Plot of the Sequence 1.

The Ramachandran plot considered the more stable when the 90% of the psi and phi values was present in the most favored region. The proline molecules were indicated as the red dots in the Ramachandran plot, the glycine molecules were indicated as the blue dots and the pre-proline molecules were indicated as the pink dots. These three molecules are major molecules which constructs the Ramachandran plot. The Ramachandran plot of the sequence 1 showed the more stable model of the Ramachandran plot as shown in the figure (4.35). Because the proline, glycine and pre- proline was present in most favored region between the psi and phi angle.

4.11.2 3D Structure of Sequence 2

The figure (4.36) showed 3D structure of sequence 2. The 3D structure was predicted by using the Swiss Modeler tool and the alpha helices, beta sheets and coils were shown in the 3D structure of the sequence 2.

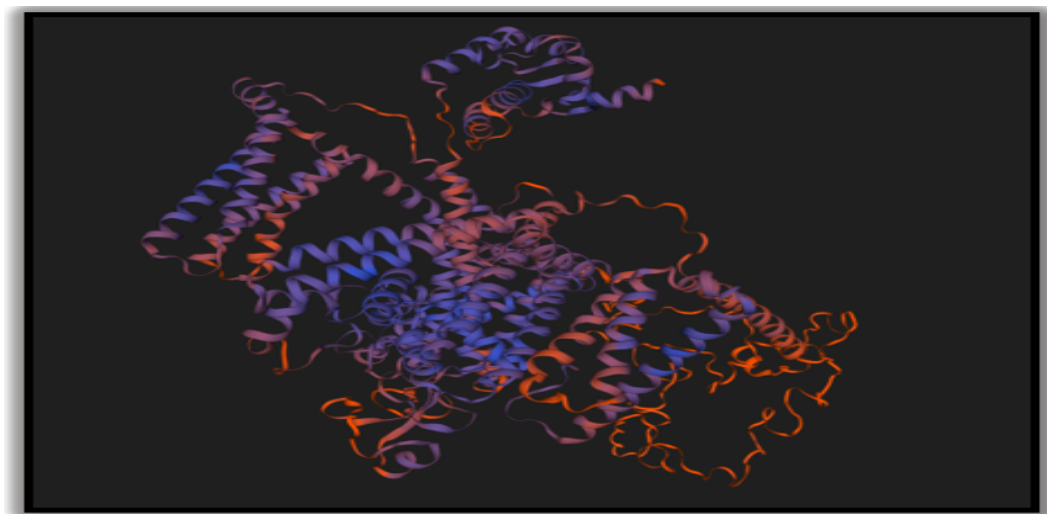


FIGURE 4.36: 3D Structure of the Sequence 2.

The Ramachandran plot was generated by the help of the Swiss Modeler tool. The (x-axis) of ramachandran diagram shows phi angle and (y-axis) of ramachandran diagram shows psi angle. From 0-180 degree the beta sheets were shown on the left hand. On the right hand from 0-180 degree, the left-handed alpha helices were shown and on the left hand from 0 to -180 degree, the right-handed alpha helices were represented. The area of the plot was divided into four regions, dark green was the mostly favored region, tea green region was the generously allowed region, the light green region was the additional allowed region and the white region was the disallowed region in the Ramachandran plot of the sequence 2 as shown in the figure (4.37).

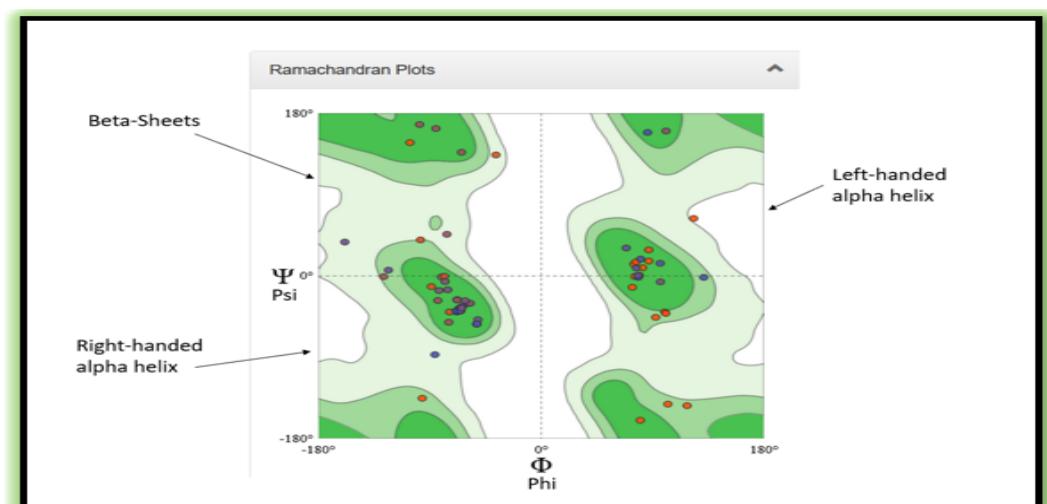


FIGURE 4.37: Ramachandran Plot of the Sequence 2.

The Ramachandran plot considered the more stable when the 90% of the psi and phi values was present in the most favored region. The proline molecules were indicated as the red dots in the Ramachandran plot, the glycine molecules were indicated as the blue dots and the pre-proline molecules were indicated as the pink dots. These three molecules are major molecules which constructs the Ramachandran plot. The Ramachandran plot of the sequence 2 showed the not stable model of the Ramachandran plot as shown in the figure (4.37). Because the proline, glycine and pre- proline was not present in most favored region between the psi and phi angle.

4.11.3 3D Structure of Sequence 3

The figure (4.38) showed 3D structure of sequence 3. The 3D structure was predicted by using the Swiss Modeler tool and the alpha helices, beta sheets and coils were shown in the 3D structure of the sequence 3.

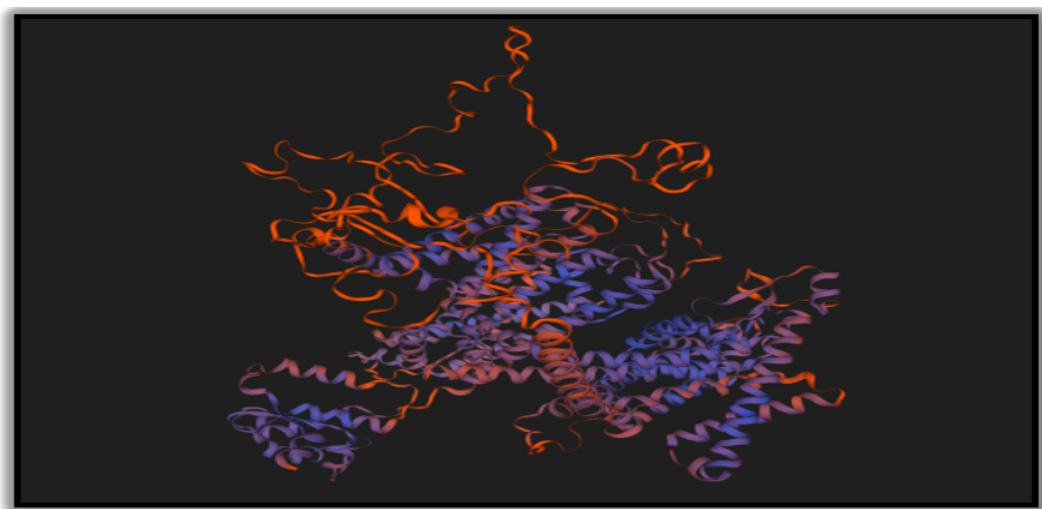


FIGURE 4.38: 3D Structure of the Sequence 3.

The Ramachandran plot was generated by the help of the Swiss Modeler tool. The (x-axis) of ramachandran diagram shows phi angle and (y-axis) of ramachandran diagram shows psi angle. From 0-180 degree the beta sheets were shown on the left hand. On the right hand from 0-180 degree, the left-handed alpha helices were shown and on the left hand from 0 to -180 degree, the right-handed alpha helices

were represented. The area of the plot was divided into four regions, dark green was the mostly favored region, tea green region was the generously allowed region, the light green region was the additional allowed region and the white region was the disallowed region in the Ramachandran plot of the sequence 3 as shown in the figure (4.39).

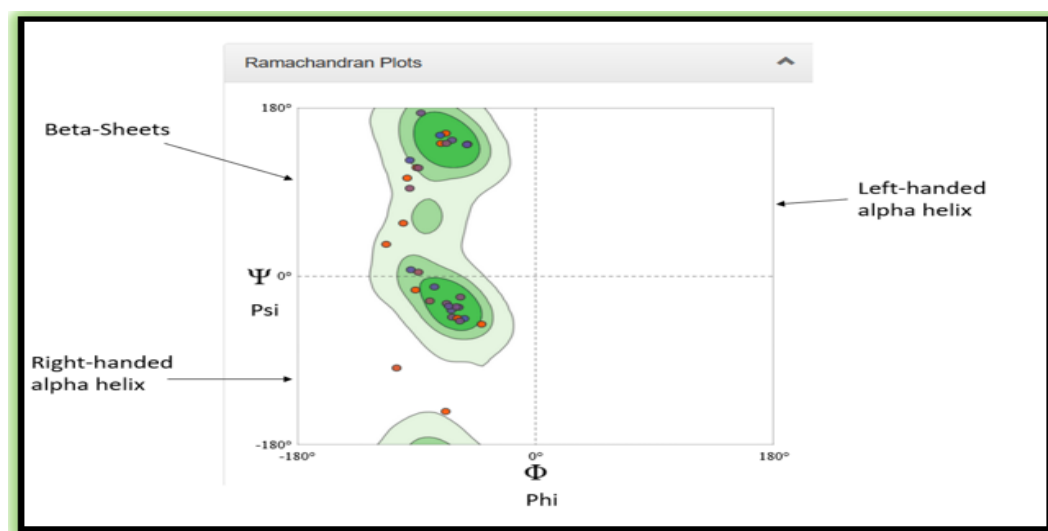


FIGURE 4.39: Ramachandran Plot of the Sequence 3.

The Ramachandran plot considered the more stable when the 90% of the psi and phi values was present in the most favored region. The proline molecules were indicated as the red dots in the Ramachandran plot, the glycine molecules were indicated as the blue dots and the pre-proline molecules were indicated as the pink dots. These three molecules are major molecules which constructs the Ramachandran plot. The Ramachandran plot of the sequence 3 showed the not stable model of the Ramachandran plot as shown in the figure (4.39). Because the proline, glycine and pre-proline was not present in most favored region between the psi and phi angle.

4.11.4 3D Structure of Sequence 4

The figure (4.40) showed 3D structure of sequence 4. The 3D structure was predicted by using the Swiss Modeler tool and the alpha helices, beta sheets and coils were shown in the 3D structure of the sequence 4.

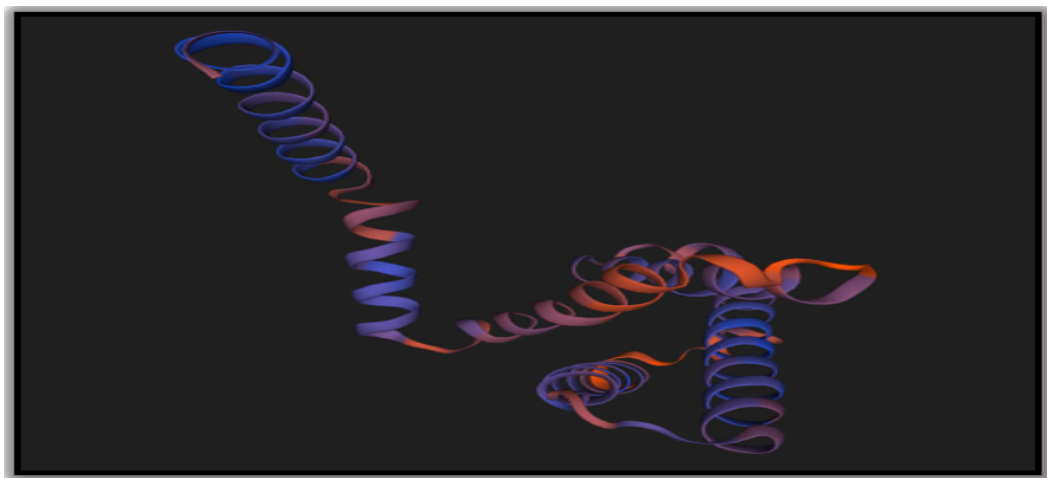


FIGURE 4.40: 3D Structure of the Sequence 4.

The Ramachandran plot was generated by the help of the Swiss Modeler tool. The (x-axis) of ramachandran diagram shows phi angle and (y-axis) of ramachandran diagram shows psi angle. From 0-180 degree the beta sheets were shown on the left hand. On the right hand from 0-180 degree, the left-handed alpha helices were shown and on the left hand from 0 to -180 degree, the right-handed alpha helices were represented. The area of the plot was divided into four regions, dark green was the mostly favored region, tea green region was the generously allowed region, the light green region was the additional allowed region and the white region was the disallowed region in the Ramachandran plot of the sequence 4 as shown in the figure (4.41).

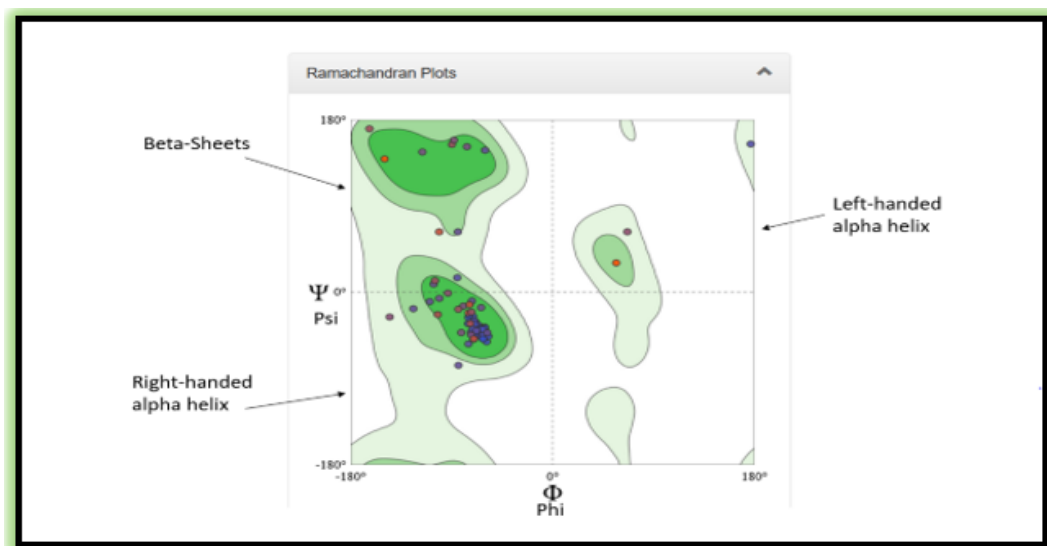


FIGURE 4.41: Ramachandran Plot of the Sequence 4.

The Ramachandran plot considered the more stable when the 90% of the psi and phi values was present in the most favored region. The proline molecules were indicated as the red dots in the Ramachandran plot, the glycine molecules were indicated as the blue dots and the pre-proline molecules were indicated as the pink dots. These three molecules are major molecules which constructs the Ramachandran plot. The Ramachandran plot of the sequence 4 showed the not stable model of the Ramachandran plot as shown in the figure (4.41). Because the proline, glycine and pre-proline was not present in most favored region between the psi and phi angle.

4.11.5 3D Structure of Sequence 5

The figure (4.42) showed 3D structure of sequence 5. The 3D structure was predicted by using the Swiss Modeler tool and the alpha helices, beta sheets and coils were shown in the 3D structure of the sequence 5.

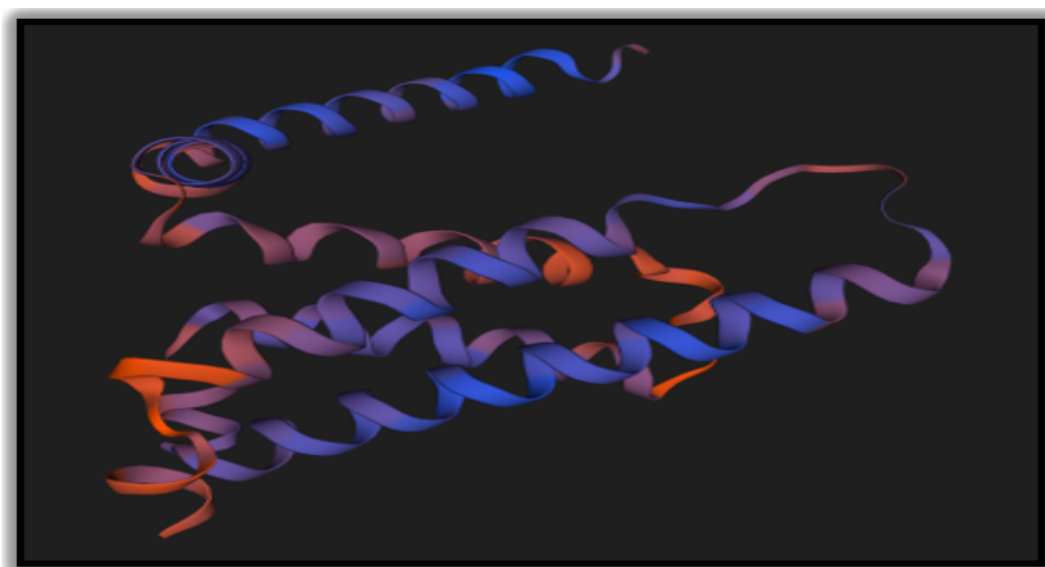


FIGURE 4.42: 3D Structure of the Sequence 5.

The Ramachandran plot was generated by the help of the Swiss Modeler tool. The (x-axis) of ramachandran diagram shows phi angle and (y-axis) of ramachandran diagram shows psi angle. From 0-180 degree the beta sheets were shown on the left hand. On the right hand from 0-180 degree, the left-handed alpha helices were

shown and on the left hand from 0 to -180 degree, the right-handed alpha helices were represented. The area of the plot was divided into four regions, dark green was the mostly favored region, tea green region was the generously allowed region, the light green region was the additional allowed region and the white region was the disallowed region in the Ramachandran plot of the sequence 5 as shown the figure (4.43).

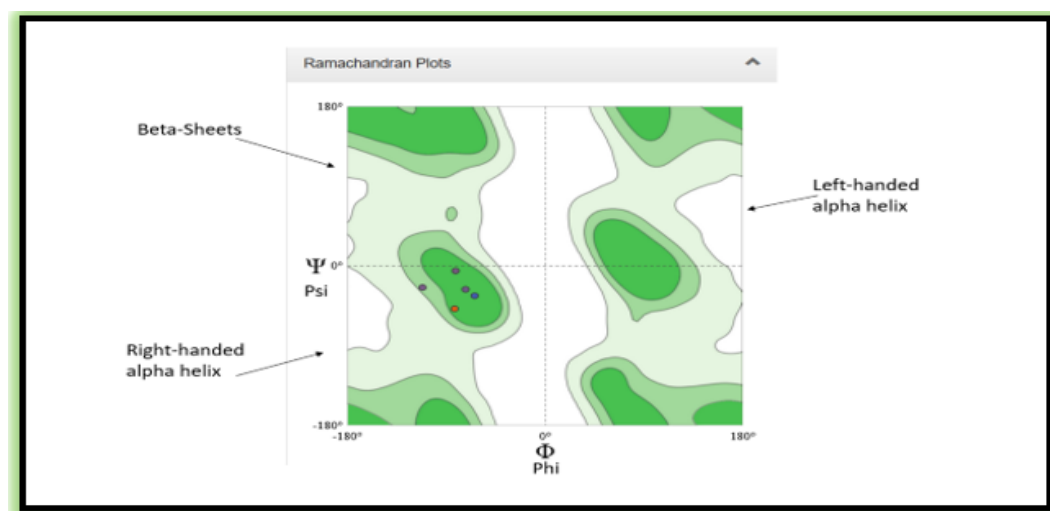


FIGURE 4.43: Ramachandran Plot of the Sequence 5.

The Ramachandran plot considered the more stable when the 90% of the psi and phi values was present in the most favored region. The proline molecules were indicated as the red dots in the Ramachandran plot, the glycine molecules were indicated as the blue dots and the pre-proline molecules were indicated as the pink dots. These three molecules are major molecules which constructs the Ramachandran plot. The Ramachandran plot of the sequence 5 showed the not stable model of the Ramachandran plot as shown in the figure (4.43). Because the proline, glycine and pre-proline was not present in most favored region between the psi and phi angle.

4.11.6 3D Structure of Sequence 6

The figure (4.44) showed 3D structure of sequence 6. The 3D structure was predicted by using the Swiss Modeler tool and the alpha helices, beta sheets and coils

were shown in the 3D structure of the sequence 6.

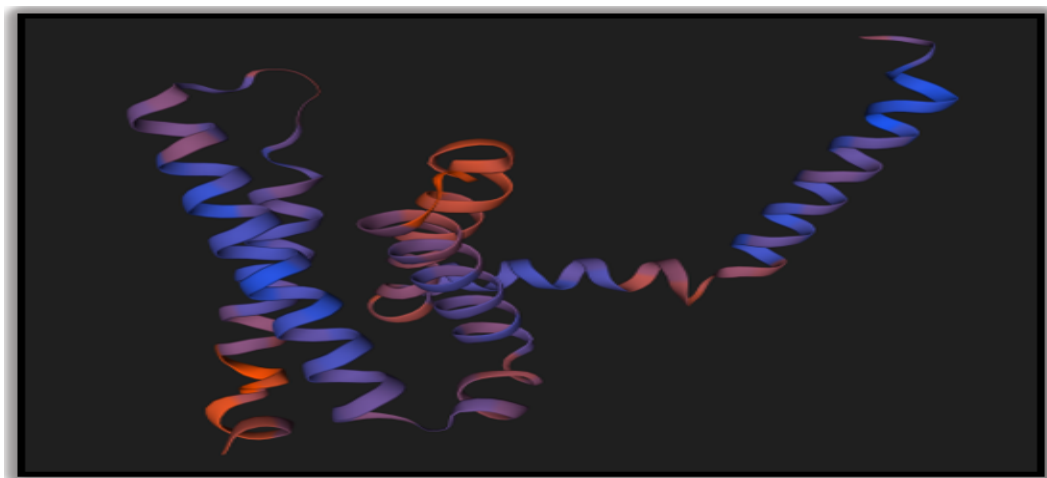


FIGURE 4.44: 3D Structure of the Sequence 6.

The Ramachandran plot was generated by the help of the Swiss Modeler tool. The (x-axis) of ramachandran diagram shows phi angle and (y-axis) of ramachandran diagram shows psi angle. From 0-180 degree the beta sheets were shown on the left hand. On the right hand from 0-180 degree, the left-handed alpha helices were shown and on the left hand from 0 to -180 degree, the right-handed alpha helices were represented. The area of the plot was divided into four regions, dark green was the mostly favored region, tea green region was the generously allowed region, the light green region was the additional allowed region and the white region was the disallowed region in the Ramachandran plot of the sequence 6 as shown in the figure (4.45).

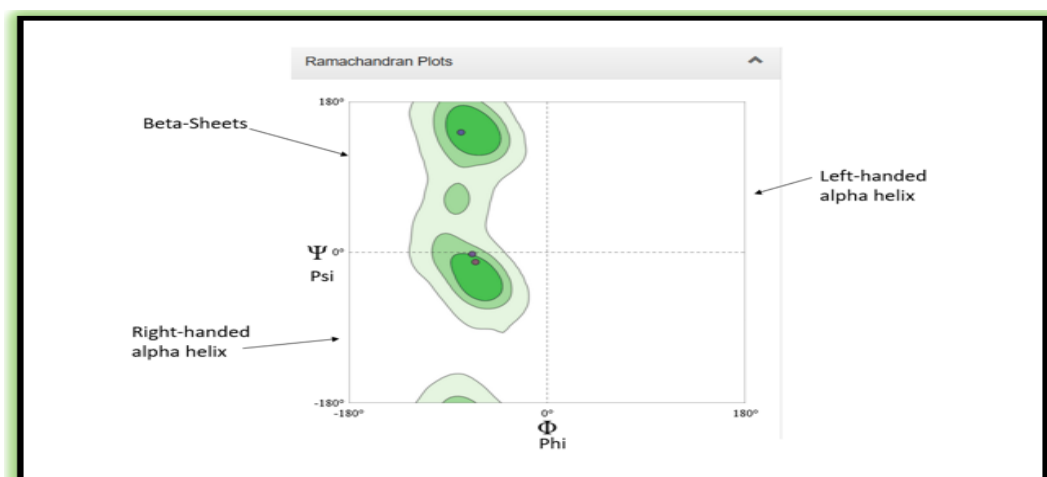


FIGURE 4.45: Ramachandran Plot of the Sequence 6.

The Ramachandran plot considered the more stable when the 90% of the psi and phi values was present in the most favored region. The proline molecules were indicated as the red dots in the Ramachandran plot, the glycine molecules were indicated as the blue dots and the pre-proline molecules were indicated as the pink dots. These three molecules are major molecules which constructs the Ramachandran plot. The Ramachandran plot of the sequence 6 showed the not stable model of the Ramachandran plot as shown in the figure (4.45). Because the proline, glycine and pre-proline was not present in most favored region between the psi and phi angle.

4.11.7 3D Structure of Sequence 7

The figure (4.46) showed 3D structure of sequence 7. The 3D structure was predicted by using the Swiss Modeler tool and the alpha helices, beta sheets and coils were shown in the 3D structure of the sequence 7.

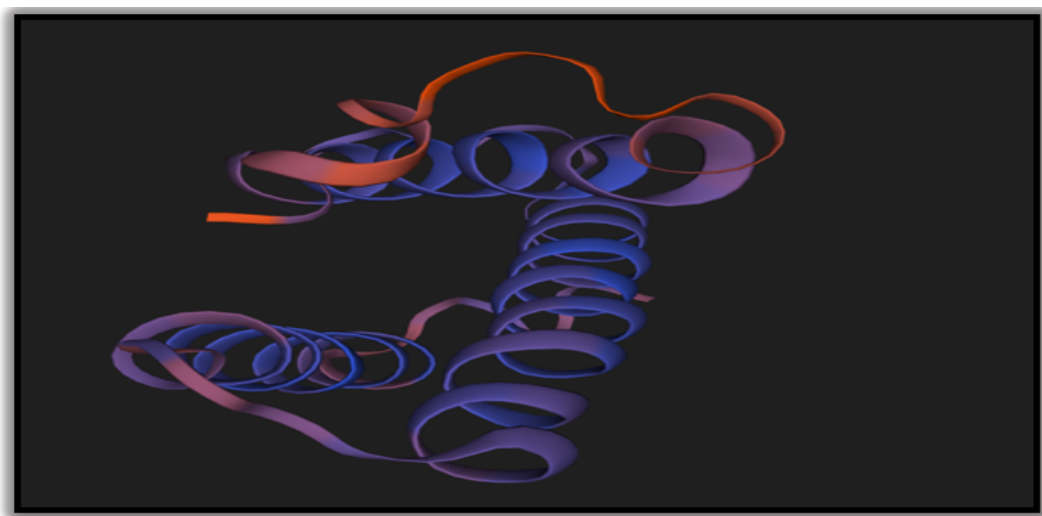


FIGURE 4.46: 3D Structure of the Sequence 7.

The Ramachandran plot was generated by the help of the Swiss Modeler tool. The (x-axis) of ramachandran diagram shows phi angle and (y-axis) of ramachandran diagram shows psi angle. From 0-180 degree the beta sheets were shown on the left hand. On the right hand from 0-180 degree, the left-handed alpha helices were shown and on the left hand from 0 to -180 degree, the right-handed alpha helices

were represented. The area of the plot was divided into four regions, dark green was the mostly favored region, tea green region was the generously allowed region, the light green region was the additional allowed region and the white region was the disallowed region in the Ramachandran plot of the sequence 7 as shown in the figure (4.47).

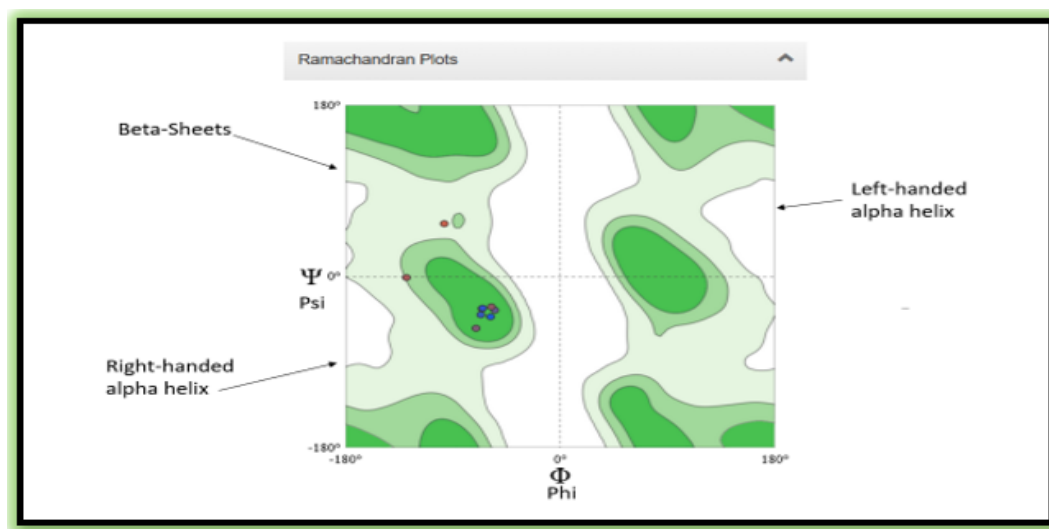


FIGURE 4.47: Ramachandran Plot of the Sequence 7.

The Ramachandran plot considered the more stable when the 90% of the psi and phi values was present in the most favored region. The proline molecules were indicated as the red dots in the Ramachandran plot, the glycine molecules were indicated as the blue dots and the pre-proline molecules were indicated as the pink dots. These three molecules are major molecules which constructs the Ramachandran plot. The Ramachandran plot of the sequence 7 showed the not stable model of the Ramachandran plot as shown in the figure (4.47). Because the proline, glycine and pre-proline was not present in most favored region between the psi and phi angle.

4.11.8 3D Structure of Sequence 8

The figure (4.48) showed 3D structure of sequence 8. The 3D structure was predicted by using the Swiss Modeler tool and the alpha helices, beta sheets and coils were shown in the 3D structure of the sequence 8.

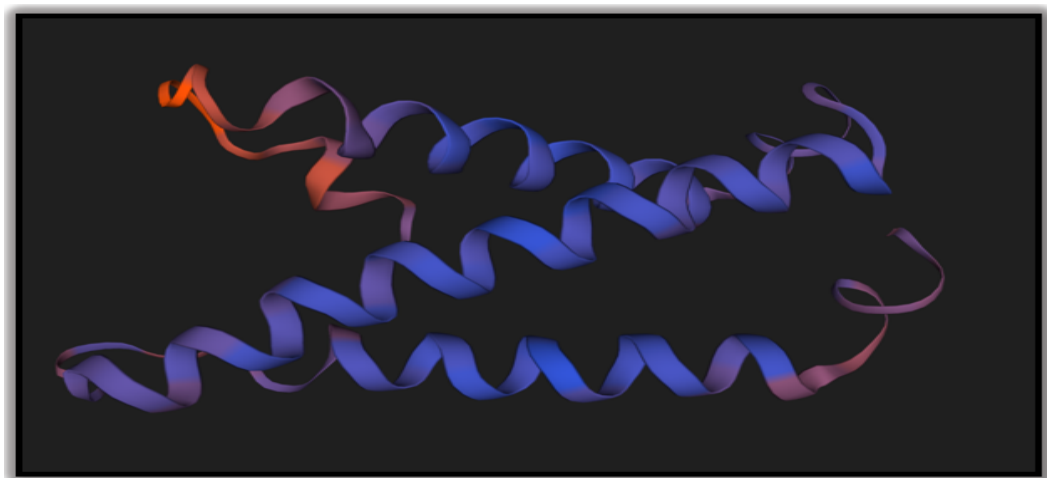


FIGURE 4.48: 3D Structure of the Sequence 8.

The Ramachandran plot was generated by the help of the Swiss Modeler tool. The (x-axis) of ramachandran diagram shows phi angle and (y-axis) of ramachandran diagram shows psi angle. From 0-180 degree the beta sheets were shown on the left hand. On the right hand from 0-180 degree, the left-handed alpha helices were shown and on the left hand from 0 to -180 degree, the right-handed alpha helices were represented. The area of the plot was divided into four regions, dark green was the mostly favored region, tea green region was the generously allowed region, the light green region was the additional allowed region and the white region was the disallowed region in the Ramachandran plot of the sequence 8 as shown in the figure (4.49).

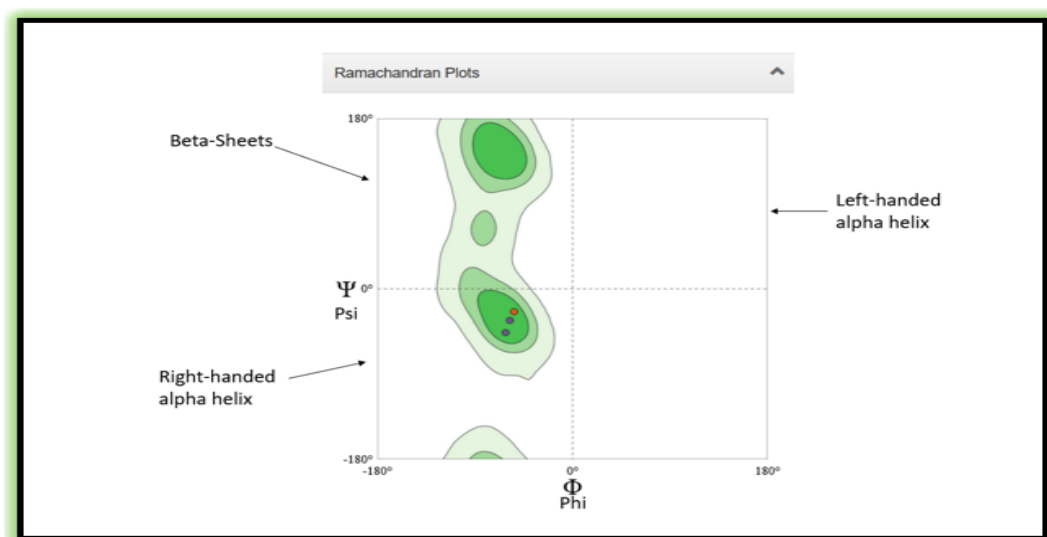


FIGURE 4.49: Ramachandran Plot of the Sequence 8.

The Ramachandran plot considered the more stable when the 90% of the psi and phi values was present in the most favored region. The proline molecules were indicated as the red dots in the Ramachandran plot, the glycine molecules were indicated as the blue dots and the pre-proline molecules were indicated as the pink dots. These three molecules are major molecules which constructs the Ramachandran plot. The Ramachandran plot of the sequence 8 showed the not stable model of the Ramachandran plot as shown in the figure (4.49). Because the proline, glycine and pre-proline was not present in most favored region between the psi and phi angle.

4.11.9 3D Structure of Sequence 9

The figure (4.50) showed 3D structure of sequence 9. The 3D structure was predicted by using the Swiss Modeler tool and the alpha helices, beta sheets and coils were shown in the 3D structure of the sequence 9.

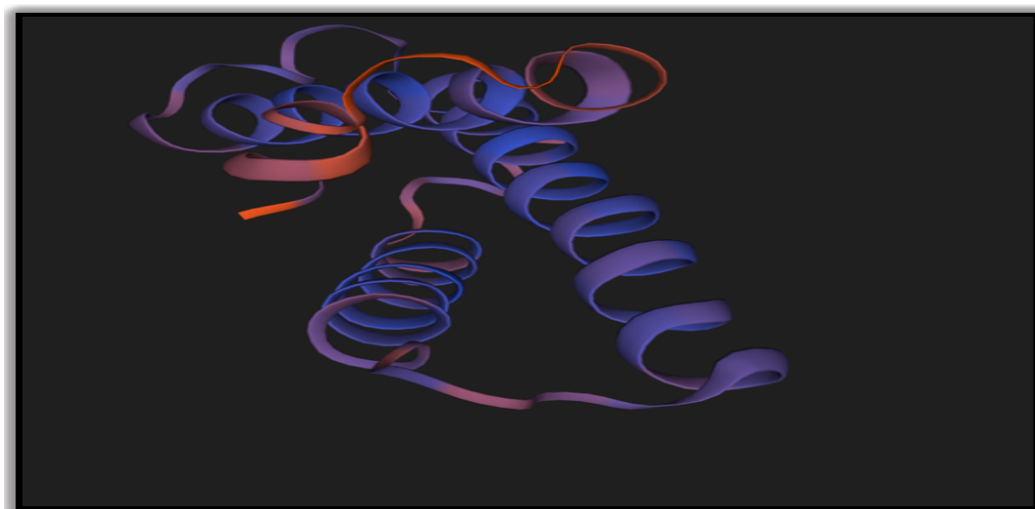


FIGURE 4.50: 3D Structure of the Sequence 9.

The Ramachandran plot was generated by the help of the Swiss Modeler tool. The (x-axis) of ramachandran diagram shows phi angle and (y-axis) of ramachandran diagram shows psi angle. From 0-180 degree the beta sheets were shown on the left hand. On the right hand from 0-180 degree, the left-handed alpha helices were shown and on the left hand from 0 to -180 degree, the right-handed alpha helices

were represented. The area of the plot was divided into four regions, dark green was the mostly favored region, tea green region was the generously allowed region, the light green region was the additional allowed region and the white region was the disallowed region in the Ramachandran plot of the sequence 9 as shown in the figure (4.51).

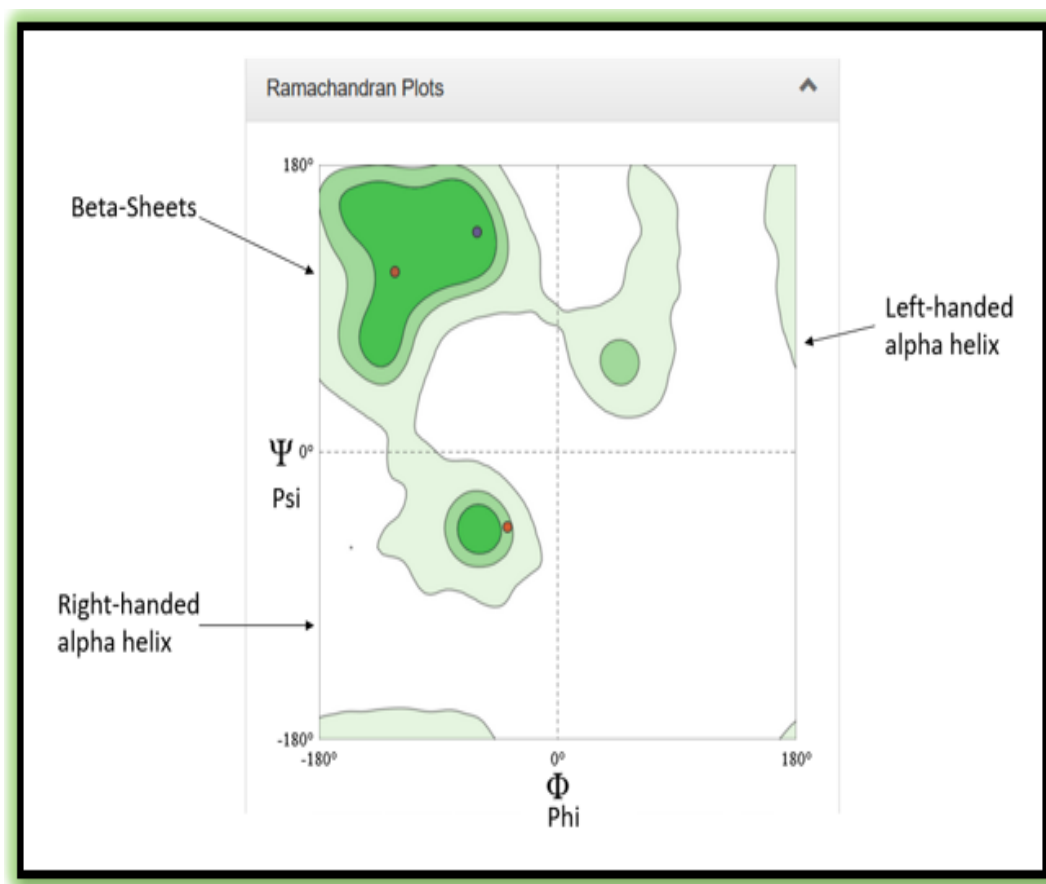


FIGURE 4.51: Ramachandran Plot of the Sequence 9.

The Ramachandran plot considered the more stable when the 90% of the psi and phi values was present in the most favored region. The proline molecules were indicated as the red dots in the Ramachandran plot, the glycine molecules were indicated as the blue dots and the pre-proline molecules were indicated as the pink dots. These three molecules are major molecules which constructs the Ramachandran plot. The Ramachandran plot of the sequence 9 showed the not stable model of the Ramachandran plot as shown in the figure (4.51). Because the proline, glycine and pre-proline was not present in most favored region between the psi and phi angle. This was used to find the angles in 3D structure of protein.

4.12 Molecular Docking of *Pediculides* (Insecticides) with KRD Sequences of Head Louse

The molecular docking of the *pediculides* such as Malathion, pyrethroids, lindane and carbaryl with the reference sequences of the knockdown resistance genes of the head louse was done to check the binding affinity of the *pediculides* with the resistance genes. These *pediculides* were considered as the ligands for the molecular docking. The structures of these *pediculides* were downloaded from the RCSB PDB in the PDB format.

4.12.1 Molecular Docking of *Pediculides* with the Reference Sequences

The 3D structures of the *pediculides* such as Malathion, pyrethroids, lindane and carbaryl were downloaded from the PDB in the PDB format. The structures of these molecules were cleaned in the Bio-discovery studio tool and using this tool the hydrogen atoms, water molecules and HETAM molecules were removed. The HETAM molecules are the previously docked ligands. The molecular docking was done by the PyRx tool and the results of molecular docking were visualized in the Bio-discovery studio tool.

The purpose of the molecular docking was to check that whether the resistance is caused by the binding of the ligands with the reference sequences or not. In the molecular docking, the three *pediculides* such as Malathion, pyrethroids and carbaryl were docked successfully with reference sequences of head louse's whole genome. But the lindane did not show any binding with the reference sequences.

From the molecular docking, it was clear that if the ligands (*pediculides*) does not bind with the proteins that were given in the form of the PDB structures then it shows resistance and if the binding energy were less than ligands (*pediculides*) bind but its binding was not stable. These factors show that the head lice of Pakistan were resistant to that ligands/*pediculides*.

So, the human head lice of Pakistan were resistant for the *pediculide* such as Lindane, whereas for the Malathion, Pyrethroids and Carbaryl the head lice have not shown any resistance. The molecular docking of the *pediculides* with the reference sequences were shown in the figure (4.52), (4.53), (4.54).

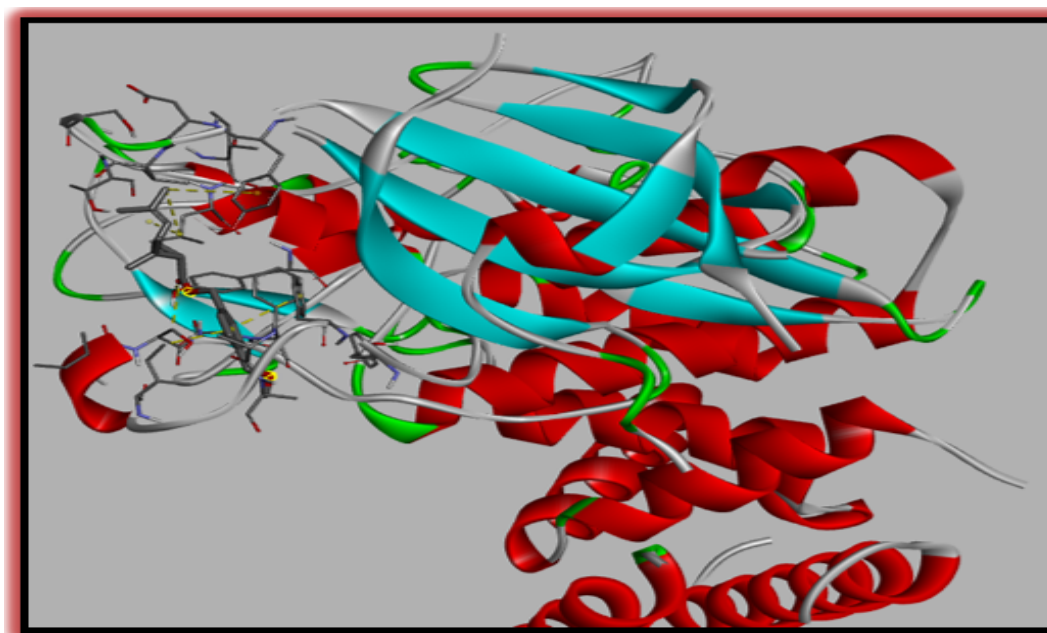


FIGURE 4.52: Molecular Docking of Sequence 1, sequence 2 and sequence 3 with the *Pediculides* (Malathion, pyrethroids and carbaryl).

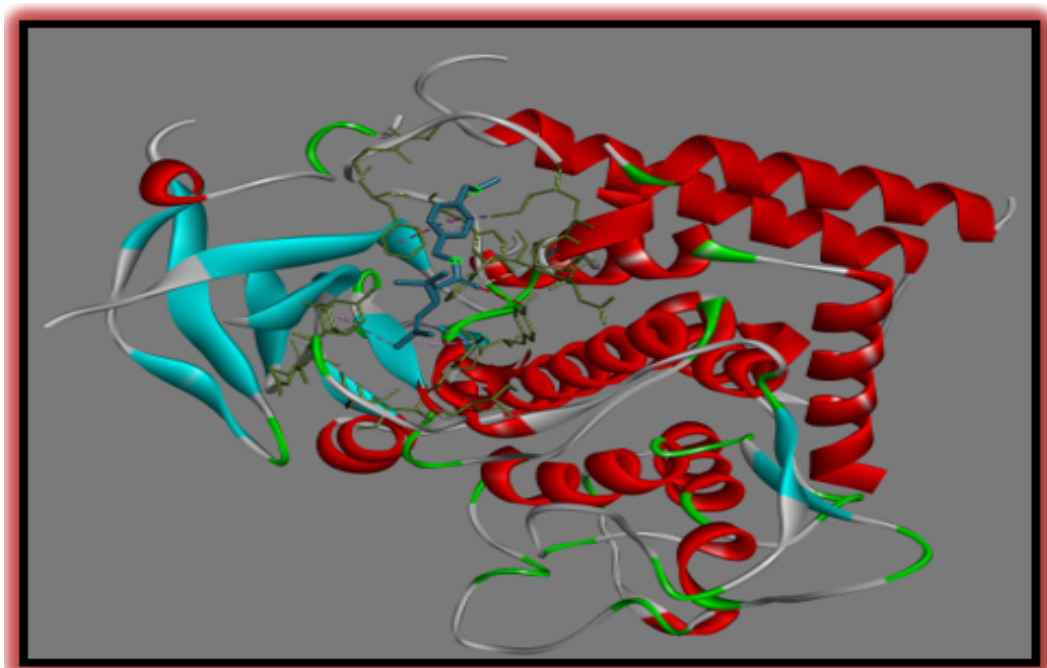


FIGURE 4.53: Molecular Docking of Sequence 4, sequence 5 and sequence 6 with the *Pediculides* (Malathion, pyrethroids and carbaryl).

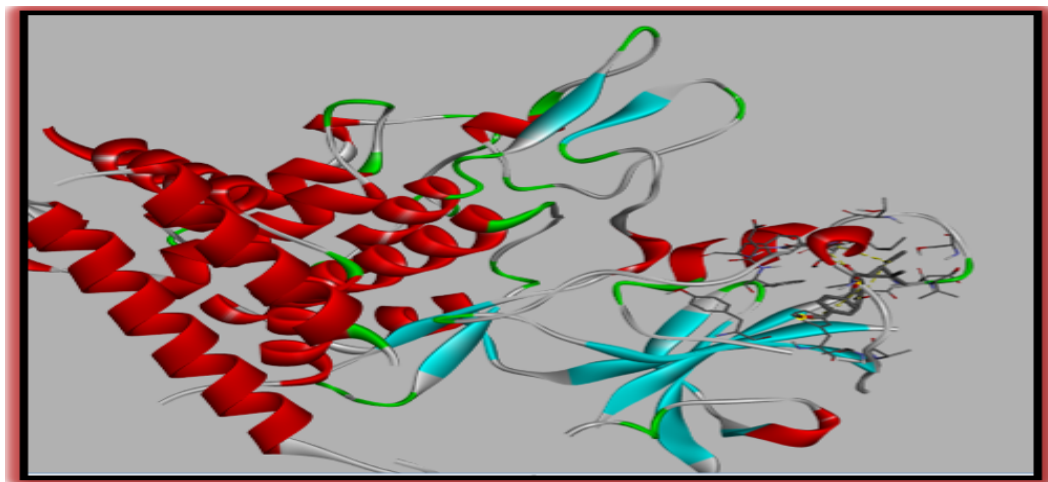


FIGURE 4.54: Molecular Docking of Sequence 7, sequence 8 and sequence 9 with the *Pediculides* (Malathion, pyrethroids and carbaryl).

4.13 Reasons of Binding of *Pediculides* with the Reference Sequences

The reason of the binding of the *pediculides* with the reference sequences in molecular docking was due to hydrogen bonding, hydrophobicity, aromatic compound as well as the binding affinity or energy present in the them. The binding of the ligands (*pediculides*) with the reference sequences (1, 2 and 3) was due to the aromatic shown in the figure (4.55) and hydrophobic was shown in the Figure (4.56) and the binding affinity were given in the table 4.10.

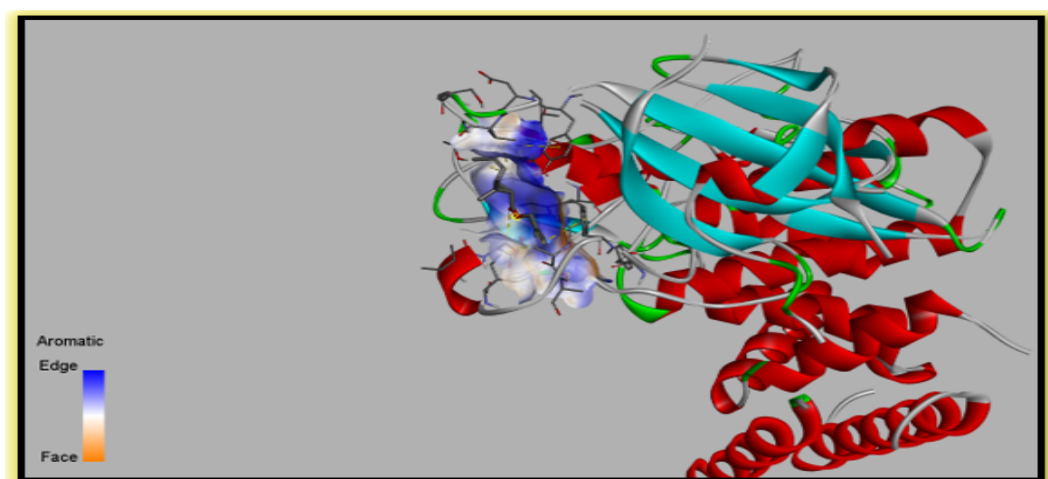


FIGURE 4.55: Binding due to Aromatic Compounds in Sequence 1, 2, 3.

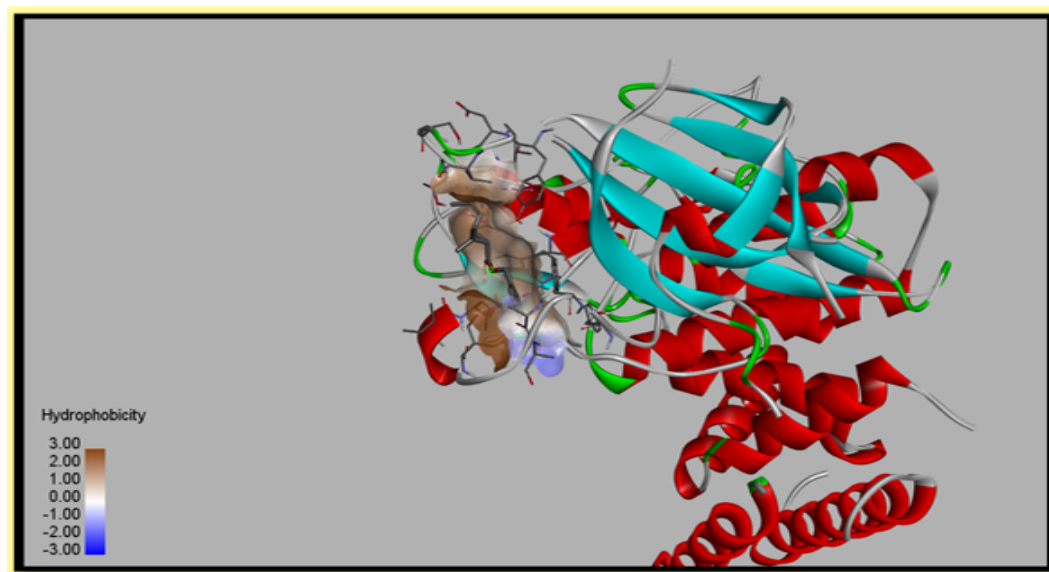


FIGURE 4.56: Binding due to Hydrophobicity in Sequence 1, 2, 3.

The binding of the ligands (*pediculides*) with the reference sequences (4, 5 and 6) was aromatic shown in the figure (4.57), hydrophobic was shown in the figure (4.58) and the hydrogen bonding was shown in the Figure (4.59) and the binding affinity were given in the table 4.10.

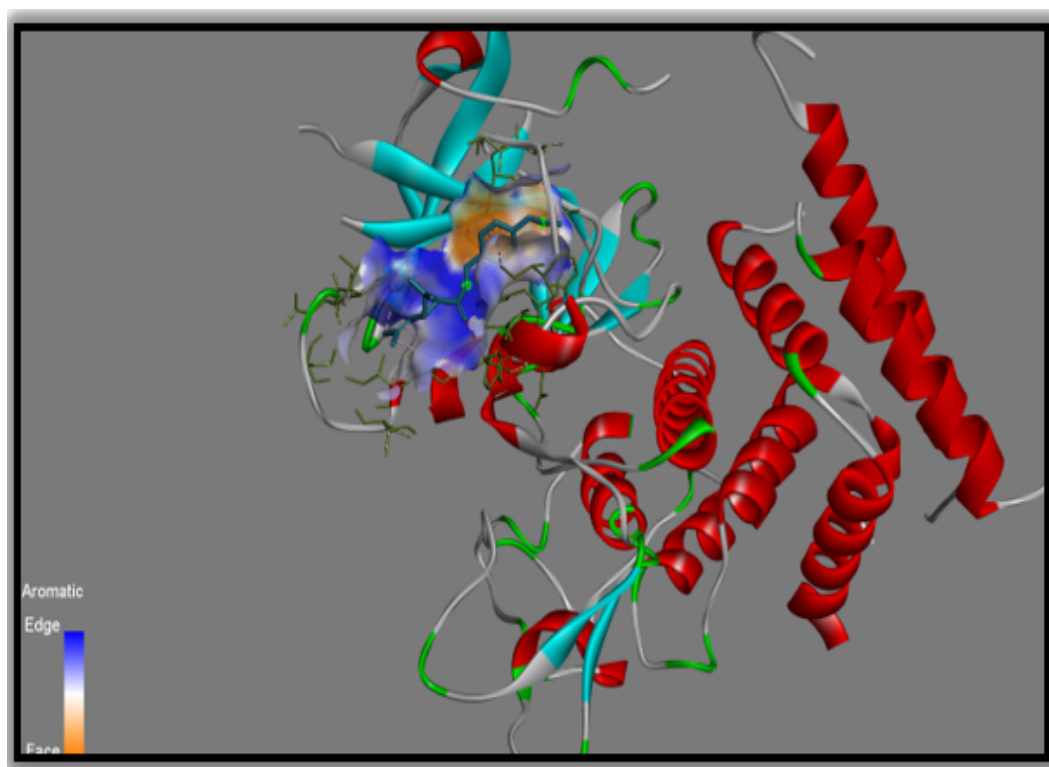


FIGURE 4.57: Binding due to Aromatic Compounds in Sequence 4, 5, 6.

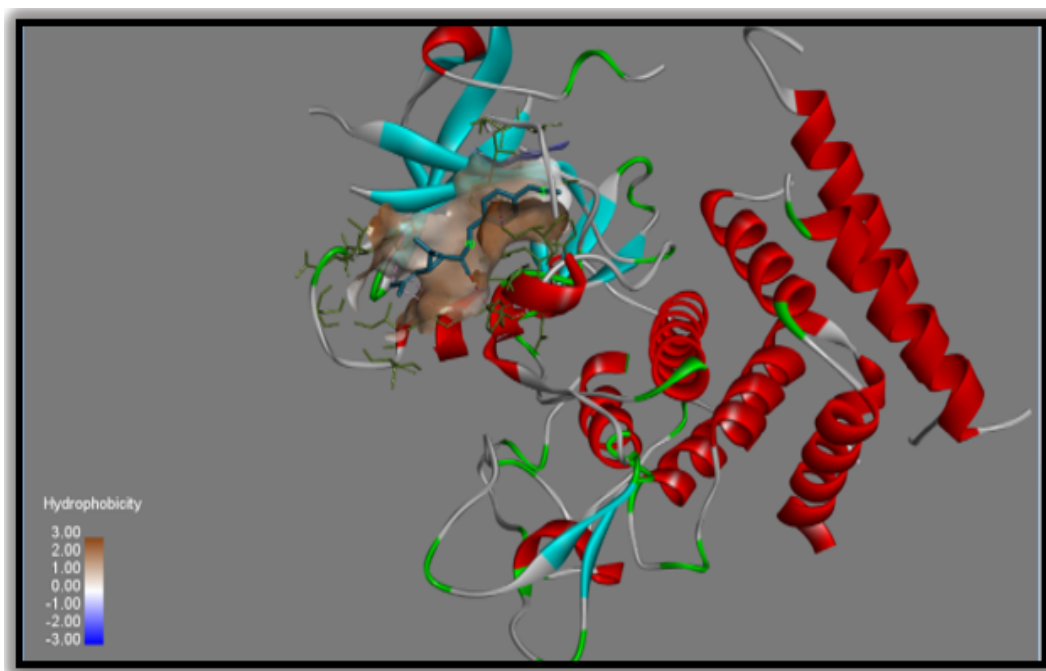


FIGURE 4.58: Binding due to Hydrophobicity in Sequence 4, 5, 6.

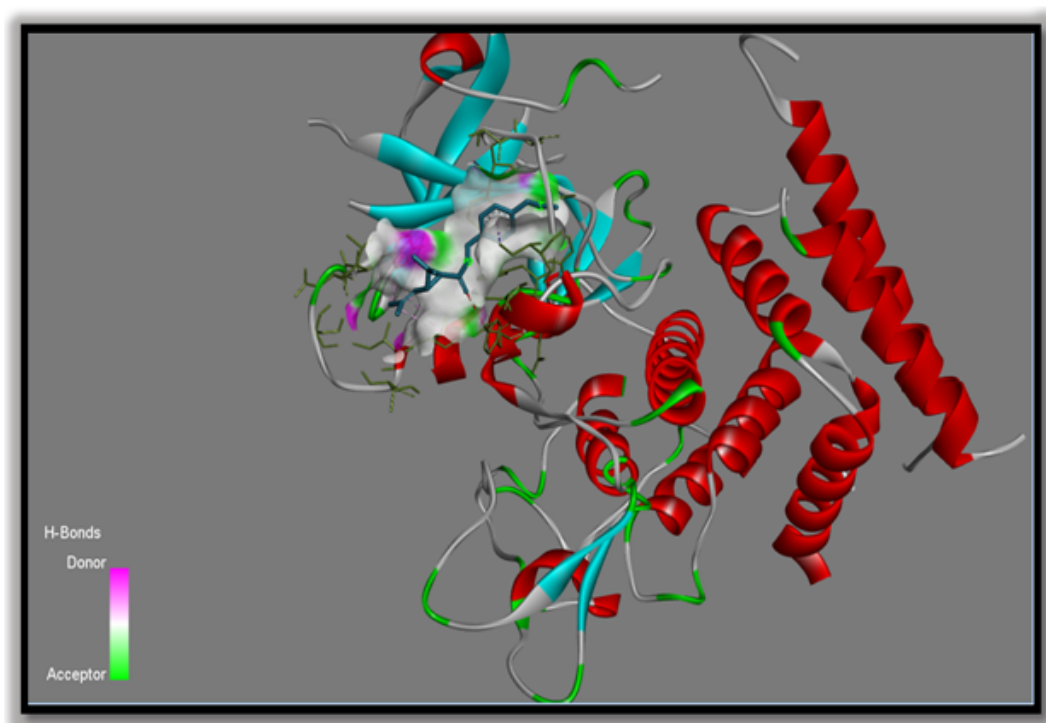


FIGURE 4.59: Binding due to Hydrogen Bonding in Sequence 4, 5, 6.

The binding of the ligands (*pediculides*) with the reference sequence 7, sequence 8 and sequence 9 was due to the hydrogen bonding was shown in the Figure (4.60) and the binding affinity were given in the table 4.10.

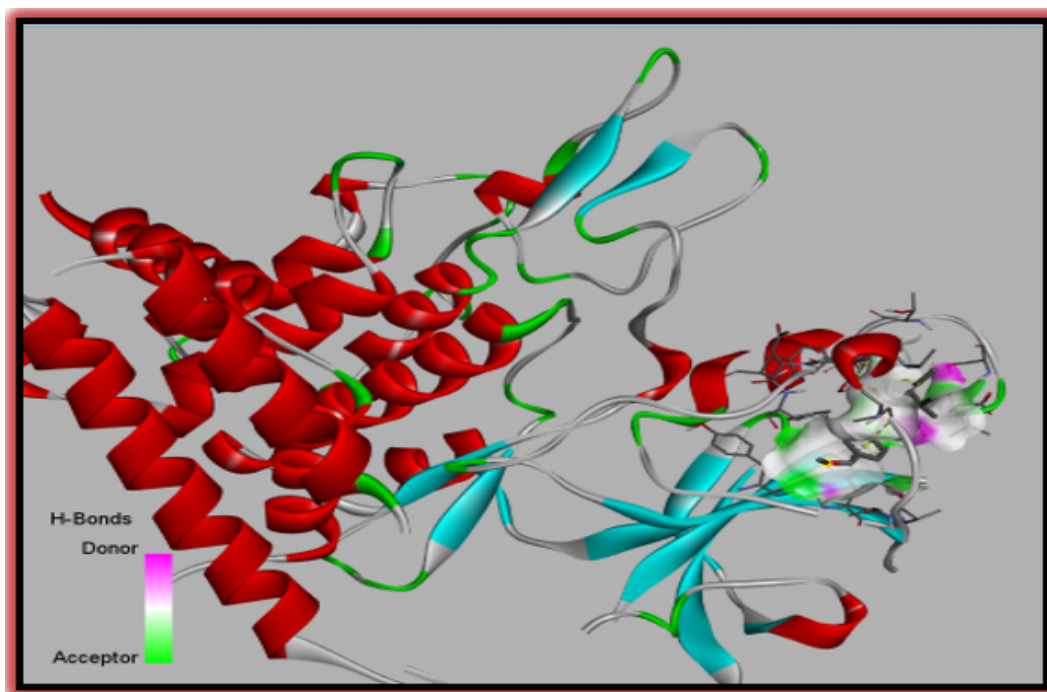


FIGURE 4.60: Binding due to Hydrogen Bonding in Sequence 7, 8, 9.

The human head lice of Pakistan were resistant for the *pediculide* such as Lindane because it was not bind with any of the reference sequences so their bind affinity was not noticing, whereas for the Malathion, Pyrethroids and Carbaryl the head lice have not shown any resistance. The binding of the Pyrethroids and Malathion was more stable with the reference sequences because of high binding affinity and the Carbaryl do not show stable binding with reference sequences because of less binding affinity which was mentioned in the table 4.10.

TABLE 4.10: Binding Affinities of the *Pediculides* (Ligands) with the Reference Sequences.

Name of Ligands	Binding Affinity of ligand with Sequence 1, 2 and 3	Binding Affinity of ligand with Sequence 4, 5 and 6	Binding Affinity of ligand with Sequence 7, 8 and 9
Pyrethroid	-8.1	-7.1	-6.1
Malathion	-6.8	-6.4	-5.9
Carbaryl	-5	-4.6	-3.4
Lindane	-	-	-

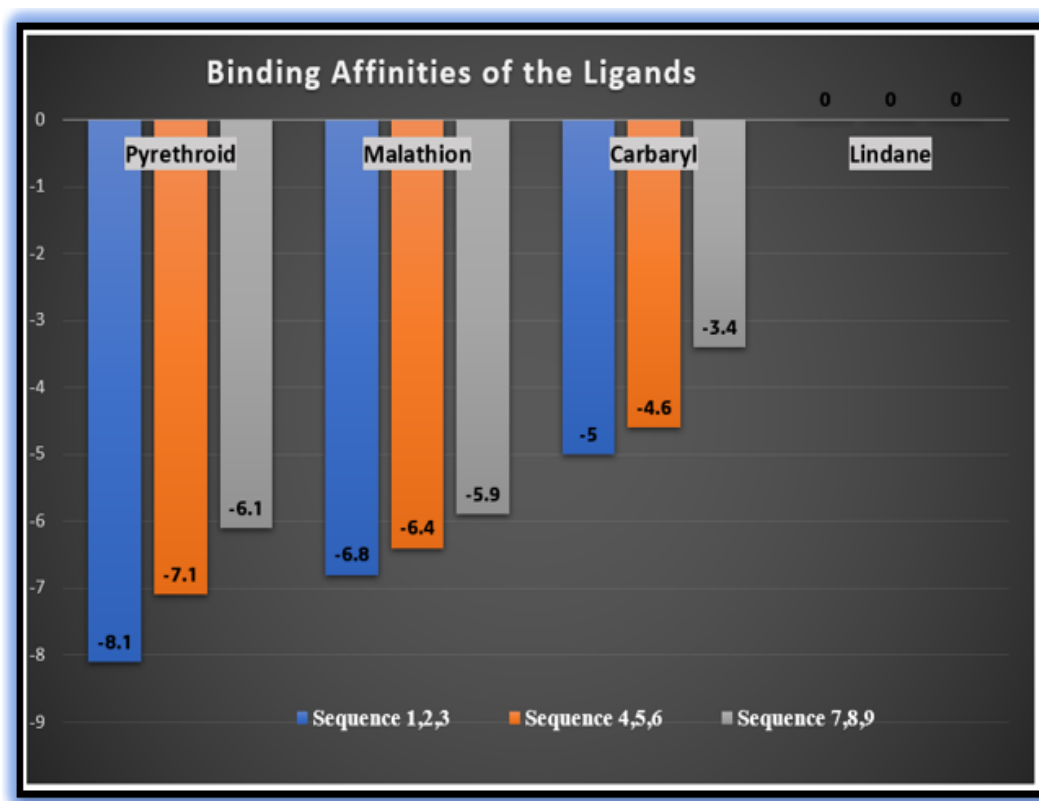


FIGURE 4.61: Graphical Representation of the Binding Affinities of the Ligands.

The figure (4.61) represent the graphical representation of the binding affinities of the ligands (*pediculides*) with the reference sequences. The blue bar represents the sequence 1, 2, 3. The orange bar represents the sequence 4, 5, 6 and the grey bar represents the sequence 7, 8, 9.

4.14 Functional Annotation and Interactions of the Reference Sequences

The interactions of the reference protein sequences were found by using the Cytoscape and STRING soft wares. The purpose of finding the interactions of the proteins was to know about the functions of the proteins as well as the interaction of the reference proteins with the other proteins. The reference protein or query protein has shown the interactions with the proteins of the body louse because the genome of head louse was not available in the databases. The query sequences

were the knockdown resistance genes which were obtained from the WG (whole genome) sequencing of the *Pediculus humanus capitis*. The interaction of query protein was noticed with the different proteins such as voltage gated calcium, sodium channel proteins, zinc finger RNA, kinase like proteins, c-AMP dependent proteins, L-type calcium channels, uncharacterized proteins and Pumilio proteins as shown in figure (4.62).

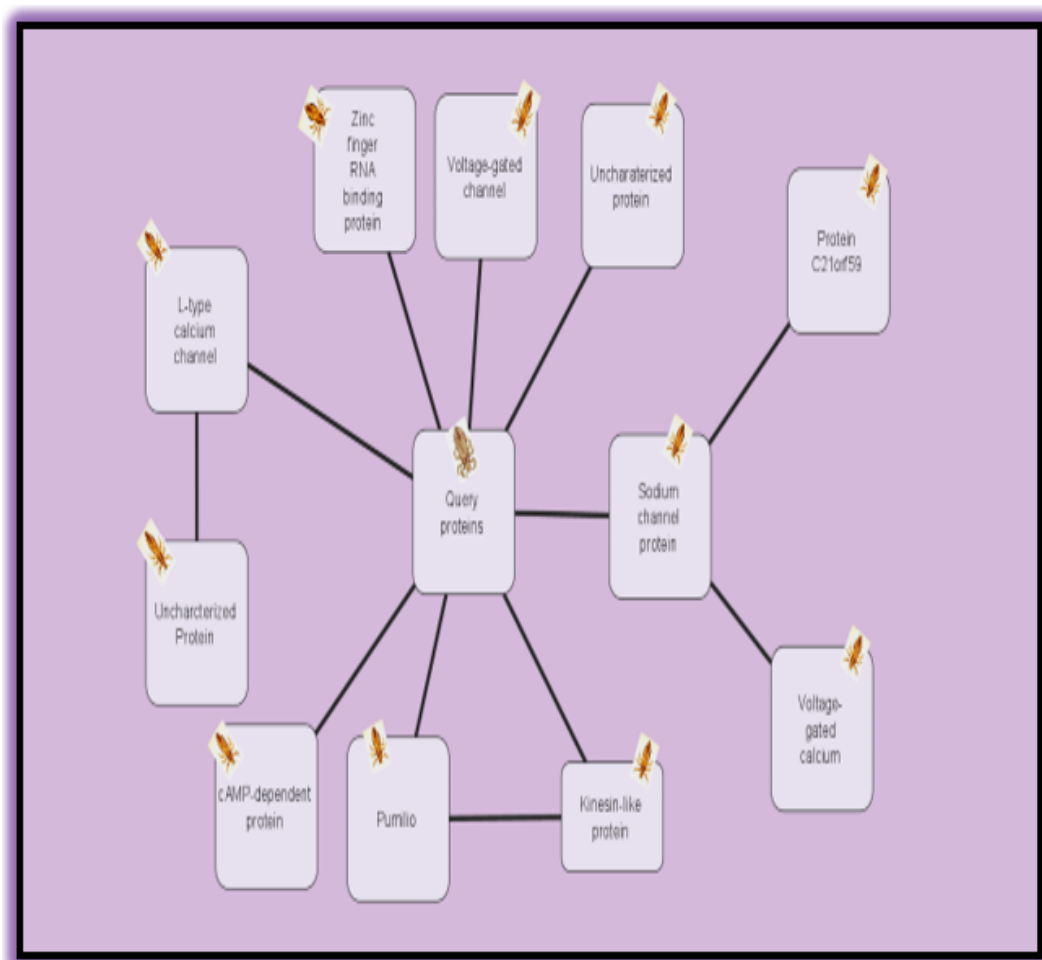


FIGURE 4.62: The Interactions of the Reference (query) Protein of head louse with Proteins of human body lice.

The table 4.11 showed the functional annotation of the mapped knockdown resistance genes on the basis of the structures of the sequences. Functional annotation was done in order to find the effects of the resistance genes in the genome of human head louse.

TABLE 4.11: Functional Annotation of the Mapped Knockdown Resistance Genes.

Sequence 1, 2, and 3	Sequence 4, 5 and 6	Sequence 7, 8 and 9
(a)Neurological System Process,	(a)Neurological System Process,	(a)Neurological System Process,
(b)Transporter Activity,	(b)Homeostatic Process,	(b)Vesicle,
(c)Plasma Membrane,	(c)Adenyl- Nucleotide Binding,	(c)Regulation of Metabolic Process,
(d)Cell Periphery,	(d)Catalytic Activity,	(d)Organelle Membrane,
(e)Transporter Activity,	(e)ATP Binding,	(e)Transmembrane Transport,
(f)It also promotes purine ribo- nucleoside binding,	(f)Pyrophos- phatase Activity,	(f)Macromolecule Biosynthetic Process,
(g)It also helps in the transporter activity.	(g)Nucleotide binding,	(g)Cellular Localization,
	(h)Ion Transport.	(h)ATPASE Activity.

Resistance is an inherited genetic feature induced by recessive allelic mutations

found in insects exposed to DDT, pyrethroids, or both at some time in their evolutionary history. Point mutations in the VSSC subunit gene that cause Kdr (M815I, T917I, L920F, etc.) have been found in resistant lice and utilised as pyrethroid resistance markers [149]. Although the presence of the *kdr* gene mutation does not guarantee clinical failure, its greater prevalence in head lice populations is consistent with reports of product failure in controlled studies. Unfortunately, because conventional *pediculicides* are widely used in many parts of the world, resistant louse populations have arisen and are fast expanding [149].

This has prompted research into the development of molecules with alternative modes of action. The most promising new *pediculicides* appear to be ivermectin and spinosad. They have sparked curiosity in novel neurotoxic modes of action. It is relatively low in mammalian toxicity and cross-resistance with routinely used conventional *pediculicides* [150].

Insecticide resistance, which leads to treatment failure, is thought to be a major cause in the rising prevalence of head louse infections [151], [152]. The freshly sequenced louse genome provides a once-in-a-lifetime chance to answer fundamental issues about the molecular pathways that govern pesticide resistance. This is critical to extending the active life of current pesticides and accelerating the development of new, more effective, and sustainable pesticide tactics [153].

Resistance mechanisms include rapid pesticide detoxification by enzyme-mediated reduction, esterification, and oxidation, which can be countered by synergists like piperonyl butoxide. Changes in acetylcholinesterase or voltage-gated sodium channels in neurons, as well as knockdown resistance (*kdr*). Clinical, parasitological, and genetic findings on resistance to traditional topical *pediculicides* show that neurotoxic pesticide therapy has lost considerable effectiveness globally [154] [155]. Resistance to synthetic pyrethroid medicines, in particular, has become noticeable, owing to their widespread usage.

Because of effectiveness and safety issues, older pesticides such as lindane and carbaryl should be avoided, since new treatment options, including non-insecticidal *pediculicides* such as dimethicone, are now available. Except in the U.K, the

organophosphate pesticide malathion is still effective in formulations containing mostly terpineol [156].

Lindane, also known as γ -hexachlorocyclohexane, is an organochlorine insecticide that is not aromatic. When *kdr* gained considerable resistance to DDT in white lice in the 1950s. But lindane, an insecticide that works on the γ -aminobutyric acid-gated chloride channel, was introduced, and soon head lice developed DDT resistance [157]. It has become a popular medication is used for white insects(lice). Lindane was formerly the most extensively used *pediculicide* in the U.S.A until the advent of pyrethroids [158]. Lindane, which is only available by prescription as a 1% shampoo, is a neurotoxic chemical that overstimulates the central fear system. It is, however, only somewhat ovicidal (today, 30-50% of eggs are not harmed) [159]. For many years, resistance has been proposed all across the world. Cure rates ranged from 43% to 91% 14 days following treatment of lindane 0.5% lotion or 1% shampoo in the 1980s [159]. In one research, one percent lindane shampoo was the least positive *pediculicide* tested in USA. Moreover, lindane, malathion, pyrethrins, and permethrin were the least positive *pediculicides* gathered in Florida and Panama, respectively. It was efficient against lice that were resistant to therapy. Only 17% and 61% of Florida and Panama lice were helpful after a 3-hour exposure, respectively [160]. However, lindane had a 93% success rate in South Korea, where all other *in vitro* trials were published in 1999 [157]. Concerns have been raised that the negative effects of lindane lead to reuse and overuse, raising the risk of skin injury or diseases [160].

From results it was clear that not only the novel mutations in the resistance causing genes and proteins were identified that was at M34I and I34F but also the insecticides (*pediculides*) were found. With the molecular docking we came to know that the human head lice of Pakistan were resistant for the *pediculide* such as Lindane, whereas for the Malathion, Pyrethroids and Carbaryl the head lice have not shown any resistance. Because the Lindane do not bind with reference sequences whereas the Malathion, Pyrethroids and Carbaryl bind with the reference sequences. This study is helpful for researchers in designing the control and treatment for the head louse infestation or *pediculosis* in Pakistan.

4.15 Submission of Mutations in NCBI

The 9 reference sequences with Noval Mutation were submitted in NCBI as a kdr gene with the Accession Id "OP136150 "

```

LOCUS      ghi3                2298 bp    DNA     linear   INV 04-AUG-2022
DEFINITION kdr mutated gene3, partial cds.
ACCESSION  OP136150
VERSION
KEYWORDS   .
SOURCE     Pediculus humanus capitis (human head louse)
ORGANISM   Pediculus humanus capitis
            Eukaryota; Metazoa; Ecdysozoa; Arthropoda; Hexapoda; Insecta;
            Pterygota; Neoptera; Paraneoptera; Psocodea; Phthiraptera;
            Anoplura; Pediculidae; Pediculus.
REFERENCE  1 (bases 1 to 2298)
AUTHORS    Ishtiaq,M., Khatoon,N. and Fazal,S.
TITLE      Direct Submission
JOURNAL    Submitted (04-AUG-2022) Daparment of Bioinformatics and
            Biosciences, Capital University of Science and Technology,
            Islamabad Expressway, Kahuta Road Zone-V Sihala, Islamabad,
            Islamabad Capital Territory, Islamabad, Punjab 46000, Pakistan
COMMENT    Bankit Comment: ALT EMAIL:muneeba2208@gmail.com
            Bankit Comment: TOTAL # OF SEQS:1

            ##Assembly-Data-START##
            Assembly Method      :: Geneious De Novo Assembler v. 2020.2;
                                   Velvet Assembler v. 2020.2
            Assembly Name        :: Headlice KDR
            Coverage              :: 6x
            Sequencing Technology :: Illumina
            ##Assembly-Data-END##

FEATURES   Location/Qualifiers
            source                1..2298
                                   /organism="Pediculus humanus capitis"
                                   /mol_type="genomic DNA"
                                   /sub_species="capitis"
                                   /db_xref="taxon:121226"
                                   /country="Pakistan"
                                   /collection_date="5/5/2022"
                                   /collected_by="Muneeba Ishtiaq"
                                   /biotype="Hair"
            gene                  <1..>2298
                                   /gene="knockdown resistance gene 3"
            CDS                   <1..>2298
                                   /gene="knockdown resistance gene 3"
                                   /codon_start=1
                                   /product="voltage-sensitive sodium channel alpha-subunit
                                   1"
                                   /translation="IIQIACRQFNMYLASPLIAYKFLQQKSIGKLSSTFPPIYTTNLD
                                   HLMGSLQQIATKSNVIIPELLEFRNYPHLVEEVRGWDAPNHITRNFSNKPGLLRDYN
                                   KVMVHRIGLIILFFLQSWRFSINMSFGSKNLIFFPKSKKILYKIMHSRVEGQATYYYY

```

FIGURE 4.63: Submission of KDR gene in NCBI.

Chapter 5

Conclusions and Recommendations

Human head louse infestation also called the *pediculosis* is the main public health concern all over the world. The control and treatment of the *pediculosis* is very significant because it is the major threat for all age group people. The insecticides which are used for the treatment of the head lice infestation are Lindane, Malathion, Pyrethroids and Carbaryl. Head lice are getting resistant to these insecticides by different mutations in their genes. Keeping in view the increase in the insecticides resistance among the head lice, the resistance genes and the mutations in these genes which are leading to resistance were identified in the current research.

The outcome of the 1st objective was that the whole genome of the head louse was sequenced and the resistance genes were identified. The total genes in the head louse genome were 9942, total proteins were 9907 and the total open reading frames were 988226. There were total nine novel resistance causing genes i.e. the knockdown resistance genes and the voltage sensitive sodium channels were identified in the head louse's genome.

The outcome of the 2nd objective was to predict the mutations in the resistance causing genes or proteins and the mutations were successfully predicted using

different computational tools. There were different mutations such as at 34th position the methionine is replaced with Isoleucine and the other mutation was that at the 34th position, the Isoleucine was replaced with the Phenylalanine.

The outcome of the 3rd objective was that the mutations were verified through the PROVEAN tool and among those mutations, the mutation M34I was deleterious and the other mutation i.e. I34F was neutral. As well as to predict the 2D and 3D structures of the mutated genes.

The outcome of the 4th objective was that the mutations were functionally annotated and their impacts on the genes in causing the resistance was studied. They have different functions which includes the cell communication, neurological system process, and transporter activity. The novel mutations were submitted in the National Centre for Biotechnology Information (NCBI) and the accession ID is **OP136150**.

The study of the resistance genes, mutations and their structures helped to understand the role of these genes and these mutations in causing the resistance among human head louse which have shown resistance against the insecticides (*pediculides*) such as Lindane and have not shown resistance against the Malathion, Pyrethroids and Carbaryl. The impacts of these mutations on causing the resistance in the head louse was studied and this study is helpful for researchers in designing the control and treatment for the head louse infestation or *pediculosis*.

The future perspectives of the research are:

- Based on the novel mutations predicted in the Pakistani head lice, the novel therapies can be designed for the control of the head louse infestation.
- The role of different proteins in the head louse's genome can be studied.
- The gene silencing and modifications in the tRNA can also be done to treat and control the head lice infestations.

Bibliography

- [1] M. Karakucs, A. Arıcı, S. Ö. Töz, and Y. Özbel, “Prevalence of head lice in two socio-economically different schools in the center of Izmir City, Turkey,” *Türkiye Parazitol Derg*, vol. 38, no. 1, pp. 32–36, 2014.
- [2] T. A. Morsy, R. G. El-Ela, M. Y. Mawla, and S. A. Khalaf, “The prevalence of lice infesting students of primary, preparatory and secondary schools in Cairo, Egypt.,” *J. Egypt. Soc. Parasitol.*, vol. 31, no. 1, pp. 43–50, 2001.
- [3] Alb. Mohammed, “Head lice infestation in schoolchildren and related factors in Mafraq governorate, Jordan,” *Int. J. Dermatol.*, vol. 51, no. 2, pp. 168–172, 2012.
- [4] K. H. Tappeh, K. H., Chavshin, A. R., Hajipirloo, H. M., Khashaveh, S., Hanifan, H., Bozorgomid, A., and Azizi, H., “Pediculosis capitis among primary school children and related risk factors in Urmia, the main city of West Azarbaijan, Iran,” *J. Arthropod. Borne. Dis.*, vol. 6, no. 1, p. 79, 2012.
- [5] R. Durand, S. Bouvresse, Z. Berdjane, A. Izri, O. Chosidow, and J. M. Clark, “Insecticide resistance in head lice: clinical, parasitological and genetic aspects,” *Clin. Microbiol. Infect.*, vol. 18, no. 4, pp. 338–344, 2012.
- [6] D. L. Reed, J. E. Light, J. M. Allen, and J. J. Kirchman, “Pair of lice lost or parasites regained: the evolutionary history of anthropoid primate lice,” *Bmc Biol.*, vol. 5, no. 1, pp. 1–11, 2007.
- [7] R. Drali, K. Mumcuoglu, and D. Raoult, “Human lice in paleoentomology and paleomicrobiology,” *Microbiol. Spectr.*, vol. 4, no. 4, p. 4, 2016.

- [8] A. Veracx and D. Raoult, “Biology and genetics of human head and body lice,” *Trends Parasitol.*, vol. 28, no. 12, pp. 563–571, 2012, doi: 10.1016/j.pt.2012.09.003.
- [9] J. E. Light, M. A. Toups, and D. L. Reed, “What’s in a name: The taxonomic status of human head and body lice,” 2008, doi: 10.1016/j.ympev.2008.03.014.
- [10] J. E. D., Raoult and V. Roux., “Geographic distributions and origins of human head lice (*Pediculus humanus capitis*) based on mitochondrial data,” *J. Parasitol.*, vol. 94, no. 6, pp. 1275–1281, 2008.
- [11] W. Li., Ortiz, G., Fournier, P. E., Gimenez, G., Reed, D. L., Pittendrigh, B., and Raoult, D., “Genotyping of human lice suggests multiple emergences of body lice from local head louse populations,” *PLoS Negl Trop Dis*, vol. 4, no. 3, p. e641, 2010.
- [12] P. Brouqui, “Arthropod-Borne Diseases Associated with Political and Social Disorder,” *Annu. Rev. Entomol.*, vol. 56, no. 1, pp. 357–374, Jan. 2011, doi: 10.1146/annurev-ento-120709-144739.
- [13] O. Chosidow, “Scabies and pediculosis,” *Lancet*, vol. 355, no. 9206, pp. 819–826, 2000.
- [14] D. Raoult and V. Roux, “The body louse as a vector of reemerging human diseases,” *Clin. Infect. Dis.*, vol. 29, no. 4, pp. 888–911, 1999.
- [15] M. A. Davarpanah, A. R. Kazerouni, H. Rahmati, R. N. Neirami, H. Bakhtiary, and M. Sadeghi, “The prevalence of pediculus capitis among the middle schoolchildren in Fars Province, southern Iran,” *Casp. J. Intern. Med.*, vol. 4, no. 1, p. 607, 2013.
- [16] H. Lapeere., “Efficacy of products to remove eggs of *Pediculus humanus capitis* (Phthiraptera: Pediculidae) from the human hair,” *J. Med. Entomol.*, vol. 51, no. 2, pp. 400–407, 2014.

- [17] M. Zahirneia, H. Taherkhani, and J. Bathaei, "Comparison assessment of three shampoo types in treatment of infestation of head lice in elementary school girl in Hamadan," *J Maz. Univ Med Sci*, vol. 49, no. 9e11, p. 16e24, 2005.
- [18] H. Feldmeier and J. Heukelbach, "Epidermal parasitic skin diseases: a neglected category of poverty-associated plagues," *Bull. World Health Organ.*, vol. 87, pp. 152–159, 2009.
- [19] J. Heukelbach and U. S. Ugbomoiko, "Knowledge, attitudes and practices regarding head lice infestations in rural Nigeria," *J. Infect. Dev. Ctries.*, vol. 5, no. 09, pp. 652–657, 2011.
- [20] A. Omidi, M. Khodaveisi, B. A. MOGHIM, N. Mohammadi, and R. Amini, "Pediculosis capitis and relevant factors in secondary school students of Hamadan, West of Iran," 2013.
- [21] A. Vahabi, Shemshad, K., Sayyadi, M., Biglarian, A., Vahabi, B., Sayyad, S., ... and Rafinejad, J., "Prevalence and risk factors of *Pediculus (humanus) capitis* (Anoplura: Pediculidae), in primary schools in Sanandaj City, Kurdistan Province, Iran," *Trop Biomed*, vol. 29, no. 2, pp. 207–211, 2012.
- [22] A. L. Donaldson, J. L. Hardstaff, J. P. Harris, R. Vivancos, and S. J. O'Brien, "School-based surveillance of acute infectious disease in children: a systematic review," *BMC Infect. Dis.*, vol. 21, no. 1, pp. 1–10, 2021.
- [23] M. E. Falagas, D. K. Matthaïou, P. I. Rafailidis, G. Panos, and G. Pappas, "Worldwide prevalence of head lice," *Emerg. Infect. Dis.*, vol. 14, no. 9, pp. 1493–1494, 2008.
- [24] A. Boutellis, L. Abi-Rached, and D. Raoult, "The origin and distribution of human lice in the world," *Infect. Genet. Evol.*, vol. 23, pp. 209–217, 2014.
- [25] C.-W. Liao, Chuang, T. W., Huang, Y. C., Chou, C. M., Chiang, C. L., Lee, F. P., ... and Fan, C. K., "Intestinal parasitic infections: Current prevalence

- and risk factors among schoolchildren in capital area of the Republic of Marshall Islands,” *Acta Trop.*, vol. 176, pp. 242–248, 2017.
- [26] A. L. Donaldson, J. P. Harris, R. Vivancos, and S. J. O’Brien, “Risk factors associated with outbreaks of seasonal infectious disease in school settings, England, UK,” *Epidemiol. Infect.*, vol. 148, 2020.
- [27] J. Heukelbach and H. Feldmeier, “Ectoparasites—the underestimated realm,” *Lancet*, vol. 363, no. 9412, pp. 889–891, Mar. 2004, doi: 10.1016/S0140-6736(04)15738-3.
- [28] S. Dogra and B. Kumar, “Epidemiology of skin diseases in school children: a study from northern India,” *Pediatr. Dermatol.*, vol. 20, no. 6, pp. 470–473, 2003.
- [29] K. Hatam-Nahavandi ., “Pediculosis capitis among school-age students worldwide as an emerging public health concern: a systematic review and meta-analysis of past five decades,” *Parasitol. Res.*, vol. 119, no. 10, pp. 3125–3143, 2020.
- [30] A. Izri and O. Chosidow, “Efficacy of machine laundering to eradicate head lice: recommendations to decontaminate washable clothes, linens, and fomites,” *Clin. Infect. Dis.*, vol. 42, no. 2, pp. e9–e10, 2006.
- [31] C. N. Burkhart and C. G. Burkhart, “Fomite transmission in head lice,” *J. Am. Acad. Dermatol.*, vol. 56, no. 6, pp. 1044–1047, 2007.
- [32] L. Meister and F. Ochsendorf, “Head lice: Epidemiology, biology, diagnosis, and treatment,” *Dtsch. Arztebl. Int.*, vol. 113, no. 45, p. 763, 2016.
- [33] B. Habedank, *Läuse–Biologie, medizinische Bedeutung und Bekämpfung*. na, 2010.
- [34] F. Kamiabi and F. H. Nakhaei, “Prevalence of pediculosis capitis and determination of risk factors in primary-school children in Kerman,” *EMHJ–Eastern Mediterr. Heal. Journal*, 11 (5-6), 988-992, 2005, 2005.

- [35] A. Buczek, D. Markowska-Gosik, D. Widomska, and I. M. Kawa, "Pediculosis capitis among schoolchildren in urban and rural areas of eastern Poland," *Eur. J. Epidemiol.*, vol. 19, no. 5, pp. 491–495, 2004.
- [36] E. S. Murray and S. B. Torrey, "Virulence of *Rickettsia prowazeki* for head lice.," *Ann. N. Y. Acad. Sci.*, vol. 266, pp. 25–34, 1975.
- [37] J. H. Kim, Previte, D. J., Yoon, K. S., Murenzi, E., Koehler, J. E., Pittendrigh, B. R., ... and Clark, J. M., "Comparison of the proliferation and excretion of *Bartonella quintana* between body and head lice following oral challenge," *Insect Mol. Biol.*, vol. 26, no. 3, pp. 266–276, 2017.
- [38] N. Amanzougaghene, F. Fenollar, D. Raoult, and O. Mediannikov, "Where are we with human lice? A review of the current state of knowledge," *Front. Cell. Infect. Microbiol.*, vol. 9, p. 474, 2020.
- [39] Á. Medina, D. López, and L. R. Vásquez, "Pediculosis capitis grave en una niña inscrita en una guardera," *Biomédica*, vol. 39, no. 4, p. 631, 2019.
- [40] J. E. Jones, "Signs and symptoms of parasitic diseases," *Prim. Care Clin. Off. Pract.*, vol. 18, no. 1, pp. 1–12, 1991.
- [41] S. Jamani ., "Head lice infestations in rural Honduras: the need for an integrated approach to control neglected tropical diseases," *Int. J. Dermatol*, vol. 58, no. 5, pp. 548–556, 2019.
- [42] P. Verma and C. Namdeo, "Treatment of pediculosis capitis," *Indian J. Dermatol.*, vol. 60, no. 3, p. 238, 2015.
- [43] H. Kalari, A. Soltani, K. Azizi, H. Faramarzi, and M. D. Moemenbellah-Fard, "Comparative efficacy of three pediculicides to treat head lice infestation in primary school girls: a randomised controlled assessor blind trial in rural Iran," *BMC Dermatol.*, vol. 19, no. 1, pp. 1–9, 2019.
- [44] M. Moemenbellah-Fard, Z. Nasiri, K. Azizi, and M. Fakoorziba, "Head lice treatment with two interventions: pediculosis capitis profile in female

- schoolchildren of a rural setting in the south of Iran,” *Ann. Trop. Med. Public Heal.*, vol. 9, no. 4, 2016.
- [45] J. A. Hunter and S. C. Barker, “Susceptibility of head lice (*Pediculus humanus capitis*) to pediculicides in Australia,” *Parasitol. Res.*, vol. 90, no. 6, pp. 476–478, 2003.
- [46] H. Feldmeier, “Treatment of pediculosis capitis: a critical appraisal of the current literature,” *Am. J. Clin. Dermatol.*, vol. 15, no. 5, pp. 401–412, 2014.
- [47] H. Feldmeier, “Pediculosis capitis: new insights into epidemiology, diagnosis and treatment,” *Eur. J. Clin. Microbiol. Infect. Dis.*, vol. 31, no. 9, pp. 2105–2110, 2012.
- [48] E. F. Kirkness, Tovar-Corona, J. M., Castillo-Morales, A., Chen, L., Olds, B. P., Clark, J. M., Reynolds, S. E., ... and Urrutia, A. O., “Genome sequences of the human body louse and its primary endosymbiont provide insights into the permanent parasitic lifestyle,” *Proc. Natl. Acad. Sci. U. S. A.*, vol. 107, no. 27, pp. 12168–73, Jul. 2010, doi: 10.1073/pnas.1003379107.
- [49] B. R. Pittendrigh, B. P. Olds, K. S. Yoon, S. H. Lee, W. Sun, and J. M. Clark, “The genomics of human lice: from the genome to the potential for future control strategies,” *Pestic. Biochem. Physiol.*, vol. 106, no. 3, pp. 172–176, 2013.
- [50] R. Shao, X.-Q. Zhu, S. C. Barker, and K. Herd, “Evolution of extensively fragmented mitochondrial genomes in the lice of humans,” *Genome Biol. Evol.*, vol. 4, no. 11, pp. 1088–1101, 2012.
- [51] A. Saghafipour, J. Nejati, A. Zahraei-ramazani, and H. Vatandoost, “Prevalence and Risk Factors Associated with Head Louse (*Pediculus humanus capitis*) in Central Iran,” vol. 5, no. 43, pp. 5245–5254, 2017, doi: 10.22038/ijp.2017.23413.1967.

- [52] L. Silva, R. de A. Alencar, and N. G. Madeira, "Survey assessment of parental perceptions regarding head lice," *Int. J. Dermatol.*, vol. 47, no. 3, pp. 249–255, 2008.
- [53] P. B. Gazmuri, B. T. Arriaza, F. S. Castro, P. N. González, K. V Maripan, and I. R. Saavedra, "Epidemiological study of Pediculosis in elementary schools of Arica, northern Chile," *Rev. Chil. Pediatr.*, vol. 85, no. 3, pp. 312–318, 2014.
- [54] M. Josébressa, A. G. Papeschi, and A. C. Toloza, "Cytogenetic Features of Human Head and Body Lice (Phthiraptera: Pediculidae)," *J. Med. Entomol.*, vol. 52, no. 5, pp. 918–924, 2015, doi: 10.1093/jme/tjv089.
- [55] J. S. Kang., "Comparison of the genome profiles between head and body lice," *J. Asia. Pac. Entomol.*, vol. 18, no. 3, pp. 377–382, 2015.
- [56] J. E. Light, M. A. Toups, and D. L. Reed, "What's in a name: The taxonomic status of human head and body lice," *Mol. Phylogenet. Evol.*, vol. 47, no. 3, pp. 1203–1216, Jun. 2008, doi: 10.1016/j.ympev.2008.03.014.
- [57] J. M. Tovar-Corona, J. M., Castillo-Morales, A., Chen, L., Olds, B. P., Clark, J. M., Reynolds, S. E., ... and Urrutia, A. O., "Alternative splice in alternative lice," *Mol. Biol. Evol.*, vol. 32, no. 10, pp. 2749–2759, 2015.
- [58] R. Kittler, M. Kayser, and M. Stoneking, "Molecular evolution of *Pediculus humanus* and the origin of clothing.," *Curr. Biol.*, vol. 13, no. 16, pp. 1414–7, Aug. 2003.
- [59] A. Boutellis, L. Abi-Rached, and D. Raoult, "The origin and distribution of human lice in the world," *Infect. Genet. Evol.*, vol. 23, pp. 209–217, 2014, doi: 10.1016/j.meegid.2014.01.017.
- [60] Gao JR, Yoon KS, Lee SH. Increased frequency of the T929I and L932F mutations associated with knockdown resistance in permethrinresistant populations of the human head louse, *Pediculus capitis*, from California, Florida, and Texas. *Pestic Biochem Physiol*; vol. 77: pp. 115–124, 2003.

- [61] Taplin D, Meinking TL, Castillero PM, Sanchez R. Permethrin 1% creme rinse for the treatment of *Pediculus humanus var. capitis* infestation. *Pediatr Dermatol*, vol. 3: pp.344–348, 1999.
- [62] Chosidow O, Chastang C, Brue C et al. Controlled study of malathion and d-phenothrin lotions for *Pediculus humanus var. capitis* infested schoolchildren. *Lancet*, vol 344: pp.1724–1727. 14, 2005.
- [63] Hipolito RB, Mallorca FG, Zuniga-Macaraig ZO, Apolinario PC, Wheeler-Sherman J. Head lice infestation: single drug versus combination therapy with one percent permethrin and trimethoprim/sulfamethoxazole. *Pediatrics*;vol.107: pp.30-45, 2001.
- [64] Gonzalez Audino P, Barrios S, Vassena C, Mougabure Cueto G, Zerba E, Picollo MI. Increased monooxygenase activity associated with resistance to permethrin in *Pediculus humanus capitis* (Anoplura: Pediculidae) from Argentina. *J Med Entomol*; vol.42: pp. 342–345, 2005.
- [65] Burkhart CG. Relationship of treatment-resistant head lice to the safety and efficacy of pediculicides. *Mayo Clin Proc*; 79: 661–666, 2004.
- [66] Feldmeier H. Treatment of pediculosis capitis: a critical appraisal of the current literature. *American journal of clinical dermatology*, vol. 15(5), pp. 401–12, 2014.
- [67] Burgess IF, Brunton ER, Burgess NA. Single application of 4% dimeticone liquid gel versus two applications of 1% permethrin creme rinse for treatment of head louse infestation: a randomised controlled trial. *BMC dermatology*, vol. 13(1), pp. 1–7. 12,2013.
- [68] Dong K, Du Y, Rinkevich F, Nomura Y, Xu P, Wang L,. Molecular biology of insect sodium channels and pyrethroid resistance. *Insect biochemistry and molecular biology*; vol. 50, pp. 1–17, 2014.

- [69] Rinkevich FD, Du Y, Dong K. Diversity and convergence of sodium channel mutations involved in resistance to pyrethroids. *Pesticide biochemistry and physiology*. Vol 106(3),pp. 93–100, 2013.
- [70] Firoozian S, Sadaghianifar A, Taghilou B, Galavani H, Ghaffari E, Gholizadeh S. Identification of novel voltage-gated sodium channel mutations in human head and body lice (Phthiraptera: Pediculidae). *Journal of medical entomology*. vol. 54(5), pp.1337–43, 2017.
- [71] Chosidow O, Giraudeau B, Cottrell J et al. Oral ivermectin versus malathion lotion for difficult-to-treat head lice. *N Engl J Med*; vol, 362, pp. 896–905, 2010.
- [72] Chosidow O. Scabies and pediculosis. *Lancet*; vol. 355, pp. 819–826, 2000.
- [73] Downs AM, Narayan S, Stafford KA, Coles GC. Effectiveness of ovide against malathion-resistant head lice. *Arch Dermatol*; vol. 141:pp. 1318, 2005.
- [74] K. Y. Mumcuoglu, “Human lice: pediculus and pthirus,” in *Paleomicrobiology*, Springer, 2008, pp. 215–222.
- [75] A. Araújo, L. F. Ferreira, N. Guidon, N. Maues Da Serra Freire, K. J. Reinhard, and K. Dittmar, “Ten thousand years of head lice infection.,” *Parasitol. Today*, vol. 16, no. 7, p. 269, Jul. 2000.
- [76] R. Drali, L. Abi-Rached, A. Boutellis, F. Djossou, S. C. Barker, and D. Raoult, “Host switching of human lice to new world monkeys in South America,” *Infect. Genet. Evol.*, vol. 39, pp. 225–231, 2016.
- [77] N. Amanzougaghene, Amanzougaghene, N., Fenollar, F., Sangare, A. K., Sissoko, M. S., Doumbo, O. K., Raoult, D., and Mediannikov, O., “High ancient genetic diversity of human lice, pediculus humanus, from Israel reveals new insights into the origin of clade b lice,” *PLoS One*, vol. 11, no. 10, pp. 1–14, 2016, doi: 10.1371/journal.pone.0164659.
- [78] A. Boutellis, R. Drali, M. A. Rivera, K. Y. Mumcuoglu, and D. Raoult, “Evidence of sympatry of clade A and clade B head lice in a pre-Columbian

- Chilean mummy from Camarones,” *PLoS One*, vol. 8, no. 10, p. e76818, 2013.
- [79] A. Boutellis ., “Borrelia recurrentis in head lice, Ethiopia.,” *Emerg. Infect. Dis.*, vol. 19, no. 5, pp. 796–8, May 2013, doi: 10.3201/eid1905.121480.
- [80] R. J. Yetman, “The child with pediculosis capitis.,” *J. Pediatr. Health Care*, vol. 29, no. 1, pp. 118–20, Jan. 2015, doi: 10.1016/j.pedhc.2014.09.002.
- [81] M. Ashfaq, S. Prosser, S. Nasir, M. Masood, S. Ratnasingham, and P. D. N. Hebert, “High diversity and rapid diversification in the head louse, *Pediculus humanus* (Pediculidae: Phthiraptera),” *Sci. Rep.*, vol. 5, no. 1, p. 14188, Nov. 2015, doi: 10.1038/srep14188.
- [82] N. Amanzougaghene Amanzougaghene, N., Fenollar, F., Sangare, A. K., Sissoko, M. S., Doumbo, O. K., Raoult, D., and Mediannikov, O., “Detection of bacterial pathogens including potential new species in human head lice from Mali,” *PLoS One*, vol. 12, no. 9, p. e0184621, Sep. 2017, doi: 10.1371/journal.pone.0184621.
- [83] N. Amanzougaghene., “Mitochondrial diversity and phylogeographic analysis of *Pediculus humanus* reveals a new Amazonian clade ‘F,’” *Infect. Genet. Evol.*, vol. 70, pp. 1–8, 2019.
- [84] S. A. Al-Shahrani, R. A. Alajmi, T. H. Ayaad, M. A. Al-Shahrani, and E. S. H. Shaurub, “Genetic diversity of the human head lice, *Pediculus humanus capitis*, among primary school girls in Saudi Arabia, with reference to their prevalence,” *Parasitol. Res.*, vol. 116, no. 10, pp. 2637–2643, 2017, doi: 10.1007/s00436-017-5570-3.
- [85] A. Boutellis, I. Bitam, K. Fekir, N. Mana, and D. Raoult, “Evidence that clade A and clade B head lice live in sympatry and recombine in Algeria,” *Med. Vet. Entomol.*, vol. 29, no. 1, pp. 94–98, 2015.
- [86] N. Amanzougaghene Molina-Cruz, A., DeJong, R. J., Charles, B., Gupta, L., Kumar, S., Jaramillo-Gutierrez, G., Barillas-Mury, C., “Head Lice of

- Pygmies Reveal the Presence of Relapsing Fever *Borreliae* in the Republic of Congo,” *PLoS Negl. Trop. Dis.*, vol. 10, no. 12, p. e0005142, Dec. 2016, doi: 10.1371/journal.pntd.0005142.
- [87] S. Sunantaraporn ., “Molecular survey of the head louse *Pediculus humanus capitis* in Thailand and its potential role for transmitting *Acinetobacter* spp.,” *Parasites vectors*, vol. 8, no. 1, pp. 1–7, 2015.
- [88] K. Candy., “Molecular survey of head and body lice, *Pediculus humanus*, in France,” *Vector-Borne Zoonotic Dis.*, vol. 18, no. 5, pp. 243–251, 2018.
- [89] M. Louni., “Detection of bacterial pathogens in clade E head lice collected from Niger’s refugees in Algeria,” *Parasites & vectors*, vol. 11, no. 1, pp. 1–11, 2018.
- [90] J. K. Park., “Characterization of the human head louse nit sheath reveals proteins with adhesive property that show no resemblance to known proteins,” *Sci. Rep.*, vol. 9, no. 1, p. 48, Dec. 2019, doi: 10.1038/s41598-018-36913-z.
- [91] C. N. Burkhart, B. A. Stankiewicz, I. Pchalek, M. A. Kruge, and C. G. Burkhart, “Molecular composition of the louse sheath,” *J. Parasitol.*, vol. 85, no. 3, pp. 559–61, Jun. 1999, doi: 10.2307/3285796.
- [92] Y. Bechah, C. Capo, J.-L. Mege, and D. Raoult, “Epidemic typhus,” *Lancet Infect. Dis.*, vol. 8, no. 7, pp. 417–426, 2008.
- [93] D. L. Bonilla, L. A. Durden, M. E. Ereemeeva, and G. A. Dasch, “The Biology and Taxonomy of Head and Body Lice—Implications for Louse-Borne Disease Prevention,” *PLoS Pathog.*, vol. 9, no. 11, p. e1003724, Nov. 2013, doi: 10.1371/journal.ppat.1003724.
- [94] S. Antinori, O. Mediannikov, M. Corbellino, and D. Raoult, “Louse-borne relapsing fever among East African refugees in Europe,” *Travel Med. Infect. Dis.*, vol. 14, no. 2, pp. 110–114, 2016.

- [95] D. Raoult, Molina-Cruz, A., DeJong, R. J., Charles, B., Gupta, L., Kumar, S., Jaramillo-Gutierrez, G., Barillas-Mury, C., “Evidence for louse-transmitted diseases in soldiers of Napoleon’s Grand Army in Vilnius,” *J. Infect. Dis.*, vol. 193, no. 1, pp. 112–120, 2006.
- [96] M. Drancourt, V. Moal, P. Brunet, B. Dussol, Y. Berland, and D. Raoult, “Bartonella (Rochalimaea) quintana infection in a seronegative hemodialyzed patient,” *J. Clin. Microbiol.*, vol. 34, no. 5, pp. 1158–1160, 1996.
- [97] J.-M. Rolain, M. Franc, B. Davoust, and D. Raoult, “Molecular detection of Bartonella quintana, B. koehlerae, B. henselae, B. clarridgeiae, Rickettsia felis, and Wolbachia pipientis in cat fleas, France,” *Emerg. Infect. Dis.*, vol. 9, no. 3, p. 339, 2003.
- [98] S. Sato., “Japanese macaques (Macaca fuscata) as natural reservoir of Bartonella quintana,” *Emerg. Infect. Dis.*, vol. 21, no. 12, p. 2168, 2015.
- [99] R. Piarroux., “Plague Epidemics and Lice, Democratic Republic of the Congo,” *Emerg. Infect. Dis.*, vol. 19, no. 3, Mar. 2013, doi: 10.3201.
- [100] L. Houhamdi, H. Lepidi, M. Drancourt, and D. Raoult, “Experimental model to evaluate the human body louse as a vector of plague,” *J. Infect. Dis.*, vol. 194, no. 11, pp. 1589–1596, 2006.
- [101] D. Raoult, “A personal view of how paleomicrobiology aids our understanding of the role of lice in plague pandemics,” *Microbiol. Spectr.*, vol. 4, no. 4, p. 4, 2016.
- [102] L. Houhamdi, P.-E. FOURNIER, R. Fang, and D. Raoult, “An experimental model of human body louse infection with Rickettsia typhi,” *Ann. N. Y. Acad. Sci.*, vol. 990, no. 1, pp. 617–627, 2003.
- [103] S. L. Kalra and K. N. A. Rao, “Typhus fevers in Kashmir state. Part II. Murine typhus,” *Indian J. Med. Res.*, vol. 39, no. 3, pp. 297–302, 1951.

- [104] P. Giroud and J. Jadin, "Infection latente et conservation de 'Rickettsia burnetii' chez l'homme, le rôle du pou," *Bull Soc Pathol Exot*, vol. 47, pp. 764–765, 1954.
- [105] N. Arricau-Bouvery and A. Rodolakis, "Is Q fever an emerging or re-emerging zoonosis?," *Vet. Res.*, vol. 36, no. 3, pp. 327–349, 2005.
- [106] B. La Scola, P.-E. Fournier, P. Brouqui, and D. Raoult, "Detection and culture of Bartonella quintana, Serratia marcescens, and Acinetobacter spp. from decontaminated human body lice," *J. Clin. Microbiol.*, vol. 39, no. 5, pp. 1707–1709, 2001.
- [107] D. Previte., "Differential gene expression in laboratory strains of human head and body lice when challenged with Bartonella quintana, a pathogenic bacterium," *Insect Mol. Biol.*, vol. 23, no. 2, pp. 244–254, 2014.
- [108] P.-J. Coulaud, C. Lepolard, Y. Bechah, J.-M. Berenger, D. Raoult, and E. Ghigo, "Hemocytes from Pediculus humanus humanus are hosts for human bacterial pathogens," *Front. Cell. Infect. Microbiol.*, vol. 4, p. 183, 2015.
- [109] J. H. Kim., "Comparison of the humoral and cellular immune responses between body and head lice following bacterial challenge," *Insect Biochem. Mol. Biol.*, vol. 41, no. 5, pp. 332–339, 2011.
- [110] J. H. Kim, K. S. Yoon, D. J. Previte, B. R. Pittendrigh, J. M. Clark, and S. H. Lee, "Comparison of the immune response in alimentary tract tissues from body versus head lice following Escherichia coli oral infection," *J. Asia. Pac. Entomol.*, vol. 15, no. 3, pp. 409–412, 2012.
- [111] A. Molina-Cruz, Molina-Cruz, A., DeJong, R. J., Charles, B., Gupta, L., Kumar, S., Jaramillo-Gutierrez, G., Barillas-Mury, C., "Reactive oxygen species modulate Anopheles gambiae immunity against bacteria and Plasmodium," *J. Biol. Chem.*, vol. 283, no. 6, pp. 3217–3223, 2008.

- [112] I. Eleftherianos, J. Atri, J. Accetta, and J. C. Castillo, “Endosymbiotic bacteria in insects: guardians of the immune system?,” *Front. Physiol.*, vol. 4, p. 46, 2013.
- [113] E. J. Muturi, C.-H. Kim, B. W. Alto, M. R. Berenbaum, and M. A. Schuler, “Larval environmental stress alters *Aedes aegypti* competence for Sindbis virus,” *Trop. Med. Int. Heal.*, vol. 16, no. 8, pp. 955–964, 2011.
- [114] J. Goldberger and J. F. Anderson, The transmission of typhus fever: with especial reference to transmission by the head louse (*Pediculus capitis*). US Government Printing Office, 1912.
- [115] G. Diatta., “Prevalence of *Bartonella quintana* in patients with fever and head lice from rural areas of Sine-Saloum, Senegal,” *Am. J. Trop. Med. Hyg.*, vol. 91, no. 2, p. 291, 2014.
- [116] E. Angelakis, J.-M. Rolain, D. Raoult, and P. Brouqui, “*Bartonella quintana* in head louse nits,” *FEMS Immunol. & Med. Microbiol.*, vol. 62, no. 2, pp. 244–246, 2011.
- [117] E. Angelakis., “Altitude-dependent *Bartonella quintana* genotype C in head lice, Ethiopia,” *Emerg. Infect. Dis.*, vol. 17, no. 12, p. 2357, 2011.
- [118] P.-E. Fournier, J.-B. Ndiokubwayo, J. Guidran, P. J. Kelly, and D. Raoult, “Human pathogens in body and head lice,” *Emerg. Infect. Dis.*, vol. 8, no. 12, p. 1515, 2002.
- [119] S. Bouvresse Ecovoiu, A. A., Ghita, I. C., Chifriuc, D. I. M., Ghionoiu, I. C., Ciuca, A. M., Bologa, A. M., and Ratiu, A. C., “No evidence of *Bartonella quintana* but detection of *Acinetobacter baumannii* in head lice from elementary schoolchildren in Paris,” *Comp. Immunol. Microbiol. Infect. Dis.*, vol. 34, no. 6, pp. 475–477, 2011.
- [120] D. Vallenet ., “Comparative analysis of *Acinetobacters*: three genomes for three lifestyles,” *PLoS One*, vol. 3, no. 3, p. e1805, 2008.

- [121] A. K. Sangaré, O. K. Doumbo, and D. Raoult, "Management and treatment of human lice," *Biomed Res. Int.*, vol. 2016, 2016.
- [122] J. M. Clark, K. S. Yoon, S. H. Lee, and B. R. Pittendrigh, "Human lice: Past, present and future control," *Pestic. Biochem. Physiol.*, vol. 106, no. 3, pp. 162–171, 2013.
- [123] O. Chosidow., "Oral ivermectin versus malathion lotion for difficult-to-treat head lice," *N. Engl. J. Med.*, vol. 362, no. 10, pp. 896–905, 2010.
- [124] S. Aditya and A. Rattan, "Spinosad: An effective and safe pediculicide," *Indian Dermatol. Online J.*, vol. 3, no. 3, p. 213, 2012.
- [125] T. L. Meinking Ecovoiu, A. A., Ghita, I. C., Chifiriuc, D. I. M., Ghionoiu, I. C., Ciuca, A. M., Bologa, A. M., and Ratiu, A. C., "The clinical trials supporting benzyl alcohol lotion 5%(Ulesfiatm): a safe and effective topical treatment for head lice (*Pediculus humanus capitis*)," *Pediatr. Dermatol.*, vol. 27, no. 1, pp. 19–24, 2010.
- [126] D. H. Kwon, J. H. Kim, Y. H. Kim, K. S. Yoon, J. M. Clark, and S. H. Lee, "Identification and characterization of an esterase involved in malathion resistance in the head louse *Pediculus humanus capitis*," *Pestic. Biochem. Physiol.*, vol. 112, pp. 13–18, 2014.
- [127] C. Foucault, S. Ranque, S. Badiaga, C. Rovey, D. Raoult, and P. Brouqui, "Oral ivermectin in the treatment of body lice," *J. Infect. Dis.*, vol. 193, no. 3, pp. 474–476, 2006.
- [128] G. Diatta, C. Abat, C. Sokhna, H. Tissot-Dupont, J.-M. Rolain, and D. Raoult, "Head lice probably resistant to ivermectin recovered from two rural girls in Dielmo, a village in Sine-Saloum, Senegal," *Int. J. Antimicrob. Agents*, vol. 47, no. 6, pp. 501–502, 2016.
- [129] N. Amanzougaghene, F. Fenollar, G. Diatta, C. Sokhna, D. Raoult, and O. Mediannikov, "Mutations in GluCl associated with field ivermectin-resistant

- head lice from Senegal,” *Int. J. Antimicrob. Agents*, vol. 52, no. 5, pp. 593–598, 2018, doi: 10.1016/j.ijantimicag.2018.07.005.
- [130] D. Sasser, S. Epis, M. Pajoro, and C. Bandi, “Microbial symbiosis and the control of vector-borne pathogens in tsetse flies, human lice, and triatomine bugs,” *Pathog. Glob. Health*, vol. 107, no. 6, pp. 285–292, 2013.
- [131] C. H. Shashindran, I. S. Gandhi, S. Krishnasamy, and M. N. Ghosh, “Oral therapy of pediculosis capitis with cotrimoxazole,” *Br. J. Dermatol.*, vol. 98, no. 6, pp. 699–700, 1978.
- [132] A. K. Sangare, J. M. Rolain, J. Gaudart, P. Weber, and D. Raoult, “Synergistic activity of antibiotics combined with ivermectin to kill body lice,” *Int. J. Antimicrob. Agents*, vol. 47, no. 3, pp. 217–223, 2016.
- [133] W. Ruankham, P. Winyangkul, and N. Bunchu, “Prevalence and factors of head lice infestation among primary school students in Northern Thailand,” *Asian Pacific J. Trop. Dis.*, vol. 6, no. 10, pp. 778–782, Oct. 2016.
- [134] D. Holland “Map to Reference” <https://www.geneious.com/tutorials/map-to-reference/> . (Founded in 2003).
- [135] D. Holland “ Translating sequences” <https://assets.geneious.com/manual/2019.1/GeneiousManuale28.html>. (Founded in 2019).
- [136] Kent, W. James. ”BLAT—The BLAST-Like Alignment Tool”. *Genome Research*. 12 (4): 656–664, 2002.
- [137] Choi Y, Chan AP. PROVEAN web server: a tool to predict the functional effect of amino acid substitutions and indels. *Bioinformatics* 31(16): 2745-2747, 2015.
- [138] Choi Y, Sims GE, Murphy S, Miller JR, Chan AP Predicting the Functional Effect of Amino Acid Substitutions and Indels. *PLoS ONE* 7(10): e46688 (2012) .

- [139] Choi Y A Fast Computation of Pairwise Sequence Alignment Scores Between a Protein and a Set of Single-Locus Variants of Another Protein. In Proceedings of the ACM Conference on Bioinformatics, Computational Biology and Biomedicine (BCB '12). ACM, New York, NY, USA, 414-417, (2012)
- [140] Gratz, N. G. Human lice: Their prevalence, control, and resistance to insecticides. A review 1985–1997. World Health Organization/Division of Tropical Diseases/WHO Pesticide Evaluation Scheme/97.8. Geneva: World Health Organization, 2021.
- [141] Heukelbach J, Wilcke T, Winter B, Feldmeier H Epidemiology and morbidity of scabies and pediculosis capitis in resource-poor communities in Brazil. *Br J Dermatol* 2005, 153(1):150-156.
- [142] Nutanson I, Steen CJ, Schwartz RA ,Janniger CK, 2008. Pediculosis capitis: an update. *Acta Dermatoven APA Vol* 17, 147-158. 4.
- [143] Durand R, Millard B, Bouges-Michel C, Bruel C, Bouvresse S, Izri A. Detection of Pyrethroid Resistance Gene in Head Lice in Schoolchildren from Bobigny, France. *J Med Entomol.* 2007;44(5):796–8.
- [144] Bouvresse S, Berdjane Z, Durand R, Bous-Gaillou J, Izri A, Chosidow O. Permethrin and malathion resistance in head lice: Results of ex vivo and molecular assays. *JAmAcadDermatol.* 2012; December.
- [145] Durand R, Bouvresse S, Berdjane Z, Izri A, Chosidow O, Clark J.M. Insecticide resistance in head lice: clinical, parasitological and genetic aspects. 2012
- [146] Thomas DR, McCarroll L, Roberts R. Surveillance of insecticide resistance in head lice using biochemical and molecular methods. *Arch Dis Child*; vol. 91: pp. 777–778, 2006.
- [147] Burgess IF, Brown CM, Peock S, Kaufman J. Head lice resistant to pyrethroid insecticides in Britain. *BMJ*;vol. 311:pp. 752, 2008.

- [148] Kristensen M, Knorr M, Rasmussen AM, Jespersen JB. Survey of permethrin and malathion resistance in human head lice populations from Denmark. *J Med Entomol*; vol. 43:pp. 533–538, 2006.
- [149] Mumcuoglu KY, Hemingway J, Miller. Permethrin resistance in the head louse *Pediculus capitis* from Israel. *Med Vet Entomol*; vol. 9:pp. 427–432, 2005.
- [150] Pollack RJ, Kiszewski A, Armstrong P. Differential permethrin susceptibility of head lice sampled in the United States and Borneo. *Arch Pediatr Adolesc Med*; vol. 153: pp.960-973, 2000.
- [151] Lee SH, Yoon KS, Williamson. Molecular analysis of kdr-like resistance in permethrin-resistant strains of head lice, *Pediculus capitis*. *Pestic Biochem Physiol*; vol. 66: pp. 130–143, 2000.
- [152] Meinking TL, Serrano L, Hard. Comparative in vitro pediculicidal efficacy of treatments in a resistant head lice population in the United States. *Arch Dermatol*; vol. 138: pp. 220–224, 2000.
- [153] Picollo MI, Vassena CV, Casadio AA, Massimo J, Zerba EN. Laboratory studies of susceptibility and resistance to insecticides in *Pediculus capitis* (Anoplura; Pediculidae). *J Med Entomol*; 35: 814–817, 1999.
- [154] Picollo MI, Vassena CV, Mougabure Cueto GA, Verneti M, Zerba EN. Resistance to insecticides and effect of synergists on permethrin toxicity in *Pediculus capitis* (Anoplura: Pediculidae) from Buenos Aires. *J Med Entomol* ; 37: 721–725, 2000.
- [155] Tomita T, Yaguchi N, Mihara M, Takahashi M, Agui N, Kasai S. Molecular analysis of a para sodium channel gene from pyrethroidresistant head lice, *Pediculus humanus capitis* (Anoplura: Pediculidae). *J Med Entomol*, vol. 40: pp. 468–474, 2003.
- [156] Hunter JA, Barker SC. Susceptibility of head lice (*Pediculus humanus capitis*) to pediculicides in Australia. *Parasitol Res* ; 90: 476–478. 26, 2009.

-
- [157] Elston DM. Drug-resistant lice. *Arch Dermatol*; vol. 139:pp. 1061–1064, 2003.
- [158] Lee SHGJ, Yoon KS, Mumcuoglu KY. Sodium channel mutations associated with knockdown resistance in the human head louse, *Pediculus capitis* (De Geer). *Pestic Biochem Physiol*;vol.75: pp.79–91, 2003.
- [159] Hodgdon HE, Yoon KS, Previte DJ. Determination of knockdown resistance allele frequencies in global human head louse populations using the serial invasive signal amplification reaction. *Pest Manag Sci*; vol. 66: pp. 1031–1040, 2010.
- [160] Kasai S, Ishii N, Natsuaki M. Prevalence of kdr-like mutations associated with pyrethroid resistance in human head louse populations in Japan. *J Med Entomol*; vol.46: pp.77–82, 2009

An Appendix

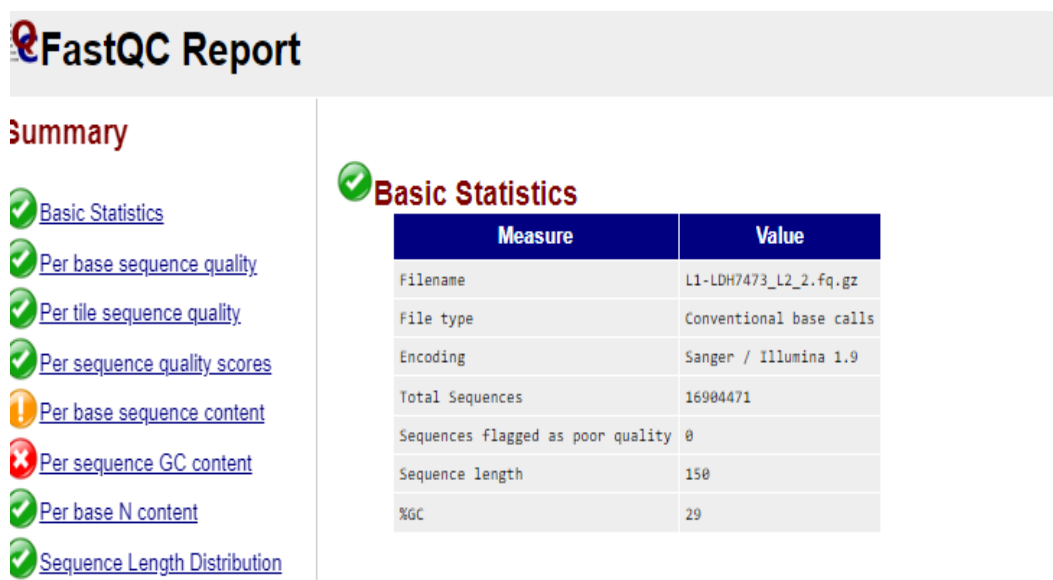


FIGURE 5.1: Basic Statistics of the Sequence.

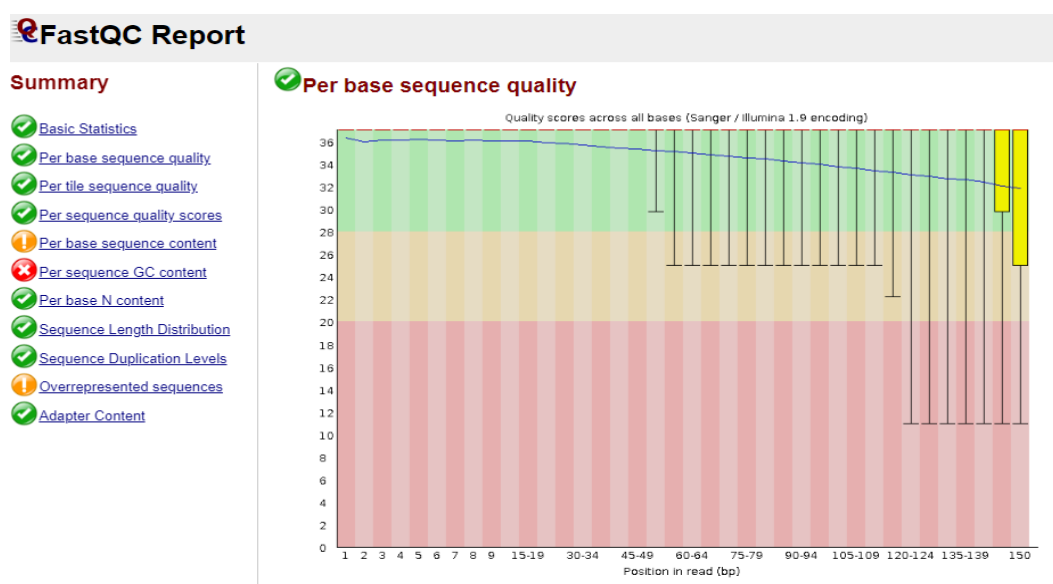


FIGURE 5.2: Per Base Quality of the Sequence.

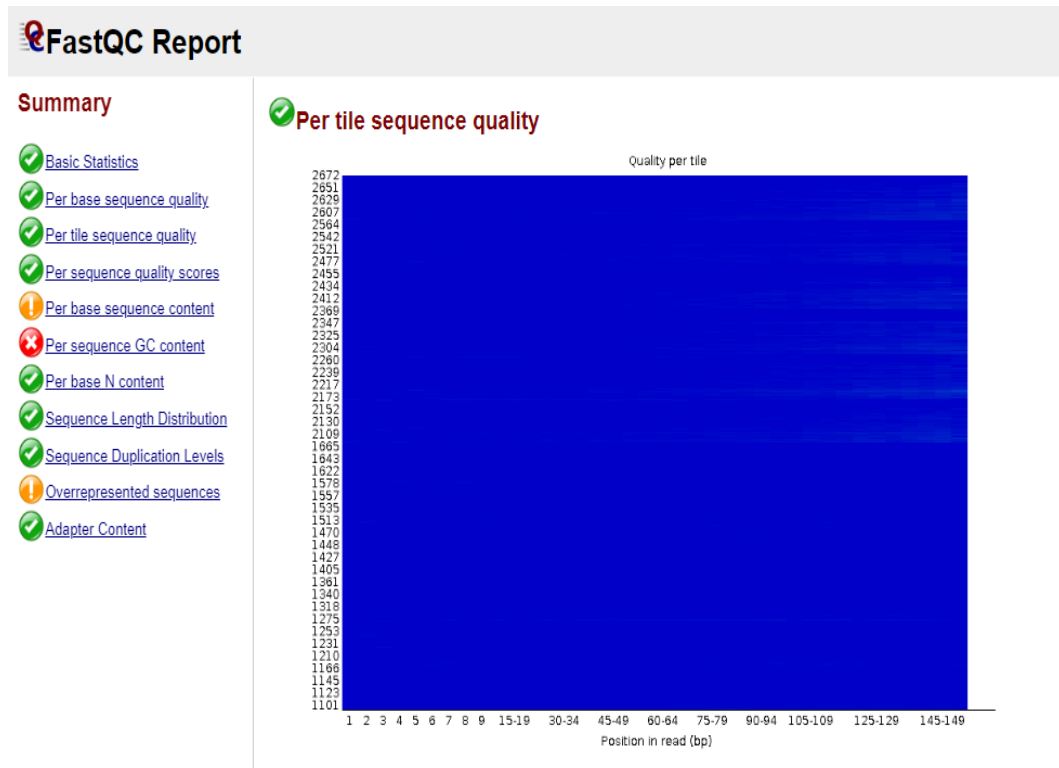


FIGURE 5.3: Quality of the Sequence per Tile.

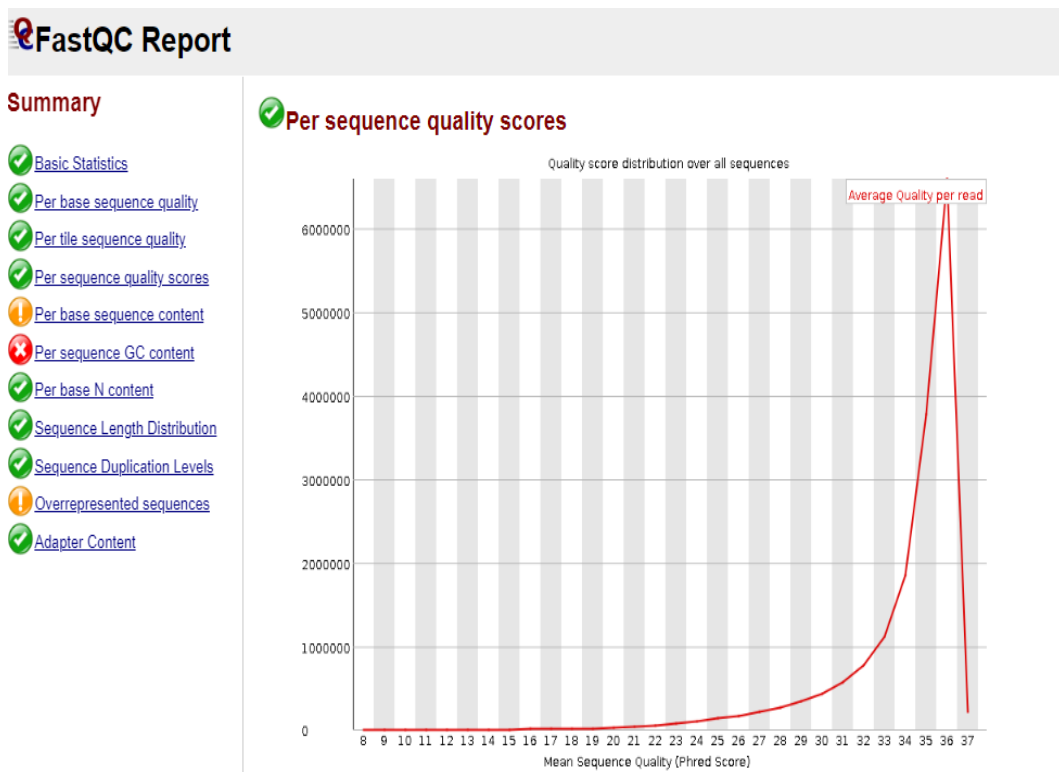


FIGURE 5.4: Per Sequence Quality Scores.

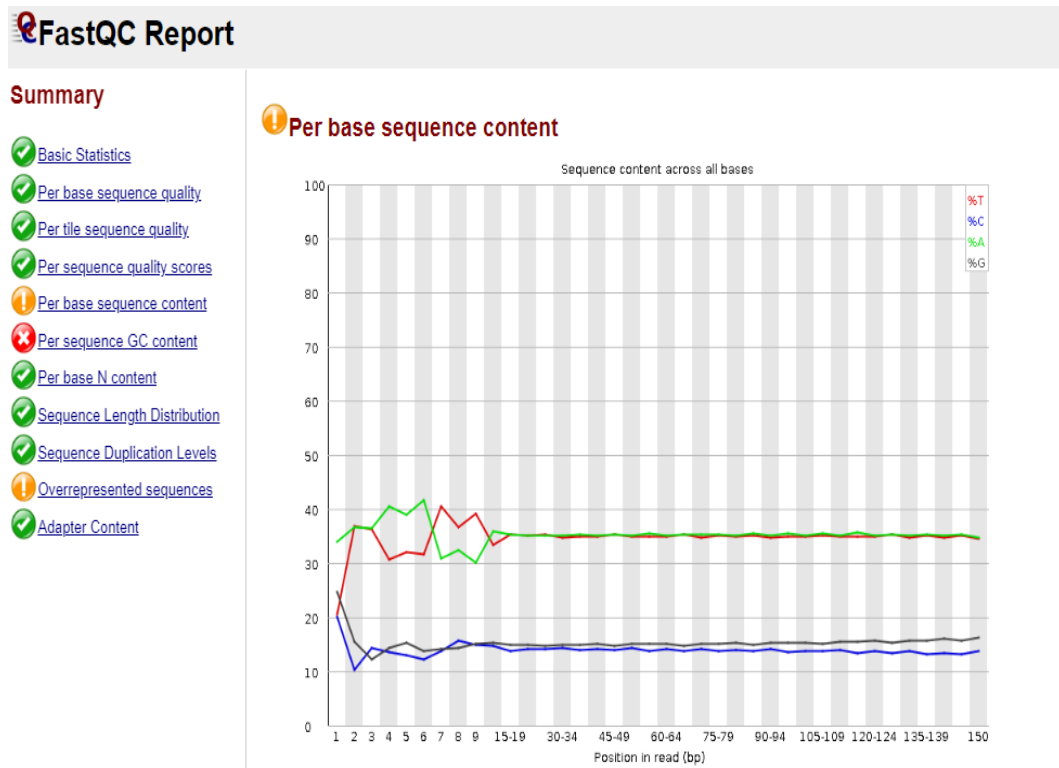


FIGURE 5.5: Per Base Sequence Content.

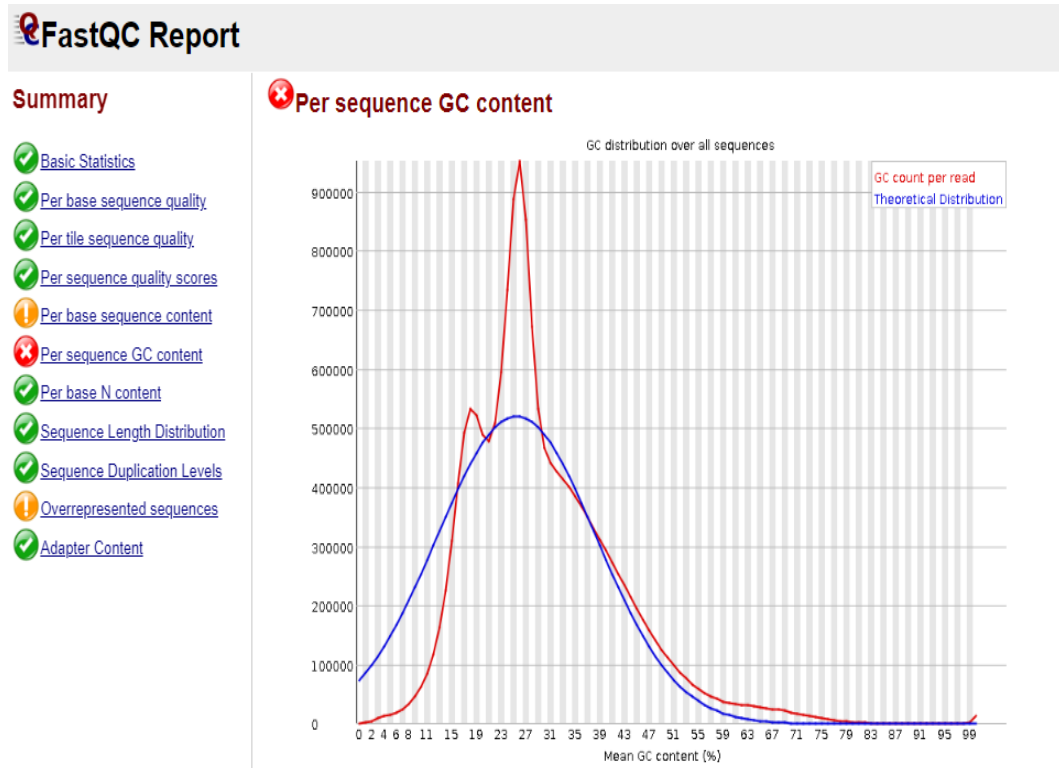


FIGURE 5.6: Per Base GC Content.

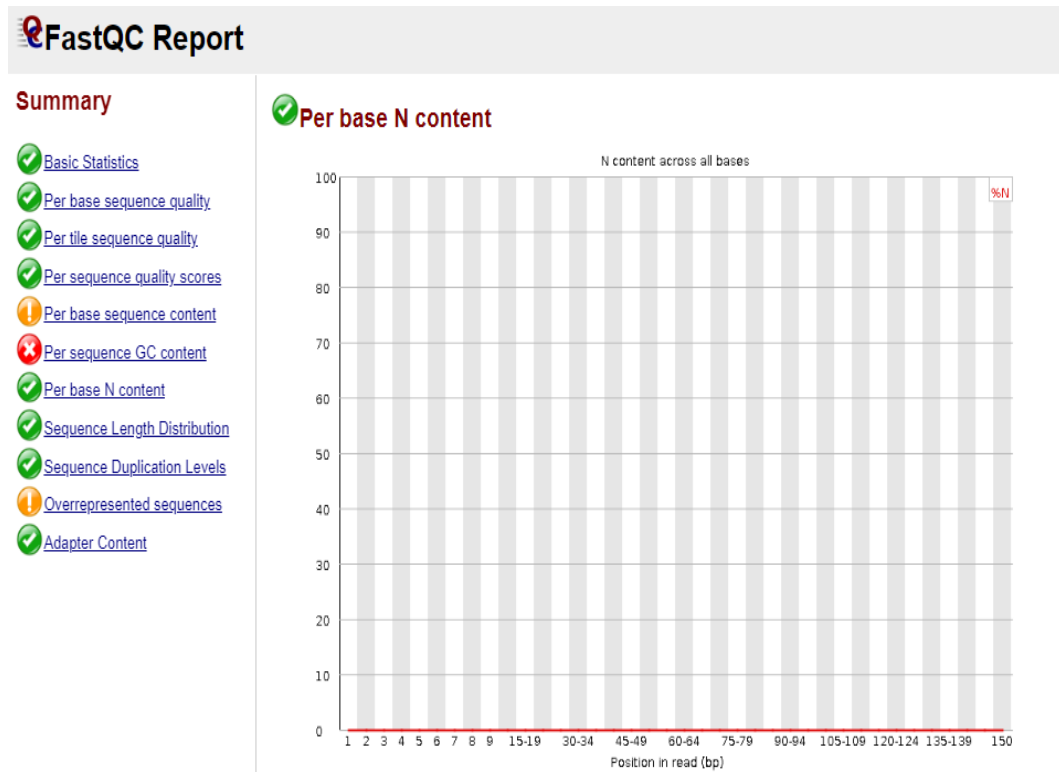


FIGURE 5.7: Per Base N Content.

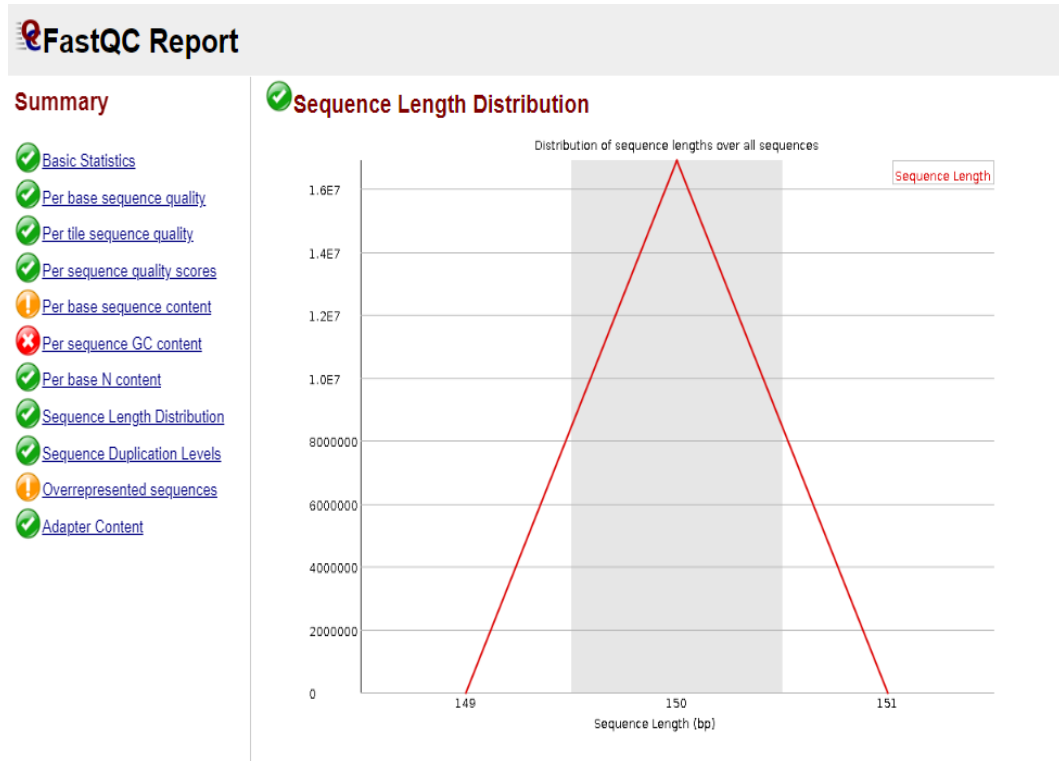


FIGURE 5.8: Sequence Length Distribution.

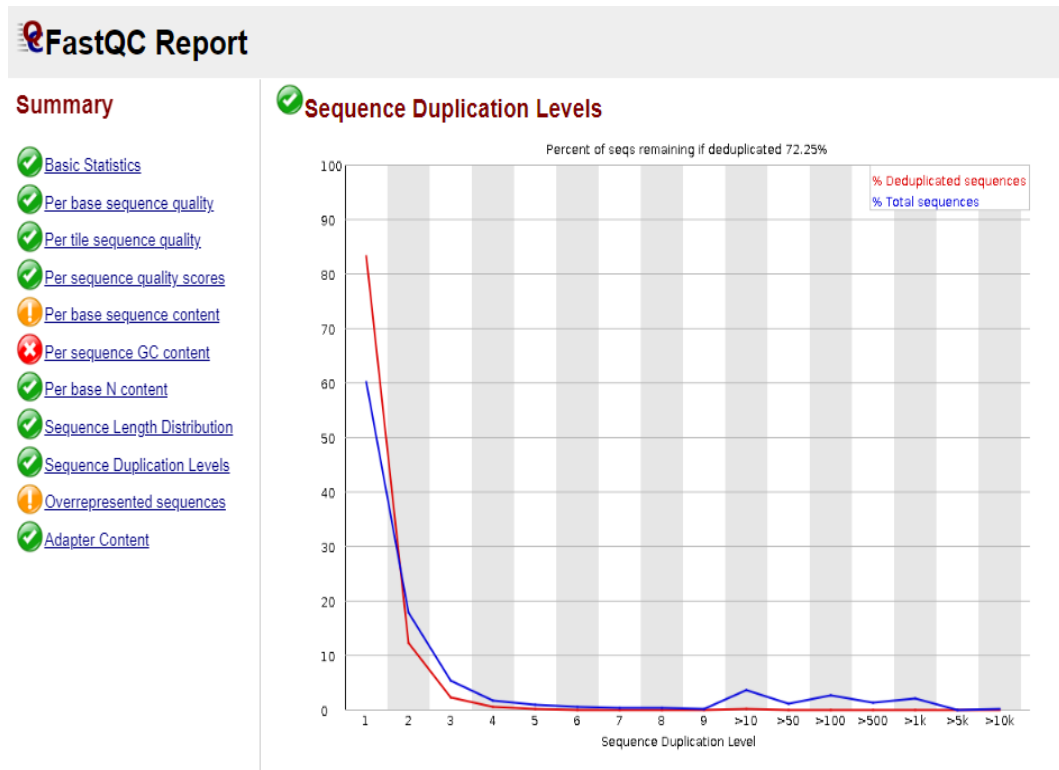


FIGURE 5.9: Sequence Duplication Levels.

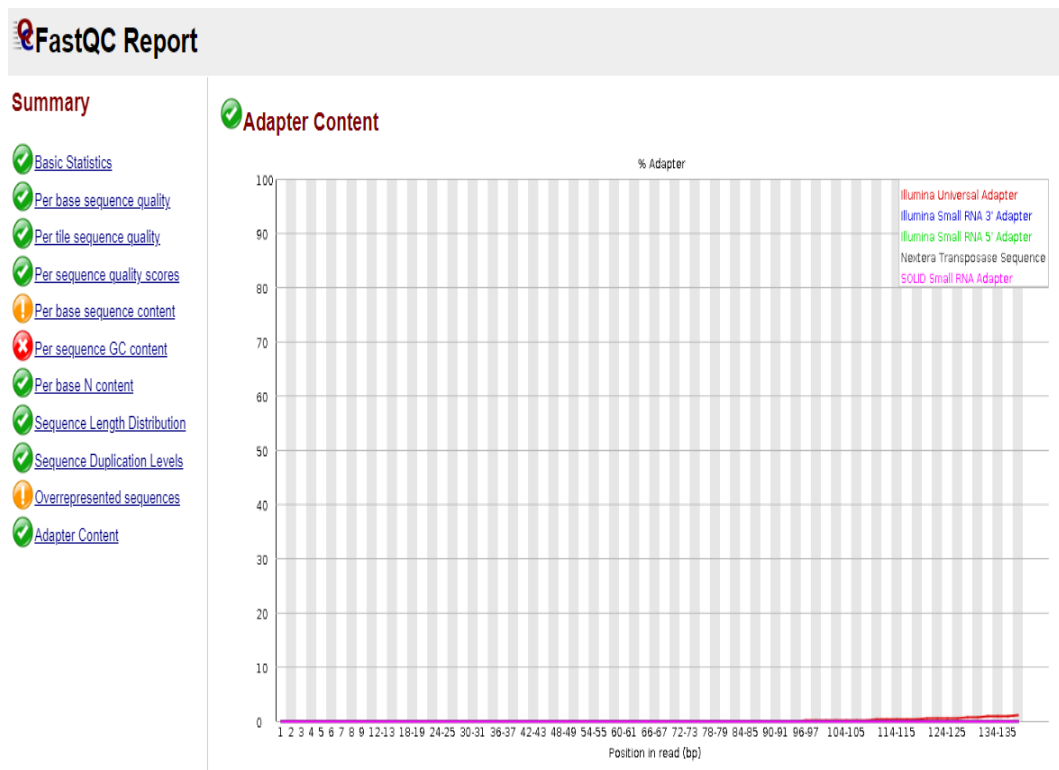
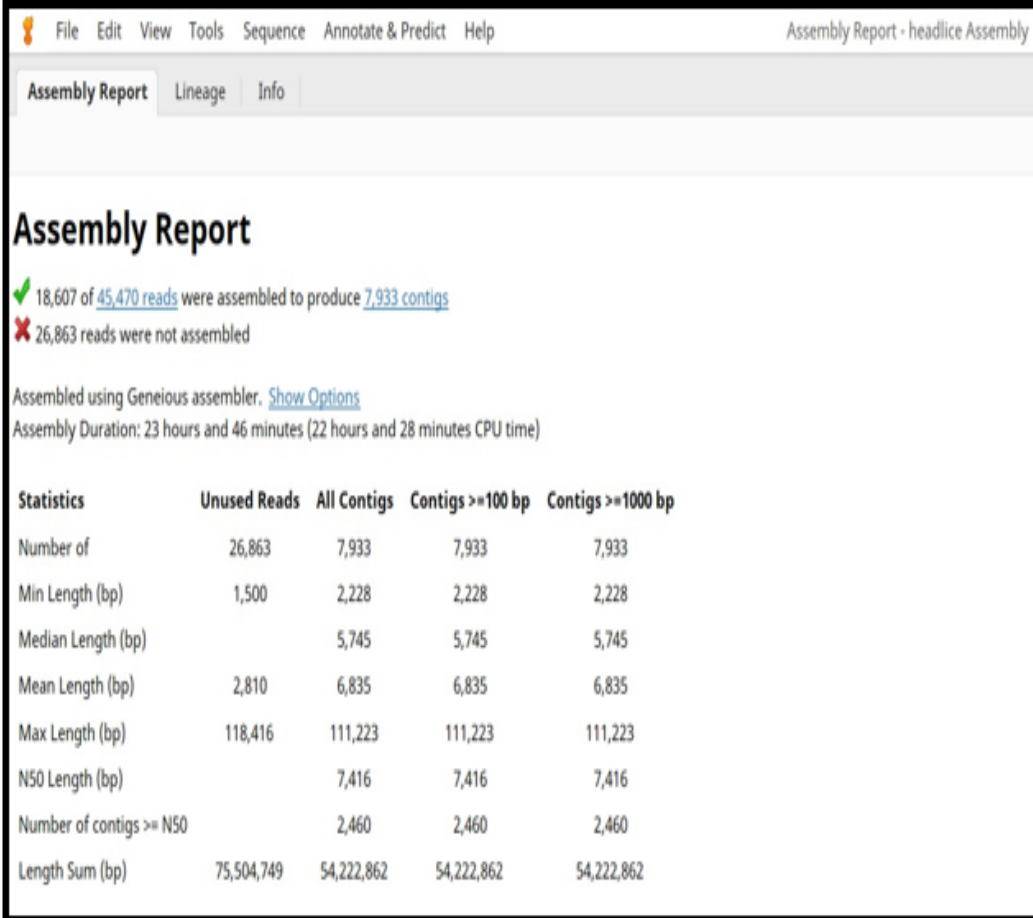


FIGURE 5.10: Adapter Content.



Assembly Report

✓ 18,607 of 45,470 reads were assembled to produce 7,933 contigs
 ✗ 26,863 reads were not assembled

Assembled using Geneious assembler. [Show Options](#)
 Assembly Duration: 23 hours and 46 minutes (22 hours and 28 minutes CPU time)

Statistics	Unused Reads	All Contigs	Contigs ≥ 100 bp	Contigs ≥ 1000 bp
Number of	26,863	7,933	7,933	7,933
Min Length (bp)	1,500	2,228	2,228	2,228
Median Length (bp)		5,745	5,745	5,745
Mean Length (bp)	2,810	6,835	6,835	6,835
Max Length (bp)	118,416	111,223	111,223	111,223
N50 Length (bp)		7,416	7,416	7,416
Number of contigs $\geq N50$		2,460	2,460	2,460
Length Sum (bp)	75,504,749	54,222,862	54,222,862	54,222,862

FIGURE 5.11: The Assembly Report provided by the Genious Prime tool.